Summer 2019

Effects of electro-osmotic consolidation of clays and its improvement using ion exchange membranes

Lucas Martin
New Jersey Institute of Technology

Copyright Warning & Restrictions

The copyright law of the United States (Title 17, United States Code) governs the making of photocopies or other reproductions of copyrighted material.

Under certain conditions specified in the law, libraries and archives are authorized to furnish a photocopy or other reproduction. One of these specified conditions is that the photocopy or reproduction is not to be "used for any purpose other than private study, scholarship, or research." If a, user makes a request for, or later uses, a photocopy or reproduction for purposes in excess of "fair use" that user may be liable for copyright infringement,

This institution reserves the right to refuse to accept a copying order if, in its judgment, fulfillment of the order would involve violation of copyright law.

Please Note: The author retains the copyright while the New Jersey Institute of Technology reserves the right to distribute this thesis or dissertation

Printing note: If you do not wish to print this page, then select "Pages from: first page # to: last page #" on the print dialog screen

ABSTRACT

EFFECTS OF ELECTRO-OSMOTIC CONSOLIDATION OF CLAYS AND ITS IMPROVEMENT USING ION EXCHANGE MEMBRANES

by
Lucas Martin

Electro-osmosis is an established method of expediting consolidation of soft, saturated clayey soils compared to commonly used methods, such as preloading with wick drains. In electro-osmotic consolidation a direct current (DC) is applied via inserted electrodes. This causes hydrated ions in the interstitial fluid to migrate to oppositely charged electrodes. Because the clay particles have a negative surface charge, the majority of ions in the interstitial fluid are positively charged. Therefore, the net flow will be towards the negatively charged electrode (cathode), where the water can be removed and thus consolidation is achieved. Certain problems, such as pH changes in the soil around the electrodes, make the method inefficient and prevent the widespread use of electro-osmotic consolidation, especially in developed nations.

There is limited experimental or theoretical analysis on how exactly an electric field removes water from clay pores. Hence in this research a new theory is developed based on colloidal chemistry. Furthermore, to a new technology using ion-exchange membranes is proposed and investigated to improve the power consumption of electro-osmotic consolidation.

The first part of this research develops a new method of estimating the expected flow of water through clayey soils (electro-osmotic conductivity) under the influence of an electric field based on work done in the area of colloid chemistry. This new method shows clear advantages over the currently used Helmholtz-Smoluchowski model. The

flowrate due to electro-osmosis and the soil consolidation is measured for different electrical conductivity values and compared with the developed theory. The results confirm the validity of the new model, showing that electrolyte composition in the interstitial fluid is a significant factor in estimating electro-osmotic consolidation. Additional laboratory tests show that electro-osmotic consolidation achieves effects similar to secondary consolidation settlement, but over a hundred times faster. This observation is used to accurately predict electro-osmotic consolidation for specific voltages.

The second part of the research described herein evaluates the ability of ion exchange membranes to improve electro-osmotic consolidation of clay soils. By inserting the membrane between the soil and the electrode a barrier is created that prevents hydrogen ions generated at the anode from moving to the cathode through the soil. When using the membrane, the change of soil pH around the anode is reduced by at least 10% and the increase in electrical resistance is slowed down by almost five times. This results in a 75% increased settlement for electro-osmotic consolidation tests with a membrane. This can prove to be a significant improvement to commercialize the use of the technology in developed nations.

EFFECTS OF ELECTRO-OSMOTIC CONSOLIDATION OF CLAYS AND ITS IMPROVEMENT USING ION EXCHANGE MEMBRANES

by
Lucas Martin

A Dissertation
Submitted to the Faculty of
New Jersey Institute of Technology
in Partial Fulfillment of the Requirements for the Degree of
Doctor of Philosophy in Civil Engineering

John A. Reif, Jr. Department of Civil and Environmental Engineering

August 2019

APPROVAL PAGE

EFFECTS OF ELECTRO-OSMOTIC CONSOLIDATION OF CLAYS AND ITS IMPROVEMENT USING ION EXCHANGE MEMBRANES

Lucas Martin

Dr. Jay N. Meegoda, Dissertation Advisor Professor of Civil and Environmental Engineering, NJIT	Date
Dr. Michael Siegel, Committee Member Professor of Mathematical Sciences, NJIT	Date
Dr. Bruno M. Goncalves da Silva, Committee Member Assistant Professor of Civil and Environmental Engineering, NJIT	Date
Dr. David W. Washington, Committee Member Associate Professor of Applied Engineering and Technology, NJIT	Date
Dr. Vahid Alizadeh, Committee Member Assistant Professor at Fairleigh Dickinson University	Date

BIOGRAPHICAL SKETCH

Author: Lucas Martin

Degree: Doctor of Philosophy

Date: August 2019

Undergraduate and Graduate Education:

- Doctor of Philosophy in Civil Engineering,
  New Jersey Institute of Technology, Newark, NJ, 2019

- Bachelor of Science in Civil Engineering,
  New Jersey Institute of Technology, Newark, NJ, 2014

Major: Civil Engineering

Presentations and Publications:

Martin, L and J.N. Meegoda (2017). "*Feasibility of ion exchange membranes to control pH changes during electro-osmotic consolidation of soft soils.*" Proceedings of the 19th International Conference on Soil Mechanics and Geotechnical Engineering; Seoul, South Korea.

Meegoda, J.N. and L. Martin (2018). "*In-situ determination of specific surface area of clays.*" Geotechnical and Geological Engineering, Volume 37, pp. 465–474.

Martin, L., V. Alizadeh, and J. N. Meegoda (2019). "*Electro-osmosis treatment techniques and their effect on dewatering of soils, sediments, and sludge: A review.*" Soils and Foundations, Volume 59, pp. 407-418.

Martin, L. and J. N. Meegoda (2019). "*Feasibility of ion exchange membranes to control p. during electro-osmotic consolidation.*" Geotechnical Testing Journal, Volume 42.

Martin, L and J.N. Meegoda (Under review). "*New model for calculating the rate of liquid flow through composite liners due to geomembrane defects*." Submitted to Géotechnique Letters, March 2019.

Martin, L, and J.N. Meegoda (Under review). "*New method to predict electro-osmotic conductivity in clays.*" Submitted to International Journal of Geomechanics, May 2019.

Martin, L and J.N. Meegoda (Under review). "*Prediction of applied voltage for electro-osmotic consolidation based on coefficient of secondary consolidation.*" Submitted to ASCE Journal of Geotechnical and Geo-environmental Engineering, July 2019.

Martin, L and J.N. Meegoda (Under review). "*Anion exchange membranes to enhance electro-osmotic consolidation.*" Submitted to Geotextiles & Geomembranes, August 2019.

Martin, L and J.N. Meegoda (Under development). "*Calculating electro-osmotic conductivity of clays based on anisotropy and porosity.*" To be submitted to Geotechnique, August 2019.

To my parents

For their unconditional love

And to Abbey

My best friend

ACKNOWLEDGEMENTS

I would like to extend my sincere gratitude to many people who supported and contributed towards the research study presented in this dissertation. This feat would have been unobtainable without my research supervisor, committee members, academic and non-academic staff, friends, and family who helped in many ways during my research.

I want to convey my sincere gratitude to my research advisor professor Jay Meegoda for his offer to join the graduate program of the New Jersey Institute of Technology and work on a Ph.D. I also thank him for numerous research opportunities he provided me, exposing me to many areas of research and developing me as a professional. His guidance and support throughout my research helped me to obtain an aptitude for research and to achieve important milestones in my life. He has also greatly influenced me and encouraged me in my goal to become a university professor. His honest and challenging advice is always valued.

I would like to thank my dissertation committee members: Vahid Alizadeh, Bruno Goncalves da Silva, and David Washington for their constructive criticism and advice to improve my work. I am grateful for their help and support provided throughout my career to improve my understanding and skills in research and teaching activities. I am especially indebted to Professor Michael Siegel for numerous consultations, which resulted in the development of the theoretical portion of the research.

I acknowledge department of Civil and Environmental Engineering for supporting me as a Teaching Assistant and providing me opportunities to teach geotechnical related

courses. I also acknowledge the Utility and Transportation Contractors Association of New Jersey for providing funding to purchase materials necessary to conduct this research through the Samuel Lucian Memorial Scholarship. I am also grateful for the I-CORPs for providing me funding to travel for conferences to present my findings and to gain more experience by talking to peers.

I also am thankful for the help provided by numerous undergraduate and high school students, especially Mateusz Rowicki and Conan Cullen. I want to thank Mrs. Heidi Young, Mr. Steven George, Mr. Nasser Channaoui, and Mr. Andrew Flory for their help and support providing me necessary access to laboratories and purchasing necessary materials and machinery to progress research. I would like to thank all my friends for their support while carrying out my studies and all the others who helped me in many ways.

Finally, I would like to thank my father, Mr. Daniel Martin and my mother, Ms. Hannelore Schultz for their loving support and my wife, Abigail Martin for her encouragement, friendship, and care during my last years of work.

TABLE OF CONTENTS

TABLE OF CONTENTS
(Continued)

TABLE OF CONTENTS
(Continued)

TABLE OF CONTENTS
(Continued)

LIST OF TABLES

LIST OF FIGURES

LIST OF FIGURES
(Continued)

LIST OF FIGURES
(Continued)

LIST OF SYMBOLS

β	*Theoretically developed electro-osmotic conductivity*
γ_w	*Unit weight of water*
δ	*Distance from particle surface to slip surface*
δ_1	*Thickness of the diffusion boundary layer of the desalting side*
δ_m	*Thickness of the diffusion boundary layer of the membrane*
ϵ	*Pore fluid permittivity*
ϵ'	*Apparent dielectric constant*
ϵ_0	*Permittivity of free space*
ϵ_r	*Relative permittivity of the pore fluid*
ζ	*Zeta potential*
κ	*Debye-Hückel parameter*
λ	*Debye length*
μ	*Pore fluid viscosity*
ρ	*Local charge density*
σ	*Soil sample electrical conductivity*
σ_{p}	*Pore fluid electrical conductivity*
ψ	*Electric potential*
ψ_m	*Potential at the midpoint between two parallel, interacting double layers*
ω	*Water content*
A	*Cross sectional area of the soil perpendicular to water flow*
a	*Capillary cross-sectional area*
a_-	*Transport numbers of the anions in the bulk*
a_-^m	*Transport numbers of the anions in the membrane*

LIST OF SYMBOLS

C	*Capacitance*
C_α	*Secondary compression index*
c	*Ion concentration*
c^0	*Ion concentration at equilibrium (in the bulk solution)*
D	*Diffusion coefficients of the anions in the bulk*
D^m	*Diffusion coefficients of the anions in the membrane*
E	*Electric field*
E_e	*Equivalent electric field*
e	*Electron charge*
e_p	*Void ratio at the end of primary consolidation*
F	*Faraday's constant*
F	*Formation Factor*
G_s	*Specific gravity of soil solids*
H	*Soil sample height*
i	*Current density*
i_{lim}	*Limiting current*
k	*Boltzmann constant*
k_e	*Electro-osmotic conductivity*
k_h	*Hydraulic conductivity*
L	*Channel width*
n	*Soil porosity*
P	*Anisotropy coefficient*
p	*Local applied pressure gradient*

LIST OF SYMBOLS

Q	*Anisotropy coefficient*
q	*Flow through clay soil*
q_{h+eo}	*Combined flow caused by electro-osmosis and a hydraulic gradient*
R	*Soil sample electrical resistance*
S_{EO}	*Settlement caused by electro-osmosis*
S_s	*Secondary consolidation*
T	*Temperature*
t	*Time*
t_1	*Time at the start of secondary consolidation*
t_2	*Time at the end of secondary consolidation period*
V_c	*Voltage on a connected capacitor*
V_o	*Initial voltage on a capacitor*
v	*Local pore fluid velocity*
w	*Clay particle thickness*
z	*Ion valence*

CHAPTER 1

INTRODUCTION

1.1 Problem Statement

When subjected to loading, clay soils will consolidate and will undergo significant settlement which can have detrimental effects on structures and pavements. Due to the low hydraulic conductivity of clay, primary consolidation takes longer time to achieve, delaying construction. Nowadays, the method most commonly used to expedite clay soil consolidation is the installation of geo-drains or wick-drains followed by preloading. Preloading is a technique by which substantial consolidation of soil can be achieved before application of actual construction loads. However, the preloading technique alone may not be satisfactory in reduction of time of consolidation to desired extent (Bhattacharya and Basack, 2011). The consolidation period can be further expedited by electro-osmotic consolidation (Bergado et al., 2000).

Electro-osmosis is an established method of improving soft, saturated clayey soils where a direct current (DC) is applied to the soil by electrodes. Due to the application of an electric field, hydrated ions in the solution are attracted to the electrodes. Because the clay particles have a net negative surface charge, the majority of ions in the interstitial fluid are positively charged. Therefore, the net flow will be towards the negatively charged electrode (cathode). If drainage is provided at the cathode, consolidation of the soil occurs, resulting in higher shear strength and lower compressibility of soils. This can be easily shown by preconsolidating a soil sample to field conditions and then applying an electric field. In a small scale lab test, a 11.4 cm high cylinder of soil of 6.4 cm in

diameter was first consolidated to 74.3 kPa to simulate field conditions under 10 feet of soil in multiple loading steps. After the samples reaches full consolidation, an electric field was applied to further drain the sample. The resulting settlement is shown in **Figure 1.1**. Regardless of pressure, when electro-osmosis was applied, a constant decrease in void ratio was observed.

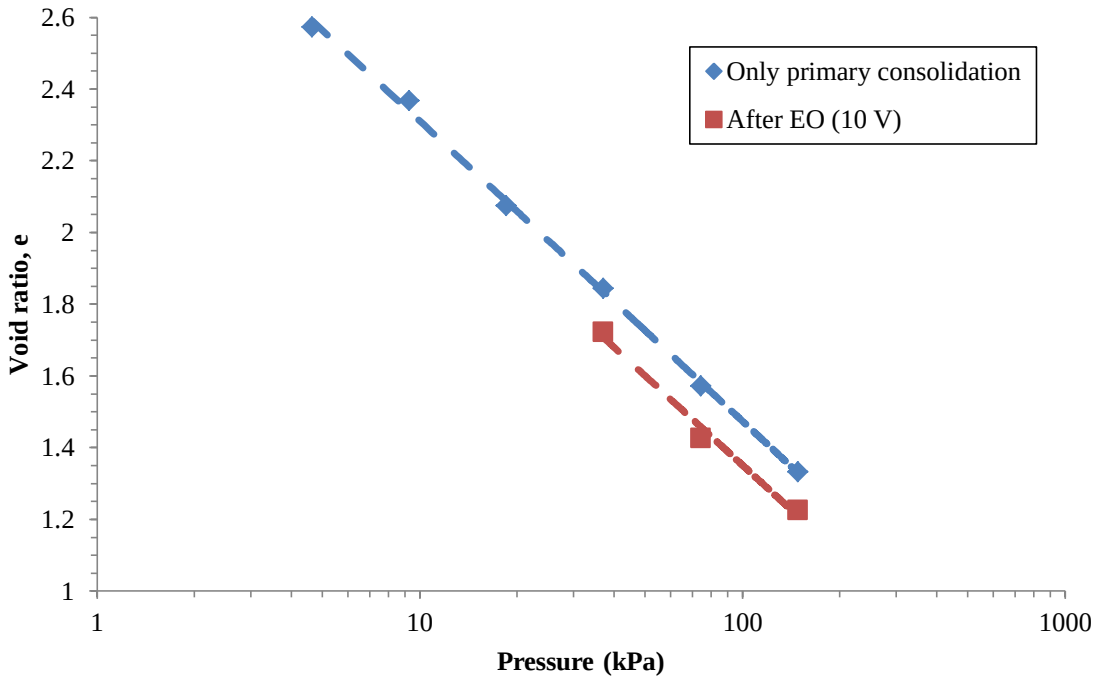

Figure 1.1 Settlement caused by electro-osmosis after full normal consolidation.
Source: Martin and Meegoda, 2019d.

Electro-osmosis was first reported by Reuss (1809). He showed that water could be made to flow through a plug of clay by applying an electric voltage. Several researchers studied different aspects of electro-osmosis (Helmholtz 1879; Perrin 1904; Smoluchowski 1921; Casagrande 1948; Veder 1981; Pamukcu et al. 1997; Shang 1998). Electro-osmosis has been studied for almost 100 years and is still not widely used in field consolidation applications. It has been extensively tested and has proven to have clear

benefits to consolidation of cohesive soils. Unfortunately, certain problems have prevented the widespread use of electro-osmotic consolidation especially in developed nations.

1.2 Theory of Electro-Osmotic Consolidation

1.2.1 Diffuse Double Layer

The Stern–Gouy double layer theory is one of the most important concepts for understanding the behavior of clayey soils. The negative surface charge of the clay particles creates a double layer of ion concentrations in the area surrounding the particles (see **Figure 1.2**). The layer closest to the clay surface is called the Stern layer and consists of a thin layer of tightly packed positive ions. These ions are strongly attracted to the negative surface charge of the clay particle and will not move under normal circumstances. The electric field created by the negative surface charge of clays still affects the area beyond the Stern layer. Beyond the Stern layer there is a second layer of mostly positive ions at high concentrations that are still attracted to the negative surface charge of the clays but are not strongly attached. Some negative charges can also be found here. This is the main layer contributing to the electro-osmotic flow. This second layer is called the diffused layer. Beyond the diffused layer the positive and negative ions in the interstitial fluid are more evenly distributed. Because the ions in the Stern layer are so tightly adsorbed by the clay particles, electro-osmotic flow actually starts at a small distance from the clay surface called the slip plane. Therefore, the actual potential at the slip plane is a little lower than the surface potential of the clay particles. This potential is

denoted as the zeta potential. Zeta potentials will differ for different soils but are usually in the range of -50 mV to -150 mV (Shang 1997).

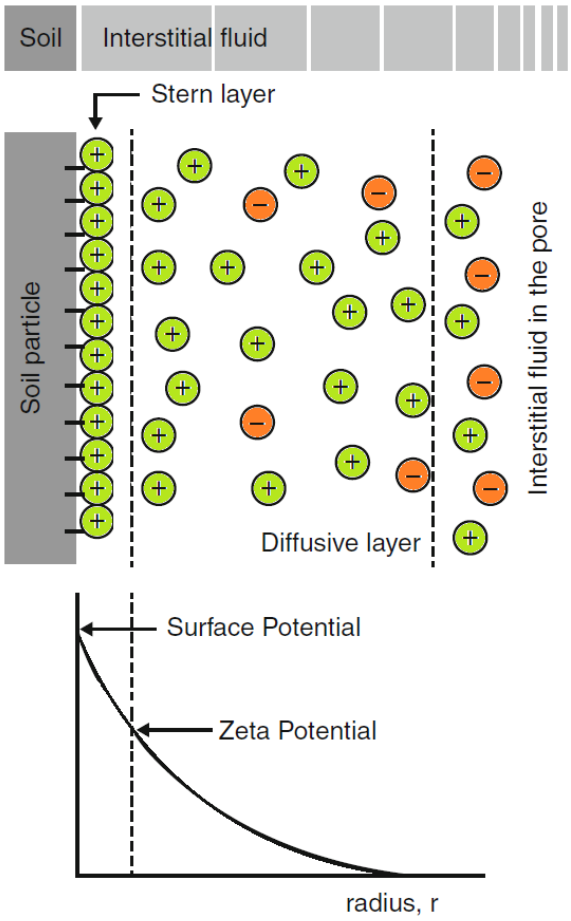

Figure 1.2 Schematic of Stern–Gouy double-layer model.
Source: Cameselle 2014.

1.2.2 Casagrande's Flow Equation

Multiple numerical models have been created to explain the electro-osmotic consolidation and its geochemical effects on the soil. The most widely used electro-osmotic flow equation for the soil system was proposed by Casagrande (1949) and is shown below

$$q = k_e EA \tag{1.1}$$

This simple model is based on Darcy's law and relates the flow caused by electro-osmotic treatment to the basic properties of the soil. It is widely used as a basis for more comprehensive models. This can then be combined with the flow due to hydrostatic pressure to yield (Mitchel and Soga, 2005):

$$q_{h+eo} = -\frac{k_h}{\gamma_w}\frac{\partial u}{\partial x} - k_e\frac{\partial V}{\partial x} \tag{1.2}$$

If water is not recirculated at the cathode, the electric field will cause negative pore water pressures at the anode that can be expressed as (Esrig 1968):

$$u_e(x) = -\frac{k_e \gamma_w}{k_h} Ex \tag{1.3}$$

Where x is the distance from the cathode to the anode and k_e is the electro-osmotic conductivity defined by Casagrande (1949). The development of the negative pore water pressure in this equation increases the effective stress in the soil, leading to consolidation during electro-osmosis. The amount of consolidation will generally be equal to the amount of water drained.

According to this equation the effectiveness of electro-osmotic consolidation is controlled by the ratio of k_e/k_h. The typical hydraulic conductivity of soils reported in electro-osmosis literature is in the range of 1×10^{-10} to 1×10^{-9} m/sec, whereas the

coefficient of electro-osmotic conductivity is in the range 1×10^{-9} to 1×10^{-8} m^2/sec/V. Hence the electro-osmotic consolidation will be significant when the ratio of k_e/k_h is higher than 0.1 (Mohamedelhassan and Shang, 2001). Due to discharge of water at the cathode, a hydraulic gradient is developed between the two electrodes. Consolidation of the soil will continue until the system reaches equilibrium where the electro-osmotic force driving water to the cathode is equal to reverse flow due to the hydraulic gradient (Mitchell and Soga, 2005) or, if the system is well drained, it will continue until electric resistance in the soil increases and prevents significant flow of current. This is most commonly the case.

1.2.3 Helmholtz-Smoluchowski Theory

One of the most the most widely used theories to model electro-osmotic flow is the Helmholtz-Smoluchowski model. This theory treats a liquid filled capillary, shown in **Figure 1.3**, as an electrical condenser with charges of one sign near the surface of the walls and opposite charges concentrated in a layer of fluid at a small distance from the walls. The latter charges cause the fluid to move as a plug flow (Mitchel and Soga, 2005). The velocity distribution is similar to that of hydraulic fluid flow through a pipe, having higher velocities at the center and decreasing as they approach the walls.

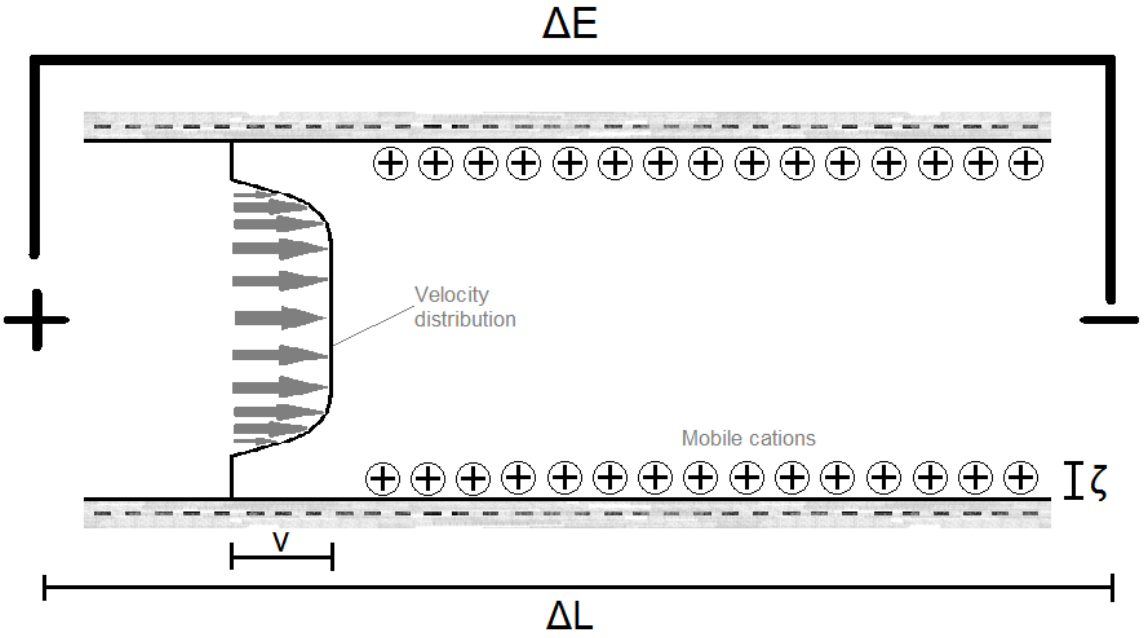

Figure 1.3 Electro-osmotic flow in the Helmholtz-Smoluchowski model.

The rate of water flow is dependent on the balance between the electrical force causing the flow and the friction between the liquid and the wall. For a single capillary tube, the flow rate can be expressed as:

$$q_a = va = \frac{\zeta \epsilon}{\mu} Ea \tag{1.4}$$

For a group of N capillaries the flow equation becomes:

$$q_A = Nq_a = va = \frac{\zeta \epsilon}{\mu} ENa \tag{1.5}$$

If the porosity is n, then the cross-sectional area of voids is nA, which must be equal to Na. Thus:

$$q_A = Nq_a = va = \frac{\zeta\epsilon}{\mu} EnA \tag{1.6}$$

If we compare this to Darcy's law, we can rewrite the equation as:

$$q_A = k_e EA \tag{1.7}$$

This will yield that the coefficient of electro-osmotic hydraulic conductivity as:

$$k_e = \frac{\zeta\epsilon}{\mu} n \tag{1.8}$$

The relationship between porosity and k_e was studied by Mohamedelhassan (1998). The results of that study for a marine sediment are shown in **Figure 1.4**.

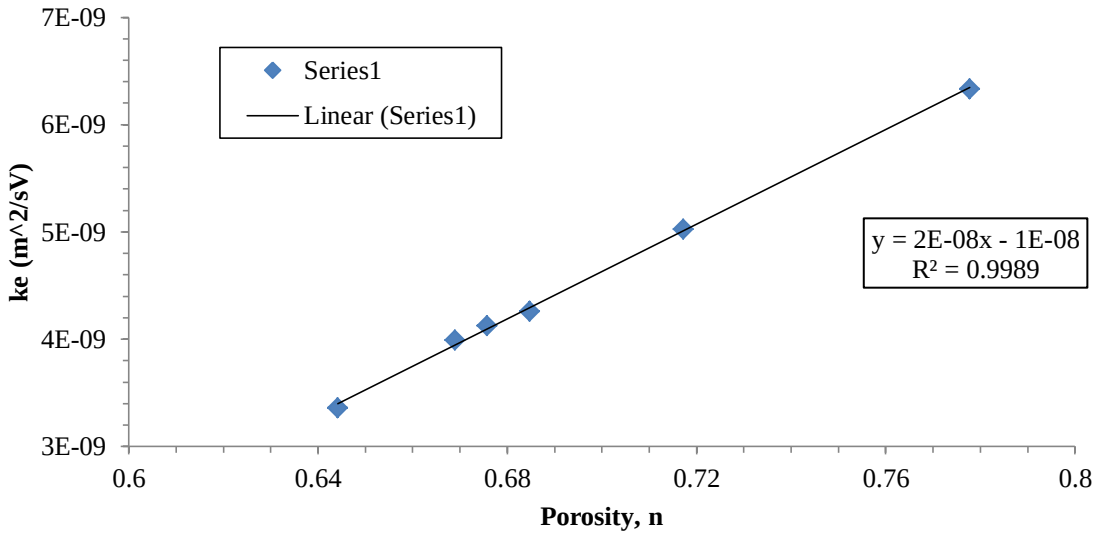

Figure 1.4 Electro-osmotic conductivity, k_e, with porosity, n.
Source: Mohamedelhassan 1998.

According to the Helmholtz-Smoluchowski model, k_e should be relatively independent of pore size. Because of this, electro-osmosis can be more effective in moving water through fine grained soils than flow caused by a hydraulic gradient (Mitchel and Soga, 2005). Values of k_e for various soils are shown in **Table 1.1**:

Table 1.1 Electro-Osmotic Conductivity Values for Various Clays

Soil Type	$\boldsymbol{k_e}$ 10^{-5} *(cm^2/sV)
London clay	5.8
Boston blue clay	5.1
Kaolin	5.7
Clay silt	5
Na-montmorillonite	2.0 to 12
Peat	0.491 to 1.57

Source: Asadi et al., 2013.

According to double layer theory, the slip plane in the clay-water electrolyte system is located a small distance away from the clay surface. The zeta potential refers to the electric potential due to the surface charge of the clay particle at the slip plane. According to this model the capacity of electro-osmosis to transport water is directly proportional to the zeta potential of the soil, which is closely related to the resistance of the soil. Also, the according to the Helmholtz-Smoluchowski theory k_e is independent of pore size while the hydraulic conductivity is. This means that electro-osmosis is more efficient in moving water through fine-grained soils than flow driven by a hydraulic gradient.

1.3 Ion Hydration

While in an aqueous solution, free ions are surrounded by a hydration shell of regularly arranged water molecules that are attracted to it. Since the water molecules are dipoles, they hydrate both positive and negative ions. This causes dissolution of ionic compounds in water. For example, for NaCl in water, the attraction between Na+ and H2O, and the attraction between Cl- and H2O is greater than between Na+ and Cl-. They separate and hydrate as conceptually shown in **Figure 1.5**.

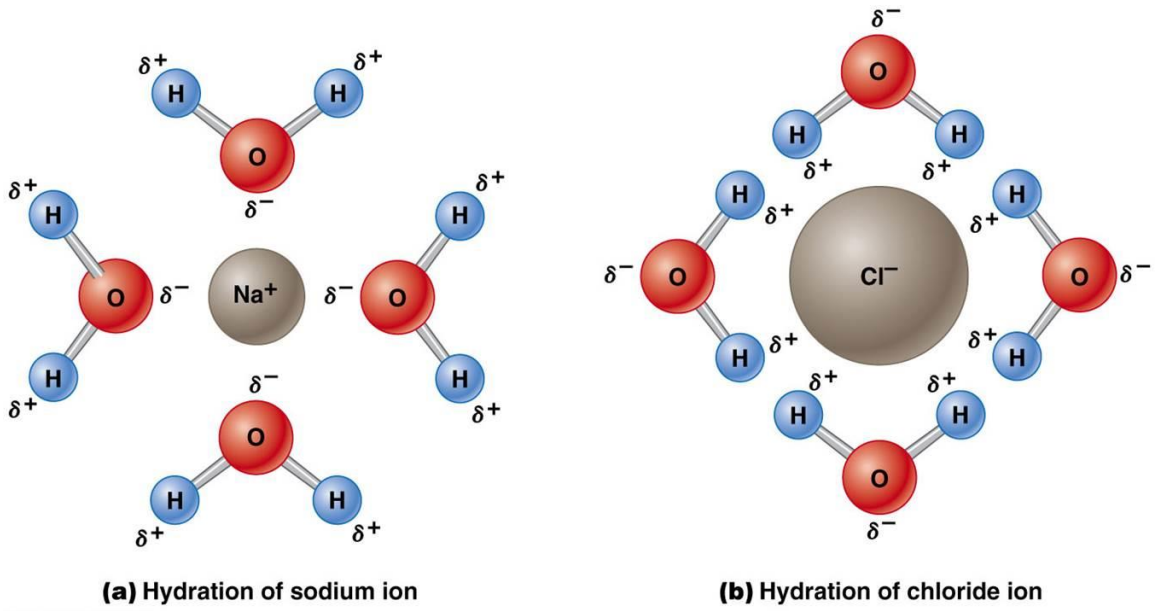

Figure 1.5 Hydration scheme for (a) sodium ions and (b) chloride ions.
Source: Hardin et al., 2010.

Hydrated ions can have multiple rings of regularly arranged water molecules. The size of the hydrated ion-water combination will depend on the ions charge and its radius without hydration. **Figure 1.6** shows hydration radii for different ions.

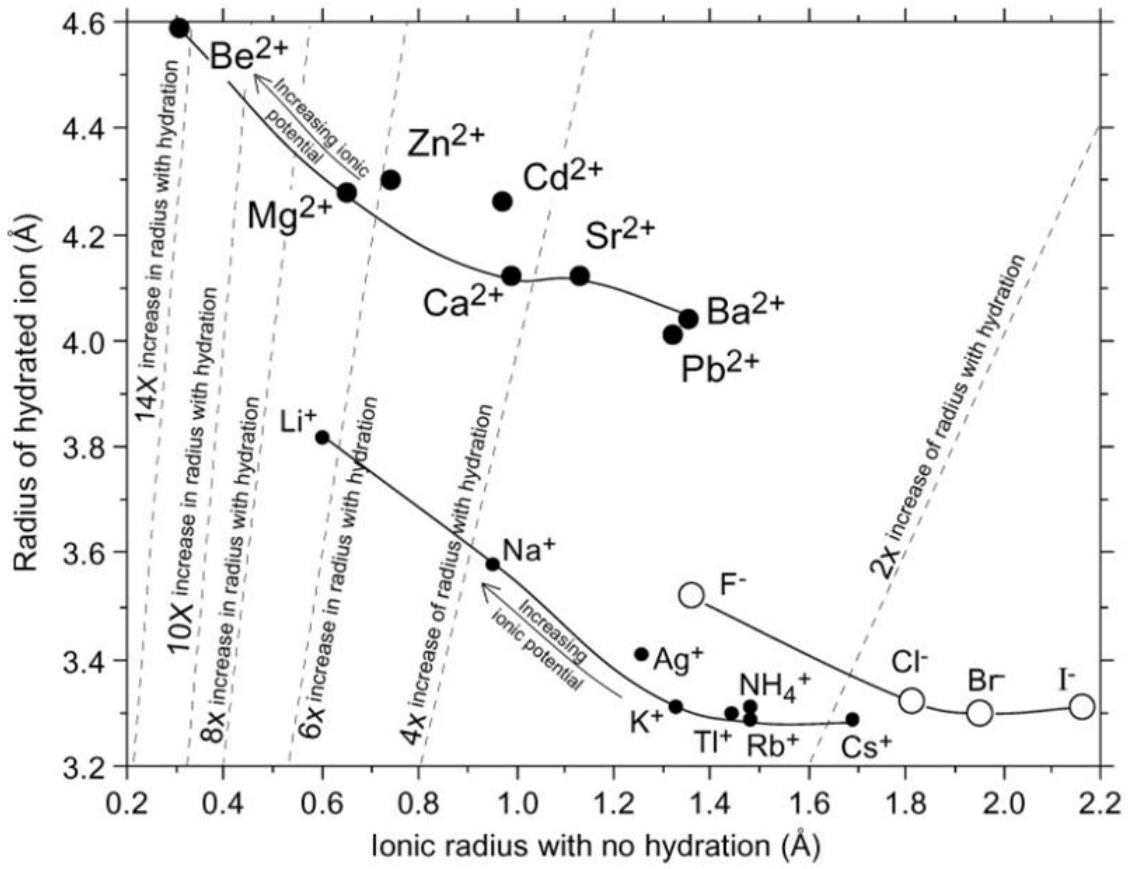

Figure 1.6 Hydration ion radii.
Source: Conway 1981.

During electro-osmosis, hydrated ions will be moved towards their oppositely charged electrodes due to the electric field. Electro-osmotic flow will occur when the drag force of cations or anions is greater than that of the other. The greater the difference, the greater flow there will be. Since clay is negatively charged and most of free ions are positive the net flow will be towards the cathode.

A higher hydration radius means the amount of water removed for a given ion is higher. For example, a hydrated Ca^{2+} ion should move more water than a hydrated Na^{+} ion, since it has a higher hydration radius, according to **Figure 1.6**. If this is true, then applying an electric potential to soil mixed with Ca^{2+} should discharge more water than

soil mixed with Na^+. This was tested on two small clay samples mixed with water containing NaCl and $CaCl_2$. The chemicals were added to deionized water until it achieved conductivity three times that of tap water. This was then mixed with soil and preconsolidated to match pressures found in the field at a depth of 10 feet. After this, an electric potential was applied for 120 hours and the water removed was measured. The results are summarized below in **Table 1.2**.

Table 1.2 Hydration Radius Effect on Water Removal Test Results

Solution	**Liquid Discharged** mL	**Conductivity of Liquid** mS/m
NaCl	4.83	189
$CaCl_2$	7.96	170

The soil treated with $CaCl_2$ drained almost twice as much water as that treated with NaCl. This shows that the type of ions in solution have a significant effect on electro-osmotic consolidation. Ion hydration is essential to water removal with electro-osmosis. The results also prove that electro-osmosis can be enhanced by treating soil with different chemical solutions. This has been investigated extensively by others (Ozkan et al. 1999, Lefebvre and Burnotte 2002, Alshawabkeh and Sheahan 2003, Mohamedelhassan and Shang 2003, Burnotte et al. 2004, Paczkowska 2005, Otsuki et al. 2007, Chien et al. 2009, Ou et al. 2009, Chang et al. 2010, Chien et al. 2011).

1.4 Negative Effects of Electro-Osmotic Consolidation

1.4.1 Introduction

The efficiency of electro-osmotic consolidation is typically measured as the amount of water removed for the power consumed. If the volume is high, then the process is more efficient and economical. This value may vary over several orders of magnitude and is dependent on multiple factors including water content, soil type, electrolyte concentration, electrolyte type, and pH. In addition to the movement of water molecules, the application of an electric field generates electrochemical and physical reactions that negatively affect the performance of the electro-osmotic consolidation, namely:

1. Crack development due to negative pore pressures and resulting extensive drying at the anode;
2. Increasing temperatures due to electric resistance
3. Corrosion of the electrodes;
4. Bubble formation at the electrodes due to electrolysis of water that reduce soil-electrode contact; and,
5. Extreme pH changes at both electrodes

1.4.2 Crack Development

Crack formation is a result of extensive drying of the soils around the anode. These cracks reduce the contact area between the soil and the electrode material, effectively increasing electric resistance. When water migrates away from the anode, the clayey soil around it shrinks, creating tensile forces that cause cracking. This is especially problematic in expansive clays. The size and quantity of cracks depends on the type of clay but all will exhibit some measure of cracking due to their cohesive properties. Additionally, crack formation is enhanced by heating of the soil due to current flow

(Burnotte et al. 2004). Crack formation can start very early in the processes, greatly hindering electro-osmotic treatment. Since the size and shape of the cracks are unpredictable and mostly unquantifiable during treatment, they can invalidate any experimental lab data. As suggested by Wu et al. (2015) and others, crack formation can be mitigated by applying electro-osmosis with preloading. The surcharge load compresses the soil as the water is drained which prevents tensile forces from creating cracks. This also provides a more accurate understating of the consolidation caused by the treatment. All tests presented here will include some form of preloading to prevent cracking.

1.4.3 Temperature

Temperature in the vicinity of the anode increases due to resistive heating associated with the application of electric power. This, in turn, will cause drying of the soil around the electrode, further increasing resistance, eventually inhibiting the electro-osmotic treatment. In a field study done on soft clay at Mont St-Hilaire, Canada, Burnotte et al. (2004) reported that the rise in temperature at the anodes and in the soil emerged as an important controlling factor. When temperatures at the anode reached values close to 100 °C, the resistivity of the system increased rapidly, resulting in a smaller effective voltage gradient in the soil and less efficient electro-osmotic consolidation. High temperatures in the soil are tentatively suggested as an explanation for the higher efficiency in the field as compared with that in the laboratory, especially for the high resistances measured near the anodes.

Rittirong et al. (2008) performed lab tests on calcareous soil to evaluate current and temperature with the use of polarity reversals. The results showed that there was a

definite relation between the temperature and the current. Initially, as the current rises, so does the temperature. Then, presumably due to drying and pH changes, increasing resistance caused the current drops. This drop is followed by a lagging temperature. Shang et al. (1996) also observed desiccation of the soil with the formation of a layer of very stiff crust at the interface between the soil and the electrodes which reduced the transferred voltage at the soil-electrode contact. Desiccation of the soil was also reported by Abiera et al. (1999) and Bergado et al. (2000) which were attributed to the generation of heat from the application of current; the heating and drying resulted in the hardening of the soil. Similar results were reported by Gray (1970), Gray and Somogyi (1977), Acar and Alshawabkeh (1996), Rutigliano et al. (2008), Ou et al. (2009), and Abou-Shady and Peng (2012). From the literature it seems heating of the soil around the anode specially is an unavoidable consequence of increasing resistance. While not the major factor governing the efficiency of electro-osmotic consolidation, it does contribute to the premature termination of the process. However, this could be mitigated or at least delayed by controlling the flow of electrical current.

1.4.4 Corrosion

Another possible electrochemical reaction is the oxidation and reduction of the electrodes. At the anode we have,

$$M \rightarrow M^{c+} + ce^{-} \tag{1.9}$$

And at the cathode,

$$M^{c+} + ce^{-} \rightarrow M \quad (1.10)$$

Where M^{n+} represents any kind of cationic species that can be reduced. These electrode reactions would be affected not only by the materials of the electrode but also the ions in the electrolyte. The oxidation of the metallic type anodes such as copper can cause corrosion and reduce the efficiency of electro-osmotic consolidation. According to Iwata et al. 2013, their short service life has impeded the widespread application of electro-osmotic dewatering. In addition, eluted metal ions, particularly those of chromium, might cause a secondary pollution issue (Mahmoud et al. 2010). Additionally, the presence of metal ions and high pH values near the cathode may result in insoluble metal hydroxides that precipitate and stick to the cathode surface, blocking the filter media (Iwata et al. 2013);

$$M^{c+} + cOH^{-} \rightarrow M(OH)_c \quad (1.11)$$

The corrosion of the electrodes also releases ions into the soil. These ions, as explained earlier, can hydrate and carry water molecules to the cathode. This effect is too small to be beneficial and consumes the electrodes, which is not economical. Also, because it is adding external ions to the process. the results of lab tests might be skewed and less accurate. To avoid this, graphite was used in all tests performed in this research.

1.4.5 Bubble Formation

The application of an electric current through water will cause electrolysis of water molecules. Water molecules dissociate and form oxygen gas and hydrogen ions at the

anode and hydrogen gas and hydroxide ions at the cathode, as shown in equations 1.12 and 1.13. At the anode:

$$2H_2O \rightarrow O_2(g) + 4H^+ + 4e^-, E_o = 1.23\ V \quad (1.12)$$

At the cathode:

$$2H_2O + 2e^- \rightarrow H_2(g) + 2(OH)^-, E_o = -0.83\ V \quad (1.13)$$

A qualitative illustration of the basic hydrolytic processes and movement of water during electro-osmosis is presented in **Figure 1.7**.

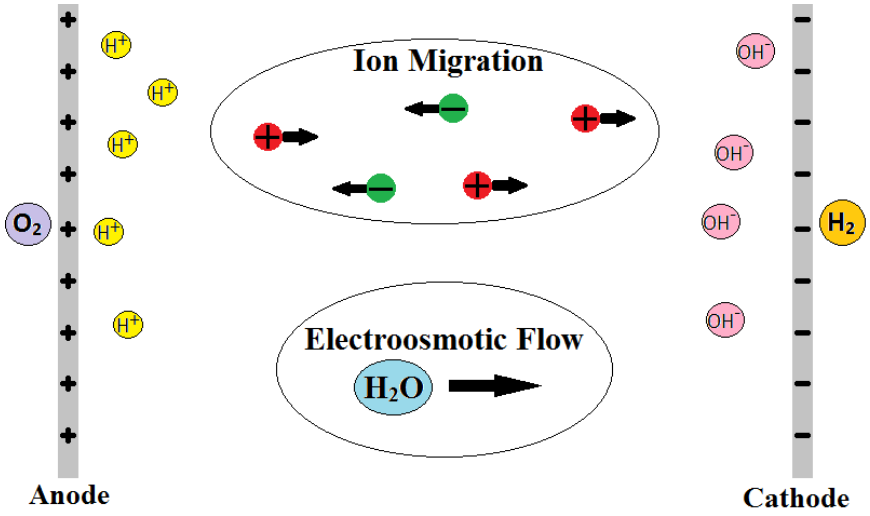

Figure 1.7 Schematic of the EO process in soil.

The energy released drives the current flow through the soil. Hydrolysis of water is especially prevalent when using uncorrodable electrode materials, since there are no

dissociating metals to release an absorb electrons. The accumulation of gas decreases contact area at the electrode-soil interface and therefore increases the electrical resistance (Mahmoud et al. 2010). This can be easily mitigated by providing a perforated cylindrical electrode and adding a slight vacuum.

1.4.6 pH Changes at the Electrodes

As the electrolysis of the water molecules proceeds, hydroxide ions are produced at the cathode and hydrogen ions are produced at the anode. This results in a pH gradient across the soil (Lockhart 1983, Yoshida 2000, Yuan and Weng 2003). Pazos et al. (2006) reports the change in pH at the anode and cathode through a few days of testing. The result is shown in **Figure 1.8**.

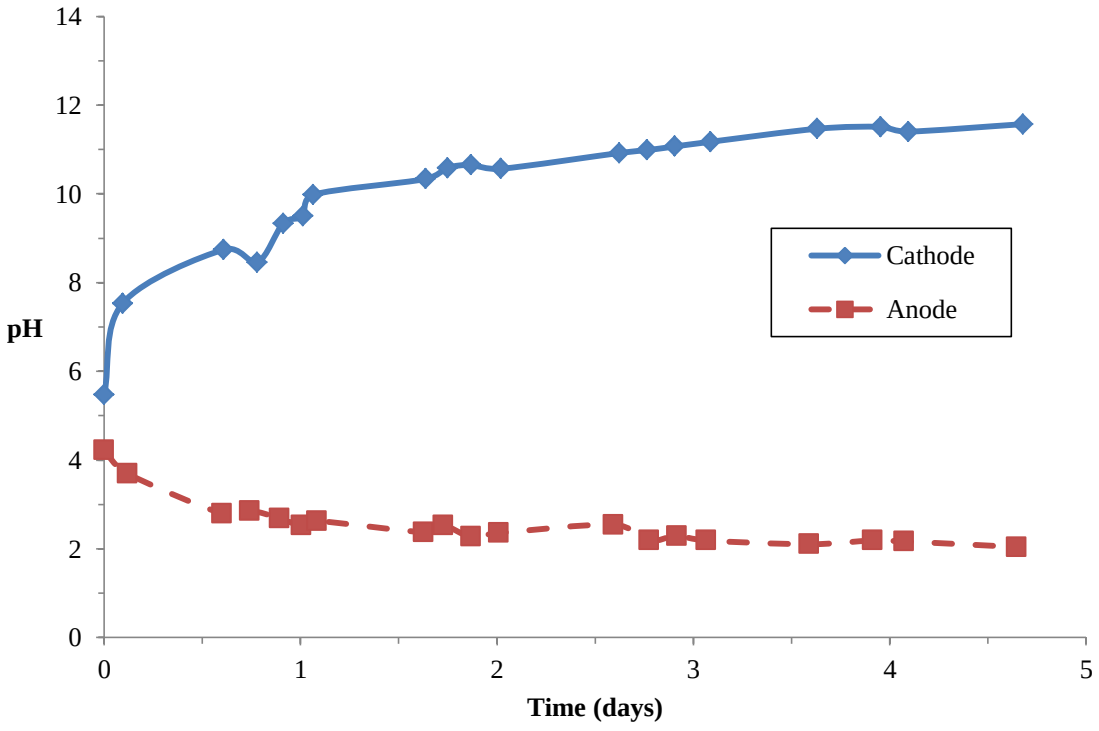

Figure 1.8 pH change at the electrodes during electro-osmosis.
Source: Pazas et al. 2006.

An acidic front produced at the anode migrates towards the cathode and a basic front produced at the cathode migrates towards the anode. The rate of electromigration could be affected by ionic mobility, and, since hydrogen ions are smaller and have 1.76 times the ionic mobility of hydroxyl ions, the acidic front generally moves faster through the soil (Alshawabkeh and Bricka, 2000). Therefore, the pH drop dominates the chemistry across the soil except for a region close to the cathode.

The basic mineral structure of clays is composed of tetrahedral sheets of silicon and oxygen and octahedral sheets of aluminum or magnesium and oxygen. The arrangement of these is shown on **Figure 1.9**.

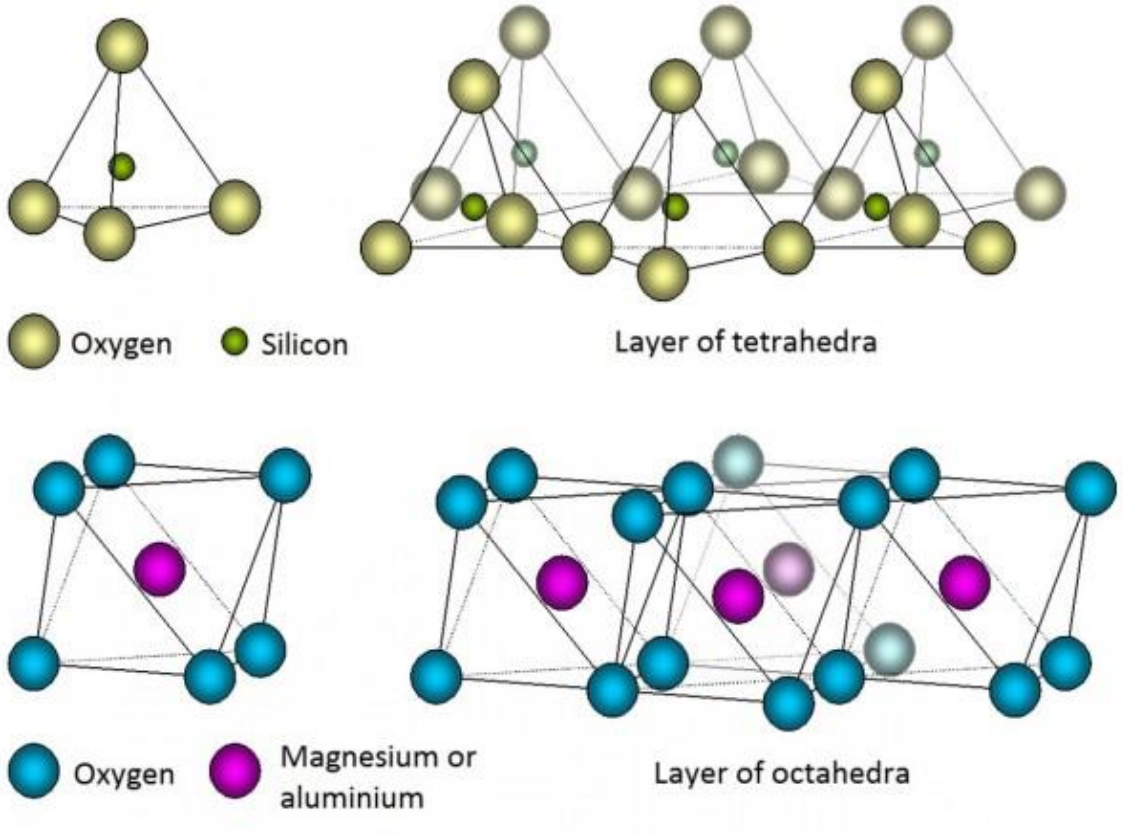

Figure 1.9 Basic clay mineral structure.
Source: Jordan 2014.

Hydroxyls are exposed on the surfaces of clay particles, giving the particles their negative surface charge. These hydroxyls have a tendency to dissociate in water,

$$(Al\ or\ Si)O^- + H^+ \leftrightarrow (Al\ or\ Si)OH \tag{1.14}$$

This is strongly influenced by pH. The higher the pH, the greater the tendency to dissociate, and vice-versa. This means that when the pH decreases due to electro-osmosis, the surface charge of clay particles becomes less negative. Additionally, alumina is an amphoteric substance, meaning it can react with both acids and bases. When the pH is low, these will ionize positive and again reduce the negative surface charge of clay particles (Mitchel and Soga 2005). When the pH in the pore fluid decreases, the exposed negative charges on the clay surface are neutralized by the H^+ ions. This causes the clay surface to have a less negative surface charge. As a result, the surface potential, and thus the zeta potential, of the clay particle are reduced. There are some exceptions to this, such as bentonite clay, that naturally buffer low pH. Since the electro-osmotic flow is directly related to the zeta potential, the electro-osmotic conductivity also decreases. The lower the pH goes, and the longer it is maintained, the less electro-osmotic flow will occur (Rabie et al. 1994, Tuan et al. 2008). Vane and Zang (1997) measured the zeta potential for clay samples under different pH levels. The results are shown below in **Figure 1.10**.

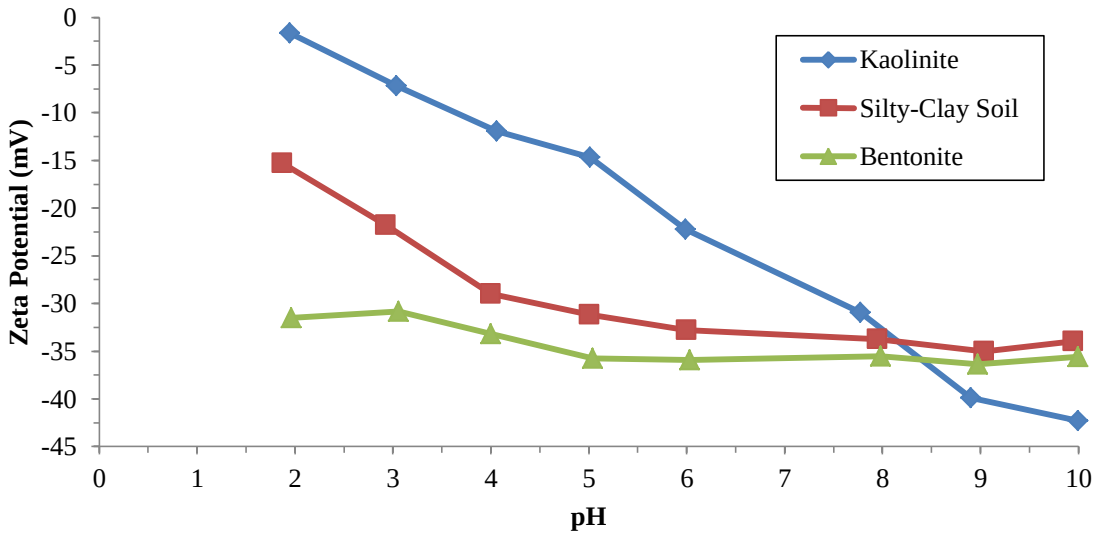

Figure 1.10 Zeta potential values for different pH levels.
Source: Vane and Zang 1997.

The drastic change in zeta potential greatly hinders electro-osmotic consolidation. Since the electro-osmotic conductivity is directly related to the zeta potential, the changes in pH alone have the potential to completely stifle the process. As shown in **Figure 1.10**, with low pH values the zeta potential can become very small, leading to small electro-osmotic consolidation based on Equation 1.8. On the cathode side, the hydroxide ions can combine with metallic ions in the soil and precipitate, clogging the pores. Eventually the electro-osmotic process stops, significantly reducing the cost efficiency of electro-osmosis. This has been one of the major setbacks for research on electro-osmotic remediation of soils contaminated with heavy metals. For reactive electrodes, such as copper and iron, oxidation and reduction of the electrodes also take place (Wu et al. 2015). Yoshida (2000) and Burnotte et al. (2004) showed in laboratory and field investigations that with continuous application of direct current, the electrical contact resistance between the electrodes (mainly the anode) and the soil is considerably

increased, leaving an effective voltage gradient in the soil too small for significant electro-osmotic consolidation. According to Iwata et al. (2013), this has impeded the widespread application of electro-osmotic dewatering. Because of the major obstacle presented by the changes in pH around the electrodes, improvements in this area can greatly increase the efficiency of electro-osmotic consolidation, enough to make it a viable technique for construction site preparation.

1.5 Conclusions

Due to the ability for rapid consolidation of soils using this technique, electro-osmosis has generated much interest in geotechnical engineering, as evidenced by the numerous laboratory studies that have been published. However, widespread use of this consolidation method is not seen in developed nations due its low electrical efficiency. Hence this research attempts to understand electro-osmotic consolidation using a theoretical analysis and then improve it using ion exchange membranes.

CHAPTER 2

PREVIOUS METHODS OF IMPROVING ELECTRO-OSMOTIC CONSOLIDATION

2.1 Introduction

Different variations of electro-osmosis application have been studied over the years to improve its consolidation results. Among then, the most popular ones are polarity reversal, intermittent current, injection of saline solutions, and the use of geosynthetics. All have shown clear improvements over conventional electro-osmosis. These are described below. The contents of this chapter have been published in Martin et al. 2019.

2.2 Polarity Reversal

Unidirectional direct current (DC) electric field has been commonly used for electro-osmotic dewatering. Theoretically, periodic reversals in direction of the electric current, and so electro-osmotic flow, eliminates the zeta-potential gradient and restores the high value of zeta-potential near the anode, thus the electro-osmotic process is restored. **Figure 2.1** shows a test performed by Rittirong et al. (2008) where current decay appears to be delayed through the use of polarity reversal. This study, however, did not look at the relationship between the cycles. A trend line has been added for this purpose and is discussed later on this chapter.

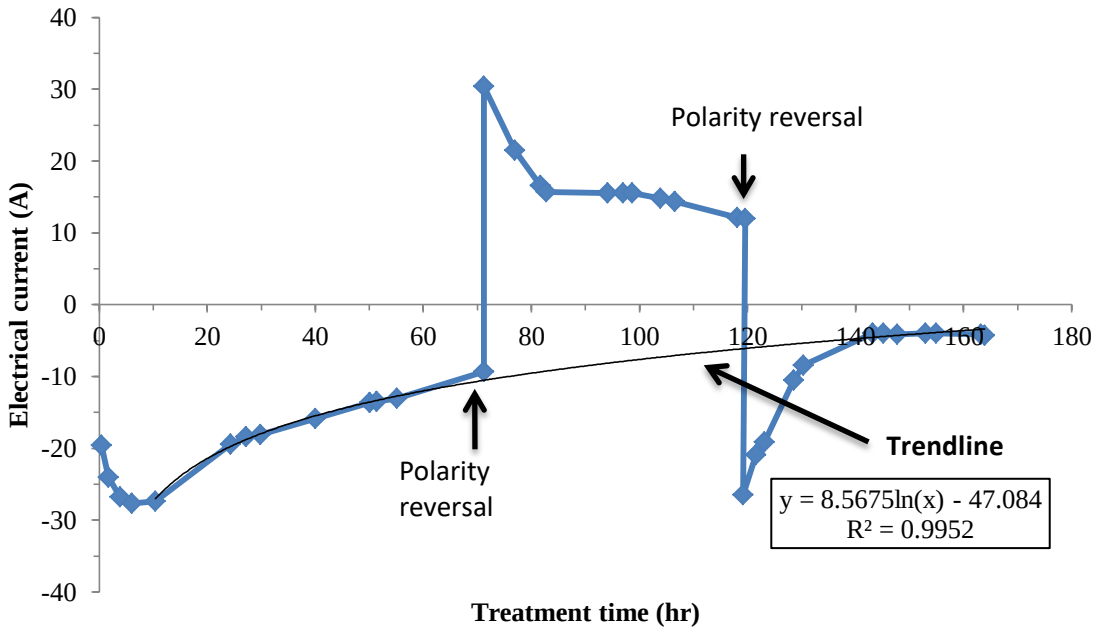

Figure 2.1 Current improvement through polarity reversal.
Source: Rittirong et al., 2008.

Gray and Somogyi (1977) performed a series of electro-osmotic tests on red mud with high water contents using electrode polarity reversals every 30 minutes. The test results showed that the temperature rise at the anode was not as high and the voltages were considerably lower in the polarity reversal modes compared with the conventional unidirectional mode (DC). Polarity reversal caused a more uniform increase in shear strength and decrease in water content compared to the asymmetrical effect of DC. It also significantly reduced the expansion of pH gradient and non-uniform electrochemical changes in the treated samples.

Yoshida et al. (1999) studied the effect of polarity reversals to reduce the electrical contact resistance during the electro-osmotic dewatering experiments. The experiments on white clay samples were performed using alternated current (AC) in the region of very low frequency (0.01 and 0.001 Hz) with constant voltage (20 and 40 V).

Both rectangular and sine waves were used. The test results showed higher final dewatered volume under polarity reversals than that under DC application. This indicates that the polarity reversal method reduced the excessive increase of the electrical contact resistance because the water moved periodically in both directions. Yoshida et al, 1999 also showed that DC removed more water than polarity reversal for the same amount of power used. However, current flow lasted longer with polarity reversal, increasing total volume of water removed past that of DC. With the use of polarity reversal the changes of pH and water content distributions within the treated samples were reduced and therefore, the dewatering could proceed more effectively. The best dewatering results were achieved by the lowest reversal frequency tested, 0.001Hz, while frequencies higher than 0.01Hz had worse results than DC. The higher frequencies, 1Hz and 50Hz, had the same dewatering as that of 0.01Hz.

Despite the reported favorable effects, some researchers pointed that the polarity reversal technique could not improve the effectiveness of electro-osmosis in terms of discharged water and undrained shear strength (Bjerrum et al. 1967, Ou et al. 2009, Chien et al. 2011, Kaniraj et al. 2011). This might be due to drying and acidic conditions near the anode being generated before the polarity is reversed. This indicates that if the interval is too long, adverse conditions will be generated such that polarity reversal has minimal impact on the treatment. If the sediments near the anode are unsaturated before the polarity is reversed, they need to be re-saturated to maintain the electro-osmotic flow in the reverse direction when it becomes a cathode (Kaniraj 2014). Chien et al. (2011) stated that the unfavorable effect of polarity reversal in their laboratory study on Taipei

clay was also due to cementation near the anode before the polarity reversal which did not allow discharge of water when it became a cathode.

2.3 Intermittent Current

Current intermittence is an alternate method of power application for electro-osmosis that has the potential to reduce power consumption and affect electrochemical reactions differently than DC application. The applied voltage gradient is intermittently turned off and then turned on again at regular intervals. For example, direct current is applied for 2 minutes, the power is turned off for 1 minute, then the process is repeated and the clayey soil receives intermittent current.

Rabie et al. (1994) demonstrated that electro-osmotic dewatering of clayey soil with interrupted power provides a 20% improvement in water removal compared to that using continuous DC (see **Figure 2.2**). Their method of power interruption involved periodically disconnecting the power supply and short circuiting the electrodes while the power was off. During the power off period, a residual current flowed through the sediments in an opposite direction to the external power supply (Rabie et al. 1994). This short circuit current reversed the electrochemical reactions which had occurred at both electrodes. This reduced the negative effects of electro-osmosis on the sample and allowed treatment time to be extended. This effect is similar to what occurs during polarity reversal treatment. The experiment also showed that the interval of current intermittence is critical to the efficiency of treatment.

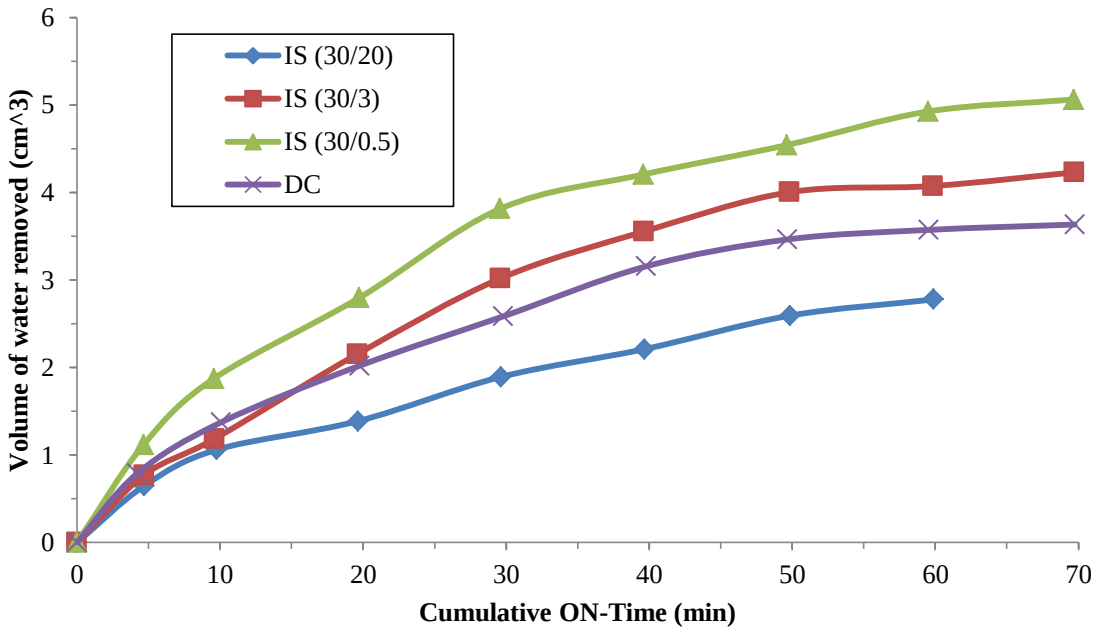

Figure 2.2 Volume of water removed over time for current intermittence at different ON/OFF intervals vs. DC.
Source: Rabie et al., 1994.

Mohamedlhassan and Shang (2001) performed a series of experiments on marine sediment and reported that with current intermittence, higher electro-osmotic flow was generated, compared with using continuous DC. According to the Casagrande (1949) equation of electro-osmotic flow, under the same voltage gradient and cell dimensions, with a high electro-osmotic flow the electro-osmotic conductivity, k_e, of clayey soil has to increase in the course of the intermittence current application. This was shown in the experiment. Thus, the current intermittence technique improved the electro-osmotic conductivity. The enhanced electro-osmotic flow might be attributed to the charge redistribution related to current interruption. Under a DC field, the electrical diffuse double layers surrounding the sediment particles will polarize and the charge orientation resulted from this polarization is against the applied electric field, which reduces the

effectiveness of the electrical field in moving water. The current intermittence allows the double layer to restore its original charge distribution, which increases the efficiency of electro-osmotic process. However, it is also possible that normal DC application decreases the coefficient of electro-osmotic conductivity due to pH changes and other factors. The effect of intermittent current in this case is simply to reduce this drop. According to Casangrande's equation, water depletion in the system will also cause a decrease in the coefficient of electro-osmotic conductivity. By allowing the residual current and hydrostatic head to redistribute water in the sample during OFF times, the intermittent current also reduces the drop in the coefficient of electro-osmotic conductivity.

The optimal current intermittence intervals to maximize the electro-osmotic flow depend on the relaxation time for the double layer to align with the applied electric field. In the current intermittence experiments by Mohamedlhassan and Shang (2001), various on/off intervals (in minutes) of 1/0.5, 2/1, 3/1.5, 4/2, and 5/2.5 were used. The optimum combination was found to be 2 minutes on and 1 minute off, which increased the k_e up to 100% compared with the continuous DC. Mohamedlhassan and Shang (2001) also showed that the open circuit is superior to the short circuit configuration used in the experiments by Rabie et al. (1994). The results are summarized in **Table 2.1**.

Table 2.1 Average k_e for Different Current Intermittence Intervals

Circuit	**ON-time** (min)	**OFF-time** (min)	**Average k_e** (m^2/sV)
Open	1	0.5	9.45E-09
Open	2	1	1.23E-08
Open	3	1.5	1.07E-08
Open	4	2	8.82E-09
Open	5	2.5	8.79E-09
Short	1	0.5	7.71E-09
Short	2	1	7.24E-09
Short	3	1.5	7.21E-09
Short	4	2	7.16E-09
DC	-	-	6.12E-09

Source: Mohamedlhassan and Shang, 2001.

The residual current in the short electric circuit may enhance the capacity of current intermittence to restore the original charge distribution of the double layer, but it also reverses the direction of the electro-osmotic flow. For the open circuit configuration, since the electric circuit between electrodes is open during the power interruption, a residual voltage exists across the sample and will reduce the energy required to recharge the sample when the power is on again. Additionally, intermittence interval is much more effective in enhancing electro-osmosis with an open circuit configuration, while a closed circuit configuration seems to have limited electro-osmosis enhancement. However, Mohamedlhassan and Shang (2001) did not explain why k_e in the short circuit configuration seems to be unaffected by intermittence interval.

Micic et al. (2001) investigated the use of current intermittence in electro-osmosis treatment of high-salinity marine sediment with steel electrodes. The investigation was

exercised with on/off intervals (in minutes) of 10/2, 4/2, and 2/2 and compared with a constant DC. It was found that the test with constant power on was the most effective in terms of increase in the undrained shear strength and decrease in water content. However, this test was the least economical because of the high power consumption and rapid corrosion of the anode. They concluded that the intermittent current method can be useful when treating marine sediment with high salinity (low resistivity) in which the current levels in the system will be high and electrode corrosion and power consumption will be too large if current intermittence is not used. This has also been shown in a large-scale laboratory study in a model tank by Lo et al. (2000). The use of intermittent current is thus shown to provide better treatment over time due to its reduction in power consumption and extension of electrode life.

Yoshida (2000) evaluated the intermittent power application to reduce the excessive increase of the electrical contact resistance with the lapse of time. The intermittent electric field was made by rectifying an AC electric field with very low frequencies (0.01 Hz and 0.001 Hz). Electro-osmotic dewatering of kaolinite was investigated under the same peak-value voltage and effective-value voltage as that under DC and AC electric fields. The results showed that the intermittent electric field which had the same peak-value voltage is capable of removing more water than that from DC field with same power. When applying power to maintain a constant voltage, the rate and the amount of removed water under current intermittence was slightly smaller than under DC, but almost the same as AC, except near the end of dewatering. Based on these findings, Yoshida (2000) concluded that the intermittent electric field considerably reduces the increase of the electrical contact resistance with time during electro-osmosis.

Other research in electro-osmosis also showed that the efficiency of treatment can be significantly improved and corrosion of the electrodes and the power consumption can be reduced if the applied current is periodically interrupted (Sprute and Kelsh 1976, Lo et al. 1991, Shang and Lo 1997). Current intermittence is thus proved a useful alternative to DC application in terms of current efficiency.

2.4 Injection of Saline Solution at the Electrodes

Several recent studies have been focused on the injection of saline solutions into clayey soil during electro-osmosis to increase its effect on dewatering. Using different injection solutions during electro-osmosis, such as NaCl, KCl, $CaCl_2$, aluminum ions, phosphoric ions, methacrylate poly cations, $Al_2(SO_4)_3$, $Mg(CH_3COO)_2$, $MgSO_4$, $Mg(NO_3)_2$, $ZnSO_4$, $AgNO_3$, NaOH, and Na_2CO_3, can enhance the effect of electro-osmosis. This method makes use of the interactions between chemical solutions and clayey soil particles, such as cation exchange and particle cementation, under the influence of an electric field (Ozkan et al. 1999, Lefebvre and Burnotte 2002, Alshawabkeh and Sheahan 2003, Mohamedelhassan and Shang 2003, Burnotte et al. 2004, Paczkowska 2005, Otsuki et al. 2007, Chien et al. 2009, Ou et al. 2009, Chang et al. 2010, Chien et al. 2011). For example, the addition of NaOH solution at the anode has a dual purpose. The OH^- ions will reduce the concentration of the H^+ ions generated at the anode. The Na^+ ions will then aid electro-osmosis by migrating towards the cathode. Saichek and Reddy (2003) showed that using NaOH to buffer the low pH and increase the effects of electro-osmosis is a valid approach. At the cathode electro-osmosis generates OH^- ions that limit the efficiency of the dewatering. Zhou et al. (2005) performed tests using different acidic

solutions introduced at the cathode to buffer the high pH. The most effective was found to be HCl. By introducing a 0.5 M HCl solution at the cathode the efficiency of electro-osmosis greatly increased. Conditioning the pH at the electrodes is thus shown to be a valid method of improving results of electro-osmotic dewatering.

Lefebvre and Burnotte (2002) carried out experiments on clay samples in which the anodes where chemically treated by injection of a saline solution at the beginning of the electro-osmotic treatment. The study showed that the injection of saline solution significantly decreased the power loss and doubled the voltage gradient. The experiment also looked at the effect of treatment on undrained shear strength. For a sample without treatment, the undrained shear strength increased by 158%. On the other hand, for two samples with electro-osmotic treatment with injection of a saline solution it increased by over 200%.

Chien et al. (2009) performed experiments on Taipei clay to study the effects of different electrolytes on water removed and zeta potential. The experiment tested NaCl, KCl, and $CaCl_2$; with different concentrations of $CaCl_2$. After testing for 24 hours at a constant applied voltage of 10 V, the drained water and zeta potential values were measured. The results are summarized in **Table 2.2**. All the above electrolytes had a beneficial effect in terms of water removal with $CaCl_2$ having the best impact. However, due to the cation exchange properties of the clay, the zeta potential of the tests using $CaCl_2$ was reduced to half that of the sodium and potassium tests. This could have adverse effects on long term treatment. Different concentrations of $CaCl_2$ had limited impact on water removal but had a major influence on the zeta potential. The lower concentration resulted in a zeta potential similar to that of the other saline solutions.

Lastly, the treatment time with application of $CaCl_2$ had limited impact on water removal and zeta potential. While a 1 day test yielded 172% increase in water removal compared to regular electro-osmosis, a 7 day trial resulted in only 22.1% increase showing that the benefits of adding saline solutions might only had an impact during the initial stages of treatment. This could be due to the negative effects of $CaCl_2$ on the zeta potential.

Table 2.2 Injections of Saline Solutions to Improve Electro-Osmosis

Test	**Chemical solution**	**Concentration** (N)	**Treatment time** (day)	**Drained water** (mL)	S_u (kPa) **Normalized position** (%)			S_u **due to injection** (kPa) **Normalized position** (%)	k_e ($\times 10^{-10}$ m^2/sV)	**Zeta potential** (mV)
					25	**50**	**75**	**50**		
EO1	Control		1	64.5	22	13	11		2.8	
EO2	Control		7	523.2	52	37	30		3.2	
EOC1	NaCl	0.1	1	127.5	24	11	9	2	5.5	-87.3
EOC2	KCl	0.1	1	152.7	26	12	12	4	6.6	-87.3
EOC3	$CaCl_2$	0.1	1	169.5	30	12	11	8	7.3	-47.3
EOC4	$CaCl_2$	0.01	1	158.2	22	13	11	0	6.8	-78.4
EOC5	$CaCl_2$	1	1	175.3	36	18	16	14	7.5	-17.7
EOC6	$CaCl_2$	1	7	683	70	41	38	18	4.1	-17.7

Source: Chien et al., 2009.

While the concentration of positive ionic species in the system may benefit the process by allowing a higher current, Hu (2008) showed that an excess of these ions will be detrimental to the overall efficiency of the treatment. The higher the concentration of ions, the higher the current through the sample will be. This translates to higher power consumption. However, the increase in removed water volume is minimal. This means that salt concentration is beneficial but will become detrimental if the concentration is too high.

Chien et al. (2011) studied the effect of injection of calcium chloride ($CaCl_2$) and sodium silicate ($Na_2O.nSiO_2$, n=3.4) solutions in a series of electro-osmotic experiments on Taipei silty clay. These chemicals are known to be non-toxic and have been used as grouting materials in sandy sediments. Perforated stainless steel tubes were installed as electrodes for injection of chemicals at the anode and drainage of fluid at the cathode. Different sequences of injection of solutions and application of voltage gradient were used. For the control test, only a voltage gradient of 50 V/m was applied for 7 days and the undrained shear strength was measured to be 39 kPa. In the second experiment, calcium chloride was injected for 1 hour and then the same voltage gradient was applied for 7 days; this increased the undrained shear strength to 49 kPa which indicates the positive effect of the short term injection prior to electro-osmotic treatment. For the third experiment, calcium chloride was injected during the application of the same voltage gradient for 7 days and the undrained shear strength changed to 25 kPa indicating the unfavorable effect of continuous injection during electro-osmotic treatment. In another test, calcium chloride was injected for 2 days followed by injection of sodium silicate for another 2 days and then the same voltage gradient was applied for the next 3 days. Undrained shear strength increased to 59 kPa indicating the positive effect of long term injection of saline solutions before the beginning of the electro-osmotic treatment. Ca^{2+} ions reduce the double layer thickness and allow a more densely packing of the particles, which is beneficial for dewatering purposes. However, as shown by Chien et al. (2009), the use of $CaCl_2$ does have adverse effects on the zeta potential that need to be considered since the electro-osmotic conductivity is proportional to the zeta potential.

2.5 Electrically Conductive Geo-Synthetics (EKG)

Electro-kinetic geo-synthetics (EKG) are new forms of electrodes based on the use of electrically conductive geo-synthetics. Electro-kinetic geo-synthetics combine the electro-osmotic function of electrically conductive polymers and the drainage, filtration and reinforcement functions of geo-synthetics. Electro-kinetic geo-synthetics are formed by incorporating conductive elements within or associated with a conventional geo-synthetic material. Alternatively the geo-synthetic material can be formed using conducting polymer. Recent research using electro-kinetic geo-synthetics has shown the potential for the application of these materials in electro-osmotic dewatering of clayey soil and mining tailings (Hamir et al. 2001, Glendinning et al. 2005, Fourie et al. 2007, and Jones et al. 2011).

Hamir et al. (2001) investigated four types EKG electrodes, including (type 1) a needle-punched geo-synthetic with a woven copper wire stringer, (type 2) a needle-punched geo-synthetic incorporating stainless-steel fibers, (type 3) a composite formed by a carbon fiber sheet sandwiched between two layers of non-woven polypropylene sheet, and (type 4) geo-composite strip reinforcement with a copper wire stringer. The effectiveness of EKG electrodes in generating negative pore pressures was compared with the copper electrodes, as the electro-osmotic dewatering is directly related to the development of negative pore pressures. If the EKG electrodes are to replace regular electrodes then the pore pressures generated should be similar, and the resulting flow rate will then be similar. Test results demonstrated that there was very little difference between the EKG type 1 and the copper electrodes; EKG types 2 and 3 appeared more

effective in generating negative pore pressure. The variations in resistance with time for types 1 and 2 and for the copper electrode are shown in **Figure 2.3**.

The EKG electrodes showed little more resistance increase than the copper electrode, especially type 1. EKG type 4 was used as ground reinforcement to study the effect of electro-osmotic dewatering on bond performance under undrained conditions. Application of a potential gradient of 30 volts in addition to surcharge loading caused a reduction in water content of the sample ranging from 5.5% for a sample with a surcharge load of 350 kPa to 14% for a sample with a surcharge load of 110 kPa. Electro-osmosis using EKG electrodes created a significant improvement in bond strength, ranging between 54-210% which was in proportion to the increase in shear strength.

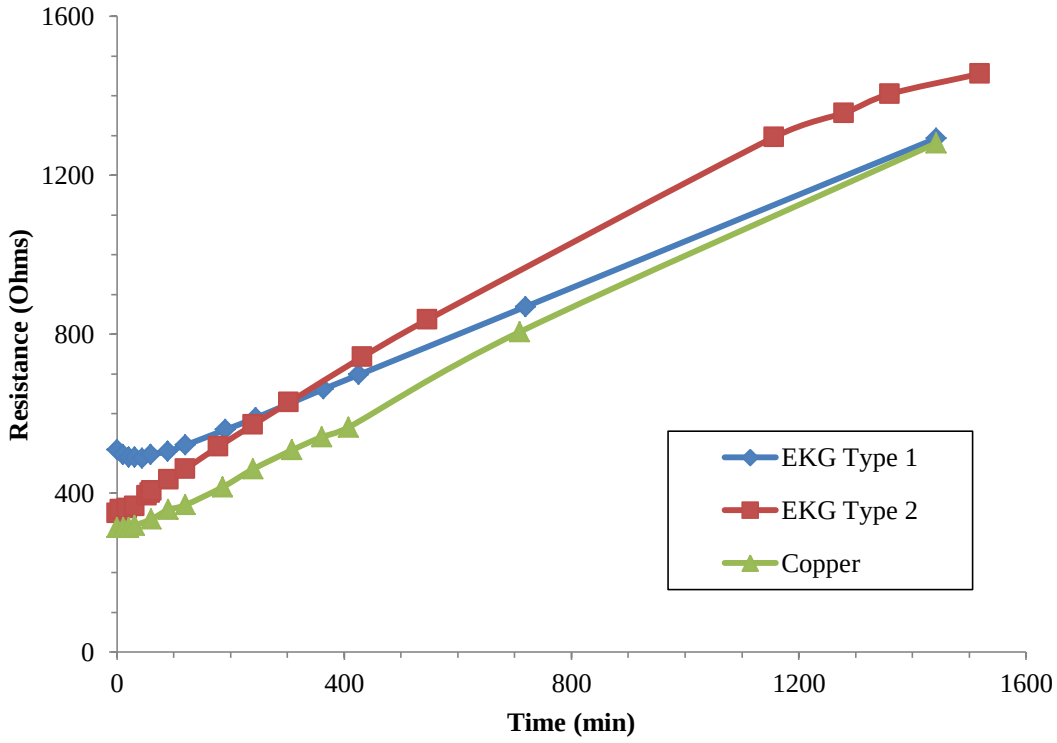

Figure 2.3 Variation of electrical resistance of copper and EKG Types 1 and 2 electrodes.
Source: Hamir et al., 2001.

Glendinning et al. (2005) demonstrated the successful use of EKG in the construction of a 4.8 m high reinforced soil wall. Clay slurry was used as backfill and was dewatered by electro-osmosis using EKG electrodes. Many potential benefits to EKG were identified. First, encasing the metallic filaments in a relatively inert polymer effectively eliminates electrode corrosion. Second, by forming the electrode as a geo-synthetic and utilizing the drainage function of geo-synthetics, EKG overcomes the problem of removing water since it provides a suitable drainage path for pore water removed with electro-osmosis. Third, geo-synthetics have the ability to take on a wide variety of shapes and forms to suit different applications. Last, making electrodes identical, polarity reversal can be easily achieved without compromising either the drainage function or electrical efficiency. Details of applications and case studies are provided in Jones et al. (2011).

Hu (2008) provides extensive research on the use of EKGs for different applications. The paper provides an analysis of the best geosynthetics to use in combination with electro-osmosis for drainage, reinforcement, filtration, separation, or containment of water and other substances in clayey soil of different types. The paper shows that carbon has the best resistance to corrosion when used for the electrically conductive filaments in EKGs. Additionally, the study reports the best treatment practices when using EKGs for different applications. These are shown in **Table 2.3**.

Table 2.3 EKG Applications

	Dewatering	Strengthening	Conditioning	Clean up
Objectives	Reduce water content	Reduces water content and increase strength	Reduces water content, increase strength, promote biological activity, pathogen reduction	Flush water through, mobilize/entrain contaminants, treat all soil, capture contaminants
Harnessed Electro-kinetic effects	Electro-osmosis	Electro-osmosis, pore pressure modification, electro-kinetic hardening	Electro-osmosis, pore pressure modification, electrolysis, Joule heating	Electro-osmosis, electrolysis, Joule heating
Electrodes configuration	Closed anode	Closed anode	Closed/semi closed anode	Open anode and cathode
Geosynthetic functions	Drainage, filtration, containment	Drainage, filtration, reinforcement	Drainage, filtration	Drainage/irrigation, filtration, sequestration
Polarity regulation	Normal polarity	Normal and reversed	Normal and reversed	Normal polarity

Source: Hu 2008.

2.6 Field Applications

Several well-documented field tests have been reported in the literature to demonstrate the successful in situ application of the electro-osmotic technique, including stabilization of excavations in clayey soil, stabilization of earth embankments, slopes and retaining walls, strengthening of clayey soil, dewatering, and improving friction pile capacity (Bjerrum et al. 1967, Chappell and Burton 1975, Lo et al. 1991, Abdel-Meguid et al. 1999, Burnotte et al. 2004, Glendinning et al. 2005, Fourie et al. 2007, Lamont-Black and Weltman 2010).

Lo et al. (1991) performed a field test to assess the effectiveness of the electro-osmotic stabilization on soft sensitive clay with original average shear strength of 20 kPa in Gloucester, Canada. The electrodes were 60.3 mm diameter perforated copper pipes to allow the drainage of water. The electrodes were installed in two square grids with different spacing of 3 m and 6 m, to investigate the influence of the spacing between the electrodes. The polarity of electrodes was reversed midway during the 32 days treatment period. Due to the polarity reversal, the undrained shear strength was uniformly increased by 60% and 40 % between the electrodes of 3 m and 6 m spacing, respectively. The dewatering removed an approximate total 4.2 cubic meters of water and was uniform over the treated area. The vane shear tests performed after 10 months showed that the shear strength remained constant, indicating that the increase in shear strength was permanent.

Burnotte et al. (2004) reported the results of a large field demonstration at Mont St-Hilaire, Canada, where a soft clay foundation of an existing road embankment was dewatered using electro-osmosis combined with chemical injection. Perforated steel pipes of 170 mm diameter were used as electrodes and pumping was used at the cathodes to make sure the water was not recirculated into the system. The clay had initial undrained shear strength of 30 kPa. The test aimed to have an over consolidation ratio (OCR) of 1.5 corresponding to a compression of 9% in 5 m of a soft clay layer. The initial profile of shear strength was compared with those obtained after the treatment at the mid-distance between the anode and the cathode, at 0.5 m from an anode, and at 0.5 m from a cathode. On average, at mid-distance between anodes and cathodes the undrained shear strength almost doubled. Thanks to the dewatering, the undrained shear strength of the clay layer

increased to 46 kPa near the cathodes and up to 190 kPa near the anodes. The desired compression of 9% was achieved uniformly after 28 days of electro-osmotic dewatering. When the treatment was terminated after 48 days the water removed was 460 L/m^2, equivalent to a compression of 12%.

In another field study Ou et al. (2009) tested the effectiveness of the injection of a calcium chloride solution followed by the injection of a sodium silicate solution. The experiment tested the use of polarity reversal and DC in combination with the saline solutions. The test consisted of injecting the solutions through the anodes and pumping out water from the cathodes. In the case of polarity reversal, the injection and pumping were also switched. The test was run for 25 day. The polarity was reversed after 12 days. The saline solution was injected during the first 4 days of treatment and during 4 days after the polarity was reversed. During DC application, the undrained shear strength of soil was increased. After the polarity was reversed, the new cathode was not able to pump water due to cementation around the electrode. This caused the water content to increase, which in turn decreased the undrained shear strength.

Lamont-Black and Weltman (2010) implemented electro-osmosis to stabilize a typical 9m high railway embankment in London with side slopes of 22°, which had been constructed by end tipping mixed fill of London clay and brick fragments, overlying alluvium and terrace gravels. A prior assessment of the embankment slope showed movement of more than 6mm a month and inclinometer readings next to the site indicated a distinct slip surface at approximately 2.5 m depth with factor of safety of 1.0 for the slope. An array of EKG electrode nails in the form of hexagons was deployed on the slope with a central cathode, from which the water could be drained. Application of a

DC potential (60-80 V) forced the water out of the ground, thus increasing material strength. After six weeks of electro-osmotic treatment and a power consumption of approximately 11.5 kwh/m^3, the shear strength of clay fill increased by a factor of 2.3, resulting in factor of safety of 1.7 for the slope, well above the required 1.3. Inclinometer readings after the treatment showed no horizontal movement. After the treatment the electrodes were left in the ground to act as soil nails to further stabilize the slope. The applied electro-osmotic technique achieved the results at 26% lower costs and with a carbon footprint of 47% lower than comparable methods using gabions and slope slackening.

2.7 Discussion

The reversal of polarity causes a switch of the electrolysis reactions. This can balance the high H+ concentration generated during the previous interval, thus maintaining an overall pH that will not greatly affect the zeta potential. The ability of the system to balance once the polarity is changed depends on the reversal interval. If drainage is available at the cathode, too many hydrated ions might be removed before reversal and the pH will be allowed to change and spread the pH front. Also, the clayey soil around the electrodes might cement and be unable to transfer current. Hence, the interval of polarity reversal is very important for the effectiveness of this technique. Yoshida et al. (1999)'s experiments with different frequencies showed that the best dewatering results were achieved by the lowest reversal frequency tested, 0.001Hz, while frequencies higher than 0.01Hz had worse results than DC. The highest frequencies, 1Hz and 50Hz, showed no difference in

dewatering. This suggests that normal high frequency alternating current is not beneficial for electro-osmotic dewatering.

Polarity reversal will create a more even distribution of water content along the path from anode to cathode, while applying a constant direct current will result in significant drying near the anode but only minor dewatering near the cathode. Simply reversing polarity will circulate water back and forth within the system. Because of this, and especially since water is not being drained to maintain current, net dewatering will not be as high as under DC. However, water molecules are being removed from the chemical structure of the clayey soil and moved to the pore spaces. In this form they are easier to remove with the help of a surcharge load.

Interestingly, while it might appear that polarity reversal delays current decay in clayey soil, it actually doesn't. Shown in **Figure 2.1** are different intervals of polarity reversal. When the polarity is switched, the current peaks for short time. However, as evidenced by the shown trend line, the current returns to the level it would have at that time had the polarity not been reversed. This disproves the idea that polarity reversal can increase treatment time. In terms of current, the only improvement it is providing is the short peaks right after the polarity is switched. Thus, the benefits of polarity reversal lay in recirculation of water and reduction of pH changes, not in the overall dewatering purposes. This can be most helpful for chemical treatment of clayey soil by recirculating a reagent with polarity reversals.

While current intermittence is subject to the same problems of DC, it is able to prolong treatment life. As the studies show, the power efficiency is increased. However, the treatment times to obtain similar dewatering results as DC are longer. This means that

current intermittence is more efficient in the long run, but DC can provide faster results if treatment time is limited and power consumption costs are not critical. While the short circuit method allows current and water recirculation to reduce resistance in clayey soil, some power is wasted to transport the recirculated water to the cathode. Thus, the OFF interval should be short to prevent too much recirculation. An open circuit on the other hand provides a benefit in power efficiency over DC since it allows the soil to relax while not draining the residual voltage.

Mohamedlhassan and Shang (2001) observed a 25% residual voltage during intermittent current OFF times. This suggests that the clayey soil might be acting as a capacitor. When the power is turned ON, the clayey soil-capacitor system stores charge and the current in the system decreases. Then, when the power is turned OFF, the clayey soil-capacitor has a residual voltage that slowly drains. This can be seen in the voltage equation for a discharging capacitor:

$$V_c = V_o * e^{-t/RC} \tag{2.1}$$

Where V_o is the voltage in the capacitor when current in turned OFF, R and C are resistance and capacitance of the clayey soil-water system, and t is the elapsed time. The resistance can be written as:

$$R = H/(\sigma * A) \tag{2.2}$$

The clayey soil capacitance can be written as:

$$C = A * \epsilon' * (\epsilon_0/H) \quad (2.3)$$

Hence, equation 2.1 can be written as:

$$V_c = V_o * e^{-t\sigma/\epsilon'\epsilon_0} \quad (2.4)$$

This might explain why intervals with the same ON/OFF ratios but higher OFF times have lower efficiency. Equation 2.4 shows that relaxation of electrical potential is a function of electrical properties of clayey soil. The $\sigma/\epsilon'\epsilon_0$ term refers to the clayey soil's electrical relaxation time. Hence equation 2.4 might have a significant implication in electro-osmotic treatment with intermittent current. If the clayey soil is allowed to relax for too long the benefit of residual voltage is lost and reactivating current requires recharge of the clayey soil. Selection of current intermittence intervals must be based on factors such as overall effectiveness of treatment, degree of electrode corrosion, and power consumption. When compared to polarity reversal, current intermittence provides the best results in terms of water removed for power consumed. Several studies have been carried out investigating these methods, but none has compared the overall effectiveness of each. To conclude which treatment procedure is better, the electro-osmotic conductivity, k_e, was calculated for each study based on Casagrande (1949)'s equation. A detailed comparison of these is presented in **Table 2.4**.

While the variables in these experiments vary, there are clear trends. The calculation of the electro-osmotic conductivity includes the discharged water and the applied electric field. The vast majority of intermittent current experiments show an

improvement in k_e while the polarity reversal tests show a reduction. For example, Yoshida (2000) and Yoshida et al. (1999) tested the same sample and electrodes. Compared to their DC electro-osmotic conductivity, the intermittent current clearly outperformed the polarity reversal. The results of these studies prove that intermittent current is superior to polarity reversal in water removal for power consumed, which is key for dewatering projects. When the polarity is reversed, the water is recirculated and energy is consumed moving the water to the new cathode. This can even create lower discharge for the same applied power as DC. **Table 2.4** also confirms that current intermittence interval, circuit type during OFF times, and wave type all influence the discharge of water. While different samples will react differently, the comparison between polarity reversal and intermittent current includes multiple types of clayey soil and still shows valid trends. Across the referenced works polarity reversal shows mostly negative efficiency of water removed for power used while intermittent current shows mostly significant improvements. This holds true despite the different clayey soil tested, electrode materials, and power application variables.

Table 2.4 Comparison Between Current Intermittence and Polarity Reversal Based on Previous Studies

Reference	Type of test	k_e for DC (m^2/sV)	k_e for IC or PR (m^2/sV)	Improvement	Electrical properties	Soil conditions
Mohamedelhassan and Shang (2001)	Intermittent current	6.15E-09	9.4453E-09	53.6%	Open 1m-ON 0.5m-OFF	Remolded marine sediment from seabed, south-west coast of Korea. Carbon-steel electrodes
			1.2285E-08	99.8%	Open 2m-ON 1m-OFF	
			1.0722E-08	74.4%	Open 3m-ON 1.5m-OFF	
			8.8235E-09	43.5%	Open 4m-ON 2m-OFF	
			8.7899E-09	42.9%	Open 5m-ON 2.5m-OFF	
			7.7142E-09	25.4%	Short 1m-ON 0.5m-OFF	
			7.2437E-09	17.8%	Short 2m-ON 1m-OFF	
			7.2100E-09	17.2%	Short 3m-ON 1.5m-OFF	
			7.1596E-09	16.4%	Short 4m-ON 2m-OFF	
Shang and Lo (1997)	Intermittent current	1.2998E-08	8.2293E-09	-36.7%	15m-ON 1m-OFF	Florida phosphate clay. Steel electrodes. Samples had different water contents
			3.5657E-08	174.3%	15m-ON 2m-OFF	
			1.3786E-08	6.1%	15m-ON 5m-OFF	
Micic et al. (2001)	Intermittent current	1.7619E-08	1.7869E-08	1.4%	10m-ON 2m-OFF	Marine clay from northwest coast of Korea. Steel electrodes.
			1.8023E-08	2.3%	4m-ON 2m-OFF	
			1.8196E-08	3.3%	2m-ON 2m-OFF	
			3.6930E-08	109.6%	4m-ON 2m-OFF	
			3.7007E-08	110.0%	4m-ON 2m-OFF Higher surcharge	

Table 2.4 (Continued)

Reference	Type of test	k_e for DC (m^2/sV)	k_e for IC or PR (m^2/sV)	Improvement	Electrical properties	Soil conditions
Yoshida (2000)	Intermittent current	1.4153E-10	1.4304E-10	1.1%	Rectangular wave f=0.001Hz	Kaolin. Platinum electrodes.
			2.1330E-10	54.0%	Sine wave f=0.001Hz	
			1.9122E-10	38.0%	Sine wave f=0.01Hz	
Hu et al. (2016)	Intermittent current	1.4416E-09	1.4736E-09	2.2%	12hr intervals	Kaolinite Suzhou, China. Iron
Kaniraj (2014)	Polarity reversal	8.3353E-10	4.9979E-10	-40.0%	PR every 8hrs	Peats and an organic soil from Sarawak, Malaysia. Copper EVD
			4.9896E-10	-40.1%	PR every 12hrs	
			5.1212E-10	-38.6%	PR every 24 hrs	
Chien et al. (2011)	Polarity reversal	5.0009E-10	1.9376E-11	-96.1%	k_e before and after PR	Taipei silty clay. Steel electrodes
Yoshida et al. (1999)	Polarity reversal	1.4672E-09	9.2994E-10	-36.6%	PR after 500s	Kaolin. Platinum electrodes.
			1.1504E-09	-21.6%	PR after 50s	
			5.9178E-10	-59.7%	PR after 5s	
			3.2870E-10	-77.6%	PR after 0.5s	
			3.2870E-10	-77.6%	PR after 0.01s	

EKGs improve on the basic electrodes by providing longer lasting electrodes that solve other problems common to normal electrodes. They will not corrode as fast as regular electrodes since they are coated with an inert polymer. Though covering the metallic filaments in a somewhat inert polymer might increase resistance, the difference is not significant, as evidenced by the presented studies. In addition to the electrical properties of EKGs, they also provide better drainage paths for water molecules that have made wick drains popular. This path not only allows water to flow out of the clayey soil systems faster, but it also helps liberate the gas bubbles generated around the electrodes due to electrolysis. While production of highly customized EKGs might cost more, they will last longer, effectively reducing costs. Because EKGs can be designed to stay in clayey soil and act as nails they can provide additional strength for little cost. EKGs also work well in combination with other enhancement techniques, especially with chemical injections by facilitating their introduction into clayey soil.

The use of saline solutions to aid in electro-osmosis is shown to be beneficial by providing new ions that will hydrate and carry water towards the cathode and buffer the large pH changes. However, close consideration must be made with regards to what type of electrolyte to use. The main factor that seems to affect electrolyte effectiveness is ease of exchange. This in turn depends mainly on the valence, ion size, and relative abundance of different ions. While Chien et al. (2011) reported that continuous injection during treatment is detrimental to the effectiveness of electro-osmosis. The tests used $CaCl_2$ which is shown to decrease the zeta potential by Chien et al. (2009). Continuous injection of other solutions might provide different results since they interact differently with clayey soil particles based on their cation exchange capacity (CEC) and the initial

structure (dispersed or flocculated). The injection of saline solutions increases the electrolytes present in clayey soil and provide a temporary boost to current and electro-osmotic flow. Unfortunately, with increased current and flow the rate of water electrolysis also increases. Hydrogen and hydroxide are produced faster at the electrodes. While most studies focused on anode conditioning, further study should be performed on the effects of conditioning at the cathode as a means to prevent precipitation and high alkalinity due to OH^- generation, which increase resistance.

The reported experiments show that injection of saline solutions to aid in electro-osmosis worked best when used prior to current application. Studies also tested the use of polarity reversal in combination with chemical injections. Ou et al. (2009) reported that sediment was cemented around the anode and this impeded the flow of water when the polarity was reversed, decreasing strength and increasing water content. However, this study was not extensive and the interval of polarity reversal was not investigated. The combined use of these two techniques could provide a substantial improvement over classic electro-osmotic treatment but electrolyte type and reversal interval must be carefully chosen. Since the polarity reversal interval depends on the amount of water drained and pH changes that occurred at the electrodes, and because adding chemical solutions increases the electro-osmotic flow of water, the intervals will have to be lower than if only polarity reversal is used.

While Ou et al. (2009) has similar issues as Chien et al. (2011), it demonstrates that injection of saline solutions improved the effectiveness of electro-osmosis in the field. The researchers concluded that polarity reversal in conjunction with chemical treatment is not beneficial. However, the reversal interval has been shown above to be a

critical variable. A shorter period between polarity reversals could provide much better results. The effectiveness of these techniques might be different in the field due to having a less controlled environment, but the benefits are still achievable.

2.8 Summary and Conclusions

In this chapter, different techniques used to enhance electro-osmotic dewatering were described and analyzed. Their improvement over the classic electro-osmotic treatment was discussed with a focus on dewatering efficiency. **Table 2.5** shows the pros and cons of each method. This study indicates that polarity reversal and intermittent current positively affected electro-osmotic treatment of clayey soil compared to DC, but that the power variation interval is critical to the success of both techniques. Polarity reversal provides a more even distribution of water removal than DC but fails in power efficiency for water removed. Current intermittence, especially under an open circuit, shows a clear increase in efficiency of water removed for power consumed. Injection of saline solutions at the electrodes was shown to provide some improvement in electro-osmotic dewatering and that it works best when application is done before testing or during the initial stages. Intermittent current suffers from the same problems that DC has with pH, thus and investigation of the effect of combining intermittent current and an injection of a buffer solution at the electrodes would be useful. Last, EKG electrodes were described and their benefits analyzed. They provide suitable replacement for classical electrodes and have additional functions. Field use of these techniques was also discussed and they have been shown to have similar effects on electro-osmotic dewatering of clayey soil in the field just as they do in the lab.

Table 2.5 Advantages and Disadvantages of Different Enhancement Techniques Compared to DC

Enhancement technique	Advantages	Disadvantages
Polarity reversal	Longer treatment time, ions are recirculated, higher power efficiency, longer electrode life, reduced pH changes	Water is maintained in the soil system, lower undrained shear strength, ON/OFF interval is critical, possible cementation and excessive ion removal
Intermittent current	Higher power efficiency for water removed, longer treatment time, longer electrode life	Lower time efficiency for water removal, ON/OFF interval is critical
Chemical injection	Increase in current flow, improved water removal at low concentrations, increase in undrained shear strength	Continuous injection is detrimental, improvement in strength is limited to immediate area around electrode, high concentrations reduce power efficiency, and higher ion valence provides better immediate water removal but can stifle long term treatment.
Geosynthetics	Cost, corrosion control, shape customization for different applications, can be used as soil nails, can be used in conjunction with the other enhancement techniques, provides a better drainage path	Minimal increase in resistance due to inert polymer coating of electric filaments

Polarity reversal, intermittent current, injection of chemical solutions at the electrodes, and use of geo-synthetics increase the overall efficiency of electro-osmotic treatment. These techniques are very promising, especially if combined. However, the improvements are not sufficient to justify use of electro-osmotic dewatering. As a result, electro-osmotic consolidation is still not widely used in construction projects. In order to reduce the excessive increase of the electrical contact resistance, improve the performance of electro-osmotic dewatering, and propel this technology into the market as

a viable consolidation option, a new approach is necessary. Additionally, a deeper understanding of the effects and mechanisms of electro-osmosis in clays are essential to properly predict and quantify the efficiency of any potential improvements.

CHAPTER 3

NEW METHOD TO PREDICT ELECTRO-OSMOTIC CONDUCTIVITY OF CLAYS

3.1 Introduction

The efficiency of electro-osmotic treatment is controlled by the electro-osmotic properties of the soil. Thus it is important to understand the properties that govern electro-osmotic phenomena in clay soils. This chapter briefly reviews an established theory of electro-osmotic conductivity of clays and then proposes a new theory based on work done in the field of colloidal chemistry. The contents of this chapter are in the process of being published in Martin and Meegoda 2019b and Martin and Meegoda 2019c.

Because of the molecular structures of clay particles, there is a negative surface charge on the wide flat sides of the particle. As discussed in Chapter 1, this negative surface charge is balanced by free ions in the interstitial fluid. A concentration gradient of these ions will develop; where the positive ions will have an increased concentration near the clay surface that decays towards the bulk concentration with the distance from the particle surface. The inverse will happen with the negative ions, i.e., lesser number of negative charges near the clay surface. This is commonly referred to as the diffused double layer. When an electric field is applied parallel to the clay surface, hydrated ions will migrate towards the oppositely charged electrodes. Since there is a predominance of positive ions in the double layer the net flow will be towards the cathode, where water can be removed. This has been the underlying principle of electro-osmotic consolidation

of soft clays. Much study has been done in an attempt to understand the mechanisms at play and develop a mathematical theory that describes this flow.

One of the earliest and more widely accepted theories is based on a model introduced by Helmholtz (1879) and refined by Smoluchowski (1914). This model is discussed in detail in chapter 1 and summarized here. The model develops an expression for the flow of water through a soil of cross-sectional area A due to an applied electric field E similar to Darcy's Law.

$$q = vA \tag{3.1}$$

Where

$$v = k_e E \tag{3.2}$$

$$k_e = \frac{\zeta \epsilon}{\mu} n \tag{3.3}$$

$$\epsilon = \epsilon_0 \epsilon_r \tag{3.4}$$

Here ζ is the potential at the slip surface of the clay particle termed the zeta potential. The actual slip plane is not at the particle surface but some small unknown distance δ away from the surface of the particle (Mitchell and Soga 2005). This occurs because there is a layer of ions that will essentially remain attached to the clay surface. In this model k_e is termed the electro-osmotic conductivity. This term essentially measures the effectiveness

of the electrical current in moving water through the soil. Thus, it is important to properly understand it. Other researchers have also proposed theories that describe the electro-osmotic conductivity. Schmid, 1950 and Schmid, 1951 develop a theory where the electro-osmotic conductivity varies with the square of the pore radius. However, the Helmholtz model still gives better results for soils (Mitchell and Soga 2005). Spiegler, 1958 proposed a model that considered the friction between the water and ions, and the pore walls but made assumptions that severely limited the model's predictive power. Its real value is in providing a relatively simple physical representation of a complex process (Mitchell and Soga 2005). To date, the Helmholtz-Smoluchowski model remained the most popular model. However, it has some important drawbacks, such as not accounting for electrolyte concentration, and tends to overestimate measured values (Mohamedelhassan, 1998). This chapter proposes a new way of calculating the electro-osmotic conductivity by adapting work done in colloid chemistry (Coelho at al., 1996).

The electro-osmotic conductivity will depend on the properties of the diffused double layer. Since the clay particle exhibits a surface charge due to its chemical structure, it can be assumed that the surface will have a constant potential. This electric potential decays away from the particle surface to a constant value at the bulk and affects the distribution of current carrying ions in the pore fluid between particles, (see **Figure 3.1**). Furthermore, when two clay particles are close enough, their respective double layers will interact. Thus, to calculate the electro-osmotic conductivity in a clay pore it is necessary to determine the potential distribution caused by the movement of ions under an electric field. The development of the relevant equations is shown below.

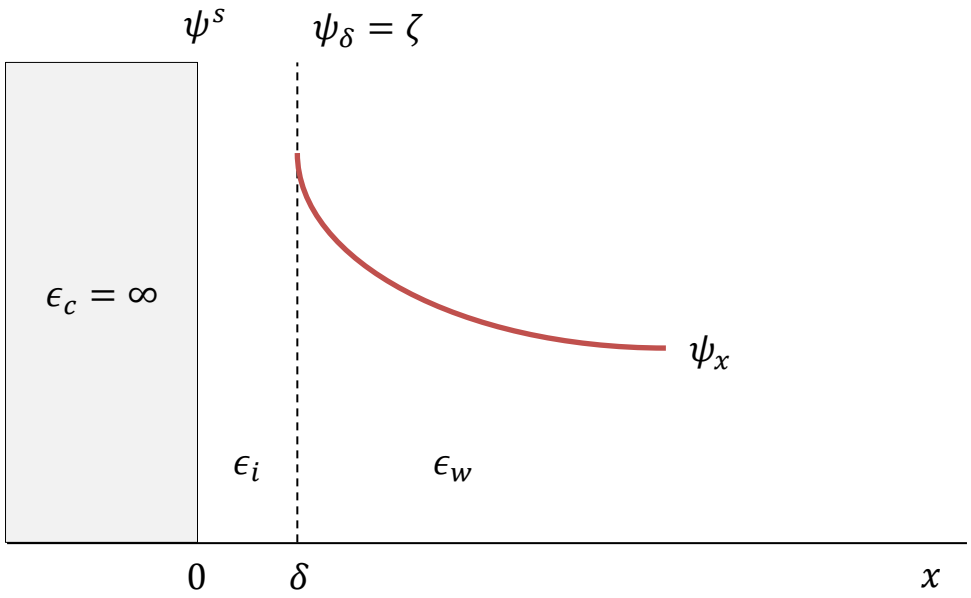

Figure 3.1 Decay of clay particle surface potential with distance from the particle.

3.2 The Poisson-Boltzmann Equation

In the region where $x > \delta$, the decay of the potential on the particle surface is given by Poisson's equation:

$$\nabla \cdot \epsilon \boldsymbol{E} = \rho \tag{3.5}$$

And

$$\boldsymbol{E} = -\nabla\psi \tag{3.6}$$

Here $\boldsymbol{E}$ is the local electric field vector. Since ϵ is constant in the pore fluid:

$$\nabla \cdot (\epsilon \nabla \psi) = -\rho \tag{3.7}$$

$$\nabla \cdot (\nabla \psi) = -\frac{\rho}{\epsilon} \tag{3.8}$$

$$\nabla^2 \psi = -\frac{\rho}{\epsilon} \tag{3.9}$$

Near the particle surface ions will congregate to valance the surface charge and their distribution is given by the Boltzmann equation:

$$c_i = c_i^0 \exp\left(\frac{-z_i e \psi}{kT}\right) \tag{3.10}$$

Where c_i represents the concentration of ions i at a given point. The charge density is given by:

$$\rho = \sum_i c_i z_i e \tag{3.11}$$

Combine Equations 3.9, 3.10, and 3.11 to obtain the Poisson-Boltzmann equation:

$$\nabla^2 \psi = -\frac{1}{\epsilon_0 \epsilon_r} \sum_i z_i e c_i^0 \exp\left(\frac{-z_i e \psi}{kT}\right) \tag{3.12}$$

This equation is well known and it describes the decay of the electric potential away from a charged surface as a function of the potential and ion concentrations at any point. This is the basis for understanding the distributions of the current carrying ions within the zone of double layer that will affect the electro-osmotic conductivity.

3.3 The Debye-Hückel Approximation

The Poisson-Boltzmann equation can be simplified using the Debye-Hückel approximation. If the electrical energy is small compared to thermal energy ($|z_i e\psi| < kT$) it is possible to expand the exponentials in Equation 3.12 as shown below

$$\nabla^2\psi = -\frac{1}{\epsilon_0\epsilon_r}\left[\sum_i z_i e c_i^0 - \sum_i \frac{{z_i}^2 e^2 c_i^0 \psi}{kT}\right] \tag{3.13}$$

Since

$$\exp\left(-\frac{A}{B}\right) \approx 1 - \frac{A}{B}$$

This approximation usually holds if $z\zeta < 51.4\, mV$ at room temperature (Hunter, 2001). Because the bulk is at equilibrium and electrically neutral, the first summation term of Equation 3.13 must be zero, thus:

$$\nabla^2\psi = \left[\frac{\sum_i {z_i}^2 e^2 c_i^0}{\epsilon_0\epsilon_r kT}\right]\psi = \kappa^2\psi \tag{3.14}$$

Where

$$\kappa^2 = \left[\frac{e^2}{\epsilon kT}\sum_i c_i^0 z_i^2\right] \tag{3.15}$$

Here κ is known as the Debye-Hückel parameter and has units of L^{-1}. The thickness of the diffused double layer is measured in terms of the inverse of this parameter:

$$\lambda = \frac{1}{\kappa} = Debye\ length \tag{3.16}$$

The region of variable potential of the double layer which extends from the slip plane to the bulk is usually in the order of 3λ to 4λ (Hunter, 2001). It is important to note that κ does not depend on properties of the clay.

3.4 Solution for the Poisson-Boltzmann Equation for Interacting Double Layers

During electro-osmotic flow the water will move through soil capillaries created between clay particles. Thus the solution to the Poisson-Boltzmann must be found for the case of two parallel plates. For a dilute clay water system, the clay particles are sufficiently separated such that the potential distributions will not interact. The solution for that case is simple. Presented here is the case for denser clay water system where diffused double layers interact such that the electric potential is never zero. **Figure 3.2** shows a

conceptual diagram of this case. Note that in this case "x" is measured from slip plane to slip plane.

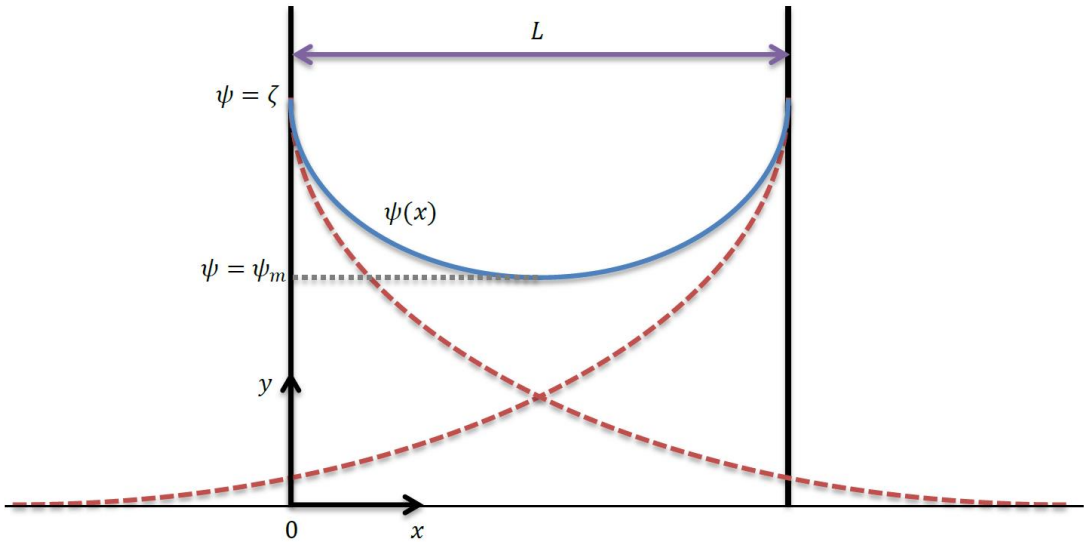

Figure 3.2 Potential distribution from two overlapping double layers. The dashed lines represent the potential distribution for each double layer if the other was not present. The full line represents the predicted potential distribution.
Source: Hunter, 2001.

The potential distribution ψ varies only with x, thus equation 3.14 reduces to

$$\frac{d^2\psi}{dx^2} = \kappa^2\psi \tag{3.17}$$

Multiplying both sides by $(2\frac{d\psi}{dx})$, the following was obtained

$$2\frac{d\psi}{dx}\frac{d^2\psi}{dx^2} = 2\kappa^2\psi\frac{d\psi}{dx} \tag{3.18}$$

Which can be easily integrated to obtain

$$\left(\frac{d\psi}{dx}\right)^2 = \kappa^2\psi^2 + C \tag{3.19}$$

In the middle of the channel, where $x = \frac{L}{2}$, $\psi = \psi_m$, and $\frac{d\psi}{dx} = 0$ and hence the constant of integration can be calculated.

$$C = -\kappa^2\psi_m^2 \tag{3.20}$$

Leading to

$$\frac{d\psi}{dx} = \kappa[\psi^2 - \psi_m^2]^{1/2} \tag{3.21}$$

To perform the second integration Hunter, 2001 suggested the following substitution

$$\psi = \psi_m \cosh(u) \tag{3.22}$$

$$d\psi = \psi_m \sinh(u)\, du \tag{3.23}$$

Substituting into Equation 3.21 and simplifying

$$\frac{d\psi}{dx} = \kappa\left[{\psi_m}^2 \cosh(u)^2 - \psi_m^2\right]^{1/2} \tag{3.24}$$

$$\frac{d\psi}{dx} = \kappa\psi_m[\cosh(u)^2 - 1]^{1/2} \tag{3.25}$$

$$\frac{d\psi}{dx} = \kappa\psi_m[\sinh(u)^2]^{1/2} \tag{3.26}$$

$$\frac{d\psi}{dx} = \kappa\psi_m \sinh(u) \tag{3.27}$$

$$\psi_m \sinh(u)\, du = \kappa\psi_m \sinh(u)\, dx \tag{3.28}$$

$$du = \kappa dx \tag{3.29}$$

Now integrating both sides

$$u = \kappa x + C \tag{3.30}$$

Substituting back into equation 3.22 gives

$$\psi = \psi_m \cosh(\kappa x + C) \tag{3.31}$$

To solve for the constant of integration the following boundary condition can be used. When $x = \frac{L}{2}$, the potential is $\psi = \psi_m$. Therefore,

$$1 = \cosh\left(\frac{\kappa L}{2} + C\right) \tag{3.32}$$

$$0 = \frac{\kappa L}{2} + C \tag{3.33}$$

$$C = -\frac{\kappa L}{2} \tag{3.34}$$

This gives

$$\psi = \psi_m \cosh\left(\kappa x - \frac{\kappa L}{2}\right) \tag{3.35}$$

It useful to present Equation 3.35 in terms of the zeta potential, which is more easily measurable than the potential at the center of the channel. When $x = 0 \rightarrow \psi = \zeta$.

$$\psi_m = \frac{\zeta}{\cosh(\frac{\kappa L}{2})} \tag{3.36}$$

Finally, substituting Equation 3.36 back into equation 3.35 gives the local electrostatic potential between two interacting double layers.

$$\psi = \zeta \frac{\cosh\left(\kappa\left(x - \frac{L}{2}\right)\right)}{\cosh\left(\frac{\kappa L}{2}\right)} \tag{3.37}$$

3.5 Development of the Electro-Osmotic Conductivity

Driven by the applied electric field, the local motion of the fluid in the neighborhood of the particle surface is governed by the Stokes equations with the body force in this case given by the applied field

$$\mu\nabla^2 v - \nabla p = -\rho \mathrm{E} \tag{3.38}$$

and

$$\nabla \cdot v = 0 \tag{3.39}$$

Assuming that inertia forces are negligible and that ion density is not affected by ion migration (because the ions replace themselves as they move from further down the channel), Equation 3.9 can be used to rewrite Equation 3.38 as

$$\mu\nabla^2 v - \nabla p = \epsilon\nabla^2\psi E \tag{3.40}$$

If the applied electric field is parallel to the particle surface the local pore fluid velocity and the potential vary only along the x direction. Thus, in the absence of an applied pressure gradient and assuming gravity is negligible Equation 3.40 can be reduced to

$$\mu \frac{d^2v}{dx^2} = \epsilon \frac{d^2\psi}{dx^2} E \tag{3.41}$$

The first integration gives

$$\mu \frac{dv}{dx} = \left[\epsilon \frac{d\psi}{dx}\right] E + C \tag{3.42}$$

This can be integrated again using the no-slip condition where $x = 0 \rightarrow v = 0 \; and \; \psi = \zeta$, to give

$$\mu v = \epsilon(\psi - \zeta)E + Cx \tag{3.43}$$

The quantity C is related to the velocity gradient beyond the double layer. In the absence of an applied pressure and for interacting double layers C must be zero, for the velocity gradients and the associated shear stresses in this region only arise in order to balance the pressure forces on the liquid (Hunter, 2001). Thus Equation 3.43 reduces to

$$v = \frac{\epsilon(\psi - \zeta)}{\mu} E \tag{3.44}$$

This equation describes the velocity of the pore fluid under an applied electric field. Comparing this to Equation 3.2 reveals that the first part of the right-hand side of Equation 3.44 is the electro-osmotic conductivity of the clay. To differentiate it from that of Equation 3.3 it will be assigned the symbol β.

$$\beta = \frac{\epsilon}{\mu}(\psi - \zeta) \tag{3.45}$$

This equation shows that the electro-osmotic conductivity varies locally within the pore space since it is influenced by the local potential. To analyze the flow of fluid through clay soil, it is useful to determine the average electro-osmotic conductivity through a given pore. First, substitute from Equation 3.37 to get

$$\beta = \frac{\epsilon}{\mu}\left[\zeta \frac{\cosh\left(\kappa\left(x - \frac{L}{2}\right)\right)}{\cosh\left(\frac{\kappa L}{2}\right)} - \zeta\right] \tag{3.46}$$

Then take the average using the formula

$$f_{avg} = \frac{1}{b-a}\int_a^b f(x)dx \tag{3.47}$$

Here Equation 3.46 will be averaged from one particle surface $(x = 0)$ to the other $(x = L)$.

$$\beta_{avg} = \frac{1}{L}\int_0^L \frac{\epsilon\zeta}{\mu}\left[\frac{\cosh\left(\kappa\left(x - \frac{L}{2}\right)\right)}{\cosh\left(\frac{\kappa L}{2}\right)} - 1\right]dx \tag{3.48}$$

$$\beta_{avg} = \frac{\epsilon\zeta}{\mu L}\left[\frac{\sinh\left(\kappa\left(x-\frac{L}{2}\right)\right)}{\kappa\cosh\left(\frac{\kappa L}{2}\right)} - x\right]_0^L \tag{3.49}$$

$$\beta_{avg} = \frac{\epsilon\zeta}{\mu L}\left[\frac{\tanh\left(\frac{\kappa L}{2}\right)}{\kappa} - L - \frac{\tanh\left(-\frac{\kappa L}{2}\right)}{\kappa}\right] \tag{3.50}$$

Using the identity $\tanh(x) = -\tanh(-x)$ Equation 3.50 reduces to

$$\beta_{avg} = \frac{\epsilon\zeta}{\mu L}\left[\frac{2\tanh\left(\frac{\kappa L}{2}\right)}{\kappa} - L\right] \tag{3.51}$$

or

$$\beta_{avg} = \frac{\zeta\epsilon}{\mu}\left[\frac{2\tanh\left(\frac{\kappa L}{2}\right)}{\kappa L} - 1\right] \tag{3.52}$$

Thus Equation 3.52 gives the average electro-osmotic conductivity through a channel between two parallel charged plates. It depends on the pore fluid's permittivity and viscosity, the pore diameter, the clay particles surface potential (expressed through the zeta potential), and the pore electrolyte's properties.

3.6 Laboratory Tests

Seven electro-osmotic consolidation laboratory tests on kaolin clay were performed. The samples were mixed with water to reach the liquid limit. The wet samples were allowed to rest for 24 hours inside a vacuum oven to remove entrapped air. After this period the samples were placed in the consolidometer and loaded to allow of normal consolidation to occur with a load equivalent to 10 feet of soil. The samples were connected to a power supply and a voltage of 2.5, 5, 7.5, 10, 12.5 and 15 volts was applied. The settlement and electrical resistance were measured. The experimental setup and testing equipment used are shown in **Figure 3.3**.

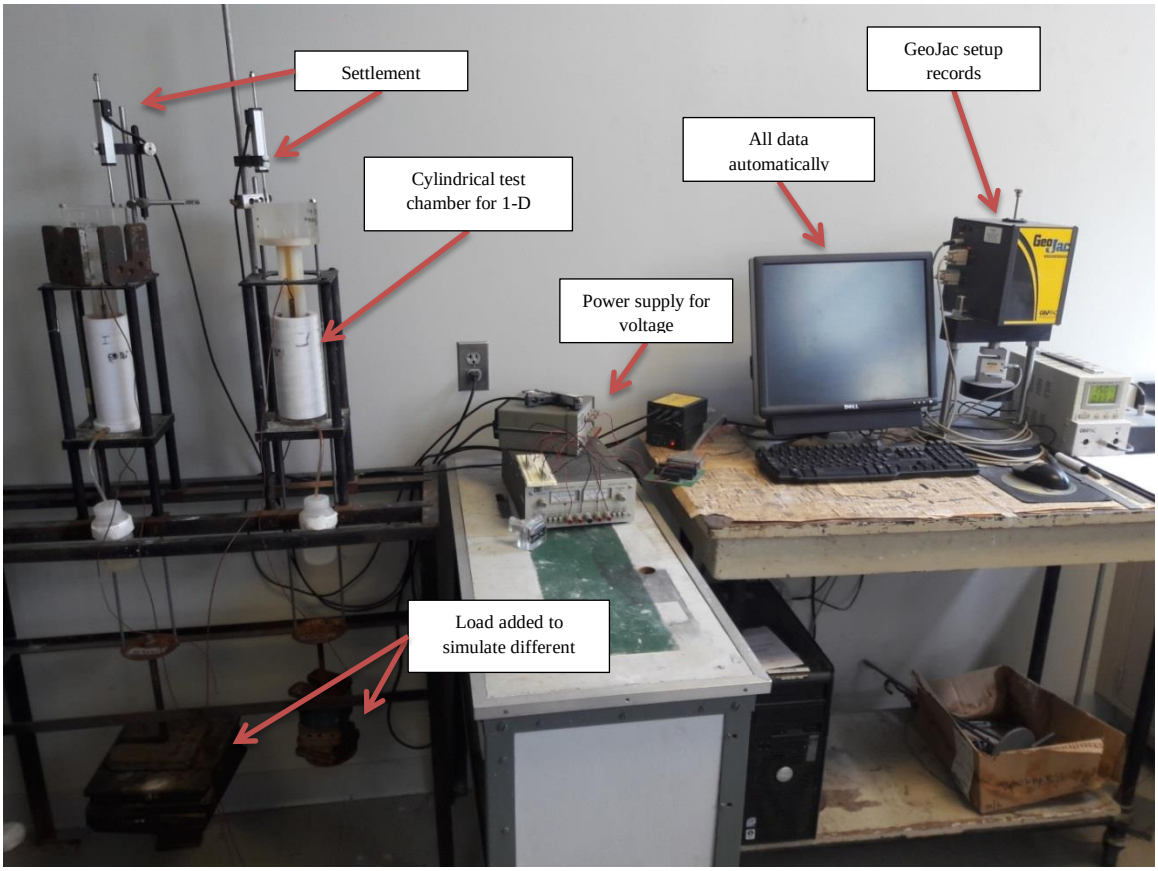

Figure 3.3 Experimental equipment and setup.

After normal consolidation under the desired load was completed, the samples were connected to the power supply. During this time, the settlement as well as the soil resistance is measured continuously. Typical data for an electro-osmotic consolidation test is shown in **Figure 3.4**.

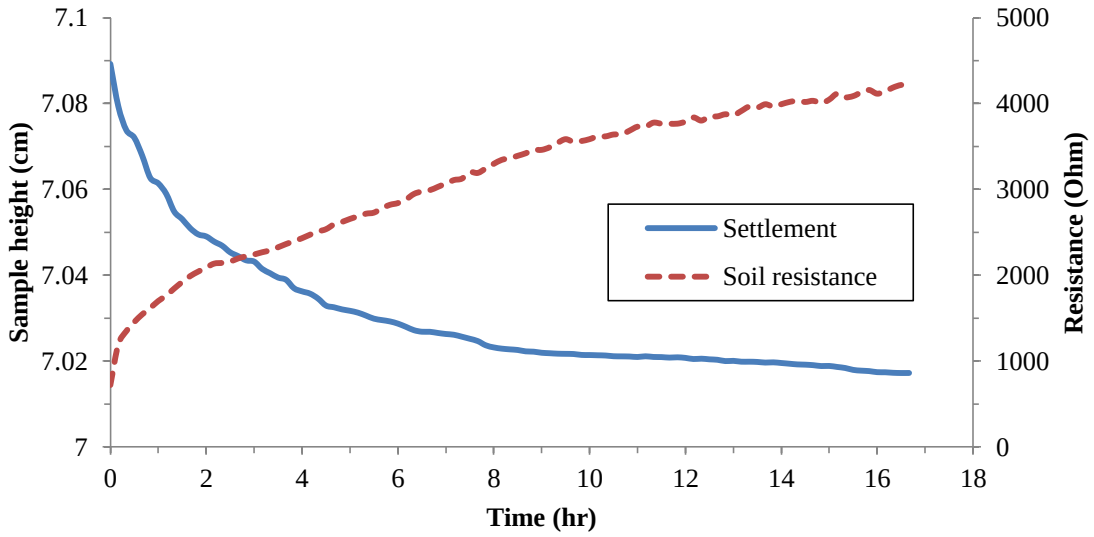

Figure 3.4 Typical experimental data for electro-osmotic consolidation.

Since the soil is saturated, the settlement measured is exactly equal to the drainage. Therefore Equations 3.1 and 3.2 can be used to calculate the experimental electro-osmotic conductivity based on the measured settlement and applied electric field. To compare to the models described the average electro-osmotic conductivity has been calculated using the settlement data in the region of relatively constant slope at the beginning of the test. For that same region of time, the resistance data is used to calculate the average electric conductivity of the sample using Pouillet's Law,

$$\sigma = \frac{H}{RA} \tag{3.53}$$

The ratio of pore fluid conductivity (σ_p) to the average electric conductivity of the sample (σ) or the formation factor ($F = \sigma_p/\sigma$) is a good indicator of the soil fabric or the soil structure which depends on the double layer thickness value shown in Equation 3.52 (Anandarajah et al., 1986, Meegoda and Arulanandan, 1986, Meegoda and Ratnaweera, 2008). The measured values of the pore fluid electrical conductivity were used to graph electrical conductivity contours. These contours, as well as the electro-osmotic conductivity found with the old model, the proposed model, and experimentally are all shown in **Figure 3.6**.

3.7 Comparison of Predicted and Measure Electro-osmotic Conductivities

Both Equations 3.3 and 3.52 describe the electro-osmotic conductivity with one key difference: the influence of pore size and pore fluid chemistry. Equation 3.3 accounts for the pore volume as porosity. It has been stated in the literature that this is one of the reasons why electro-osmotic consolidation works well in fine grained clayey soils. Contrary to the hydraulic conductivity, the electro-osmotic conductivity does not depend on pore size, only on porosity (Mitchell and Soga 2005). A more rigorous development of an electro-osmotic conductivity coefficient has led to Equation 3.52. This shows that the electro-osmotic conductivity does in fact depend on pore size. However, a simple analysis of the function $f(x) = \frac{\tanh(x)}{x}$ shows that as the pore size gets smaller, the electro-osmotic conductivity increases. Pore size depends primarily on soil type. It can be estimated but not accurately measured, especially since it will not be constant throughout the soil mass.

Equation 3.52 takes into account the properties of the electrolyte in the pores. This means that a more accurate understanding can be obtained of the electro-osmotic conductivity and what influences it. The variation of the electro-osmotic conductivity can be calculated for different pore electrolytes while keeping the other properties of the system constant. This can then be compared to the electro-osmotic conductivity predicted by the Equation 3.3. This was done for 4 different electrolyte concentrations using typical values for the other properties. The electro-osmotic conductivities were plotted as a function of water content assuming 100% saturation. To optimally compare results, Equations 3.3 and 3.52 were first non-dimensionalized as shown in Equations 3.54 and 3.55.

$$\frac{\mu}{\zeta\epsilon}k_e = n \tag{3.54}$$

$$\frac{\mu}{\zeta\epsilon}\beta_{avg} = \frac{2\tanh\left(\frac{\kappa L}{2}\right)}{\kappa L} - 1 \tag{3.55}$$

Figure 3.5 shows channel geometry used and **Table 3.1** shows the values used for the constants. Based on **Figure 3.5**, the channel width L and the porosity can be calculated for different water contents ω as follows

$$L = wG_s\omega \tag{3.56}$$

$$n = \frac{L}{L + w} \tag{3.57}$$

Hence the L value in Equation 3.55 can be replaced by n. The comparison of non-dimensionalized electro-osmotic conductivity values from Helmholtz-Smoluchowski model as well as from the proposed model shows that both models show that the electro-osmotic conductivity is a function of the soil porosity. In addition to the soil porosity, the electro-osmotic conductivity based on the proposed model is also a function of the diffused double layer thickness.

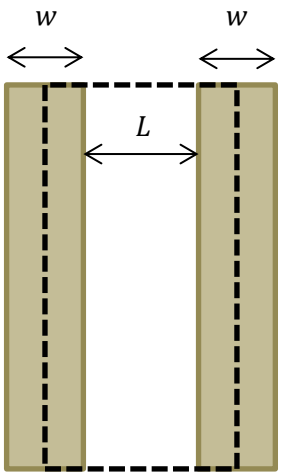

Figure 3.5 Channel geometry between two clay particles of thickness w.

Table 3.1 System Constants

Constants	Symbol	Value	Unit
Fluid relative permittivity	ϵ_r	80.2	
Permittivity of free space	ϵ_0	8.85E-12	F/m
Fluid viscosity	μ	0.001002	s*Pa
Zeta potential	ζ	-0.03	V
Electron charge	e	-1.60E-19	C
Avogadro constant	N_a	6.0221E+23	
Valence (z:z)	z	1	
Boltzmann constant	k	1.38E-23	J/K
Temperature (20 °C)	T	293.15	K
Thickness of clay particle	w	100.00	nm
Specific gravity of solids	G_s	2.7	
Plastic limit	PL	30%	
Liquid limit	LL	90%	

The analysis was performed for a 1:1 electrolyte of sodium chloride at different concentrations. The results of the laboratory tests along with the predictions based on the two models are shown in **Figure 3.6**. Electrical conductivity contours of the pore fluid were also plotted with the laboratory tests data of the electro-osmotic conductivity. **Figure 3.6** demonstrates that the proposed equation for calculating electro-osmotic conductivities provides a comprehensive model by taking into account pore electrolyte properties, which the Helmholtz-Smoluchowski model overlooks. Hence the proposed model can provide a more accurate approximation of the effect of electro-osmotic consolidation. This agrees with the literature, which shows that addition of saline solutions at the electrodes increases the flow of water (Ozkan et al. 1999; Lefebvre and Burnotte 2002; Burnotte et al. 2004; Paczkowska 2005; Chien et al. 2009; Ou et al. 2009;

Chang et al. 2010; Chien et al. 2011). Therefore, the proposed model could provide an explanation for that phenomenon.

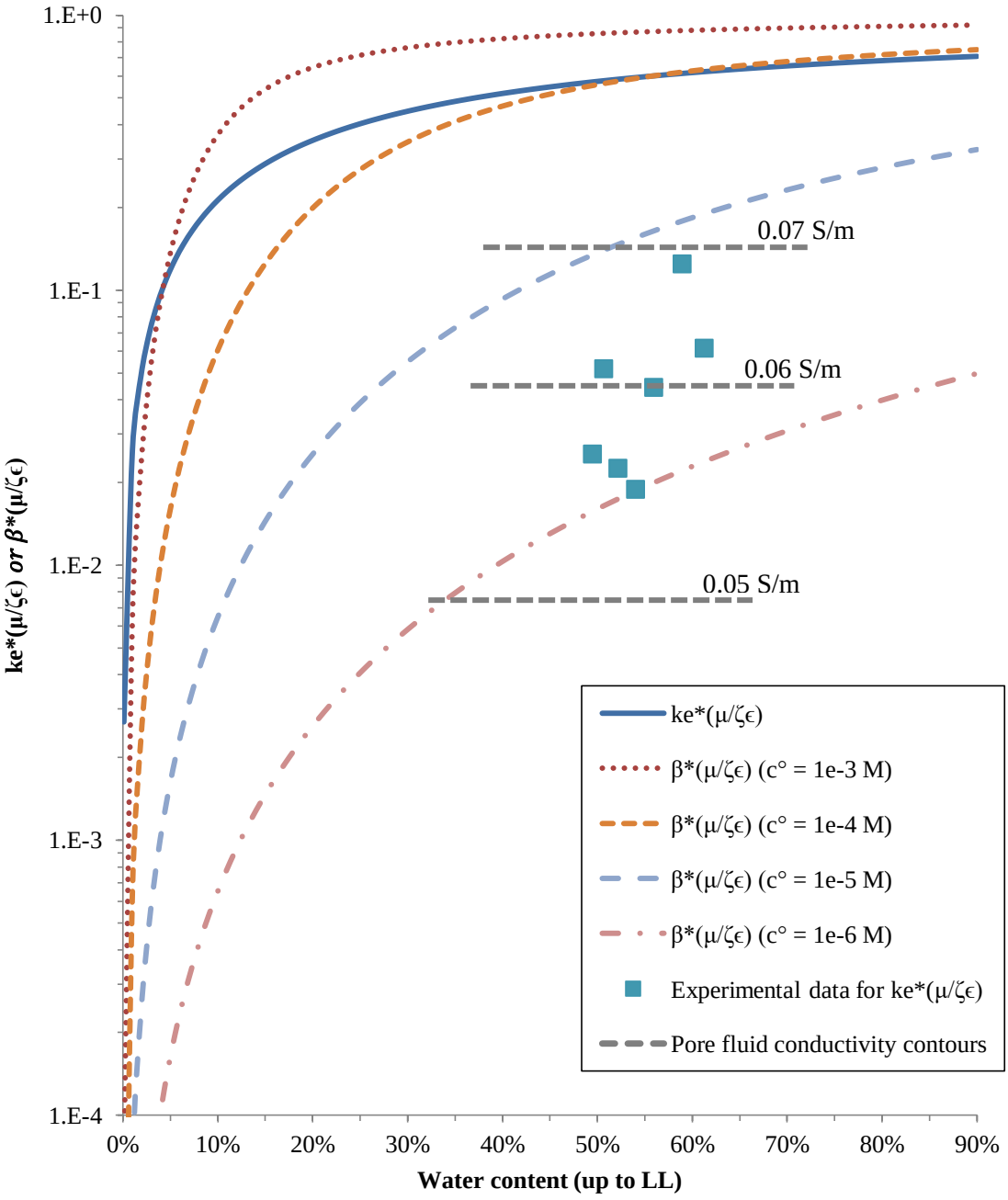

Figure 3.6 Electro-osmotic conductivities based on different models.

3.8 Estimating Electro-Osmotic Conductivity of Anisotropic Clay

3.8.1 Introduction

In typical soil clay particles are aligned in all directions. Channels parallel to the applied electric field will have the highest electro-osmotic conductivity while channels perpendicular to the applied electric field will have the lowest electro-osmotic conductivity. Thus, it is reasonable to estimate the total soil electro-osmotic conductivity by calculating a weighted average of the electro-osmotic conductivity of parallel and perpendicular channels. The weights of each channel type are given by the anisotropy of the sample. Thus, if the porosity, type of clay, and anisotropy are known, the total soil electro-osmotic conductivity can be more accurately calculated.

This section develops the electro-osmotic conductivity for the case of a channel perpendicular to the applied electric field. Additionally a laboratory test was conducted to calculate the anisotropy of a lab sample of kaolinite. This was then used to estimate the electro-osmotic conductivity and compare it to experimental measurements.

3.8.2 Electro-Osmotic Conductivity for a Channel Perpendicular to the Applied Electric Field

The main difference between and parallel and a perpendicular channel is that in a parallel channel the applied electric field does not affect the distribution of charges in the double layer created by the clay surface. The ion density is not affected by ion migration because the ions replace themselves as they move from further down the channel. In a perpendicular channel, in fact for any non-parallel channel, the electric field creates an uneven distribution of charges. Because the applied electric field cannot be directly included in the derivation of the electro-osmotic conductivity, it can instead be simulated

with an equivalent electric field parallel to the channel and by changing the surface potential of one of the clay surfaces to obtain the same uneven distribution of charges. For this, a potential distribution between two parallel surfaces of different surface potential is required. **Figure 3.7** shows a conceptual sketch of this distribution.

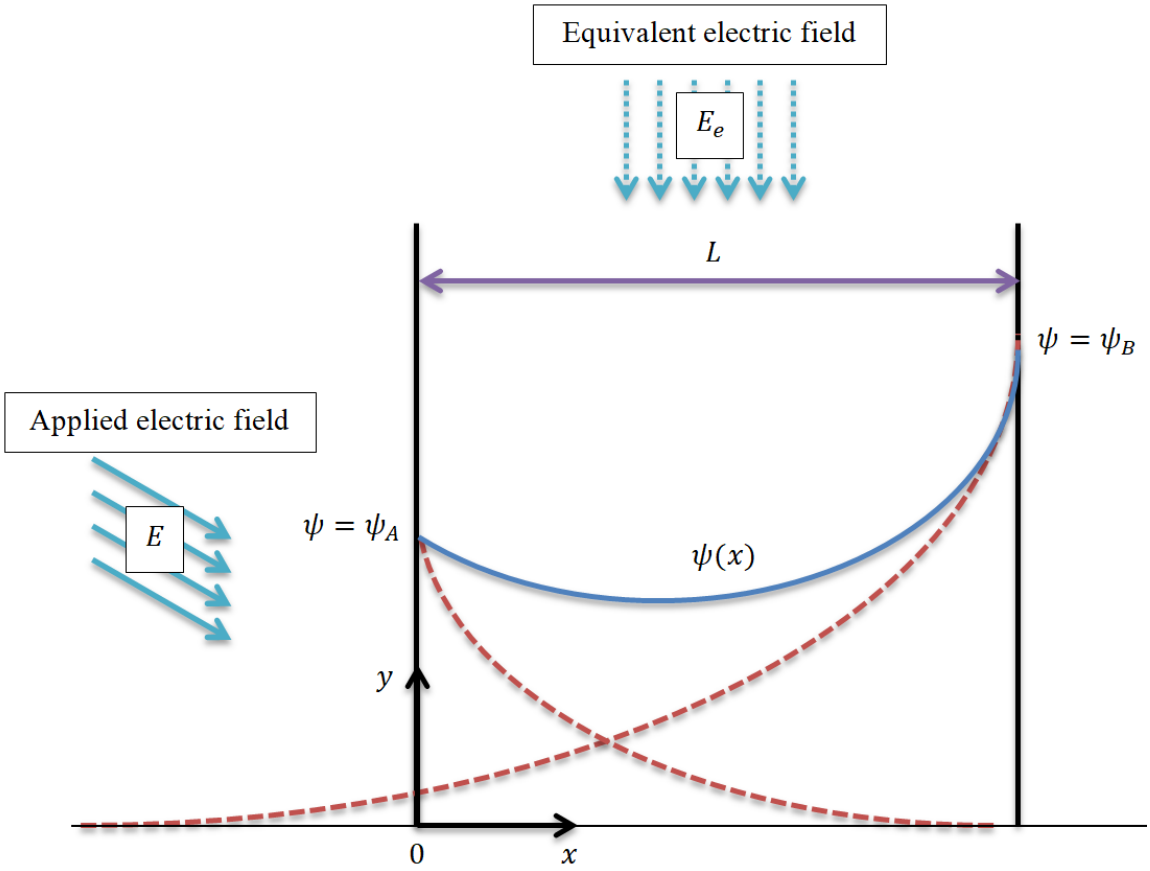

Figure 3.7 Potential distributions from two overlapping double layers with different surface potentials. The dashed lines represent the potential distribution for each double layer if the other was not present. The full line represents the predicted potential distribution.

Chakraborty (2015) showed that the potential distribution between two parallel plates of different surface potential is given by

$$\psi = \psi_A \cosh(\kappa x) + \frac{\psi_B - \psi_A \cosh(\kappa L)}{\sinh(\kappa L)} \sinh(\kappa x) \tag{3.58}$$

This is true for any values of ψ_A and ψ_B , and if $\psi_A = \psi_B$ then the expression simplifies to the case of a parallel channel described earlier in this chapter. Driven by the applied electric field, the local motion of the fluid in the neighborhood of the particle surface is governed by the Stokes equations with the body force in this case given by the equivalent electric field following Poisson's equation. If the equivalent electric field is parallel to the particle surface the local pore fluid velocity and the potential vary only along the x direction. Thus, in the absence of an applied pressure gradient and assuming gravity is negligible Stoke's equation can be reduced to

$$\mu \frac{d^2 v}{dx^2} = \epsilon \frac{d^2 \psi}{dx^2} E_e \tag{3.59}$$

Integrating twice gives

$$\mu v = \epsilon E_e \psi + C_1 x + C_2 \tag{3.60}$$

The constants of integration can be solved with the following boundary no-slip conditions:

1. When $x = 0$, $\psi = \psi_A$, and $v = 0$. This gives $C_2 = -\epsilon E_e \psi_A$
2. When $x = L$, $\psi = \psi_B$, and $v = 0$. This gives $C_1 = \frac{\epsilon E_e}{L}(\psi_A - \psi_B)$

Substituting back into Equation 3.60

$$v = \left[\frac{\epsilon}{\mu}\left(\psi - \psi_A + \frac{x}{L}(\psi_A - \psi_B)\right)\right] E_e \tag{3.61}$$

This equation returns the flow velocity of the pore fluid as a function of location inside the pore due to the equivalent electric field. The coefficient of the equivalent electric field is the electro-osmotic conductivity for a channel perpendicular to the applied electric field.

$$\beta_{90} = \frac{\epsilon}{\mu}\left(\psi - \psi_A + \frac{x}{L}(\psi_A - \psi_B)\right) \tag{3.62}$$

Combining Equations 3.58 and 3.62 will solve for the electro-osmotic conductivity.

$$\beta_{90} = \frac{\epsilon}{\mu}\left(\left[\psi_A \cosh(\kappa x) + \frac{\psi_B - \psi_A \cosh(\kappa L)}{\sinh(\kappa L)} \sinh(\kappa x)\right] - \psi_A + \frac{x}{L}(\psi_A - \psi_B)\right) \tag{3.63}$$

Then take the average using the formula

$$f_{avg} = \frac{1}{b-a}\int_a^b f(x)dx \tag{3.64}$$

Here Equation 3.63 will be averaged from one particle surface $(x = 0)$ to the other $(x = L)$.

$$\beta_{90avg} = \frac{1}{L}\int_0^L \frac{\epsilon}{\mu}\left(\left[\psi_A \cosh(\kappa x) + \frac{\psi_B - \psi_A \cosh(\kappa L)}{\sinh(\kappa L)} \sinh(\kappa x)\right] - \psi_A + \frac{x}{L}(\psi_A - \psi_B)\right) dx \tag{3.65}$$

$$\beta_{90avg} = \frac{\epsilon}{\mu L}\int_0^L \psi_A \cosh(\kappa x) + \frac{\psi_B - \psi_A \cosh(\kappa L)}{\sinh(\kappa L)} \sinh(\kappa x) - \psi_A + \frac{x}{L}(\psi_A - \psi_B) dx \tag{3.66}$$

$$\beta_{90avg} = \frac{\epsilon}{\mu L}\left[\frac{\psi_A}{\kappa}\sinh(\kappa x) + \frac{\psi_B - \psi_A \cosh(\kappa L)}{\kappa \sinh(\kappa L)} \cosh(\kappa x) - \psi_A x + \frac{(\psi_A - \psi_B)}{2L} x^2\right]_0^L \tag{3.67}$$

$$\beta_{90avg} = \frac{\epsilon}{\mu L}\left[\frac{\psi_A}{\kappa}\sinh(\kappa L) + \frac{\psi_B - \psi_A \cosh(\kappa L)}{\kappa \sinh(\kappa L)} \cosh(\kappa L) - \psi_A L + \frac{(\psi_A - \psi_B)}{2L} L^2 - \frac{\psi_A}{\kappa}\sinh(0) - \frac{\psi_B - \psi_A \cosh(\kappa L)}{\kappa \sinh(\kappa L)} \cosh(0) + \psi_A(0) - \frac{(\psi_A - \psi_B)}{2L}(0)^2\right] \tag{3.68}$$

$$\beta_{90avg} = \frac{\epsilon}{\mu L\kappa}\left[\psi_A\left(\sinh(\kappa L) - \frac{\cosh^2(\kappa L)}{\sinh(\kappa L)} - \frac{\kappa L}{2} + \frac{\cosh(\kappa L)}{\sinh(\kappa L)}\right) + \psi_B\left(\frac{\cosh(\kappa L)}{\sinh(\kappa L)} - \frac{\kappa L}{2} - \frac{1}{\sinh(\kappa L)}\right)\right] \tag{3.69}$$

Using the identity $sinh^2(p) - cosh^2(p) = -1$ gives

$$\beta_{90avg} = \frac{\epsilon}{\mu L\kappa}\left[\psi_A\left(\frac{\cosh(\kappa L) - 1}{\sinh(\kappa L)} - \frac{\kappa L}{2}\right) + \psi_B\left(\frac{\cosh(\kappa L) - 1}{\sinh(\kappa L)} - \frac{\kappa L}{2}\right)\right] \tag{3.70}$$

And finally, using the identity $\tanh\left(\frac{p}{2}\right) = \frac{\cosh(p)-1}{\sinh(p)}$ gives the final equation for electro-osmotic conductivity through a pore

$$\beta_{90avg} = \frac{\epsilon}{\mu}(\psi_A + \psi_B)\left(\frac{\tanh\left(\frac{\kappa L}{2}\right)}{\kappa L} - \frac{1}{2}\right) \tag{3.71}$$

Even though this equation has been derived for a channel perpendicular to the applied electric field it will still work for an electric field in any direction as long as the corresponding surfaces potentials ψ_A and ψ_B are calculated based on the orientation. For example, for the case where the applied electric field is parallel to the channel $\psi_A = \psi_B = \zeta$, thus Equation 3.71 reduces to that derived earlier for a parallel channel

$$\beta_{avg} = \frac{2\zeta\epsilon}{\mu}\left(\frac{\tanh\left(\frac{\kappa L}{2}\right)}{\kappa L} - \frac{1}{2}\right) \tag{3.72}$$

3.8.3 Calculating Equivalent Surface Potentials

The equivalent surface potentials ψ_A and ψ_B will depend on the orientation and the intensity of the applied electric field (see **Figure 3.8**). One of the potentials will remain the same as the clay particle's actual surface potential, known as the zeta potential. The other will change to produce an equivalent electric field across the width of the pore.

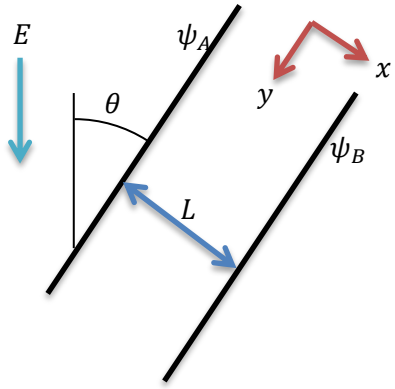

Figure 3.8 Orientation θ of pore channel with respect to applied electric field E.

The equivalent electric field in the y-direction drives flow through the channel and can be calculated as

$$E_y = Ecos(\theta) \tag{3.73}$$

The equivalent electric field in the x-direction does not drive flow through the channel but influences the double layer potential distribution. From this the equivalent surface potentials ψ_A and ψ_B can be calculated.

$$E_x = Esin(\theta) = \frac{(\psi_A - \psi_B)}{L} = \frac{\Delta\psi}{L} \tag{3.74}$$

From this, the change in necessary in one of the surface potentials can be calculated as

$$\Delta\psi = ELsin(\theta) \tag{3.75}$$

Thus, the surface potentials can now be calculated

$$\psi_A = \zeta + \Delta\psi \tag{3.76}$$

And

$$\psi_B = \zeta \tag{3.77}$$

The channel spacing *L* can be calculated from common soil properties where the variable *w* represents the typical particle thickness

$$L = wG_s\omega \tag{3.78}$$

3.8.4 Calculating the Electro-Osmotic Conductivity for Anisotropic Clay

The electro-osmotic conductivity can now be calculated for a typical clay under and applied electric field using a weighted average of the conductivity through parallel and

perpendicular channels. Combing Equations 3.71, 3.72, and 3.75-3.77 and setting $\theta = 90°$ for perpendicular channels gives

$$\beta = \frac{\epsilon}{\mu} * \left(\frac{\tanh\left(\frac{\kappa w G_s \omega}{2}\right)}{\kappa w G_s \omega} - \frac{1}{2} \right) * \frac{P(2\zeta) + Q(2\zeta + E w G_s \omega)}{P + Q} \tag{3.79}$$

This model describes the electro-osmotic conductivity for a saturated clay soil based on the properties of the clay ($w, G_s, \omega, \zeta, P, and\ Q$), the properties of the pore fluid ($\epsilon, \mu, and\ \kappa$), and the applied electric field (E). Most of these quantities are simple to test for or estimate or are usually available in the literature. The anisotropy coefficients P and Q must be tested for since they will depend on the clay's loading history. This new model can provide useful estimates of flow using the classical equation for flow through soil under an electric field (Mitchel and Soga, 2005)

$$q = AE\beta \tag{3.80}$$

3.8.5 Laboratory Test for Anisotropy of Electro-Osmotic Conductivity

Equation 3.79 suggests that the electro-osmotic conductivity might be a vector, whereas it's used as a scalar in the geotechnical profession. A qualitative laboratory test was performed to measure the value of the electro-osmotic conductivity for a soil when an electric field is applied in different directions. The soil used was commercially available brown kaolin with a liquid limit of 90. To prepare the soil for testing, it was thoroughly mixed with water to the liquid limit and slowly preloaded to 200 kPa.

To consolidate the soil a Teflon cylinder was used. The cylinder was closed on the bottom by a porous electrode plug that applies a voltage but also allows for water drainage. The top of the cylinder has an extractable electrode with similar setup. Load can then be applied on the top electrode to imitate stress conditions in the field. To track the settlement of the sample high precision GeoJac® settlement probes are placed on top of each cylinder.

The samples were consolidated using electro-osmosis with and without a membrane and applying an electric field corresponding 160 V/m. One test received a vertical electric field, in the same direction as the overburden pressure. The other received a horizontal electric field through a modified electrode and drain built into the wall of the cylinder. The settlement was tracked for each. The test was terminated after 40 hours.

The results for the settlement tests using electro-osmosis in different directions are shown in **Figure 3.9**. The test where a horizontal electric field was applied shows a significantly higher settlement. This is likely the case because the soil fabric is expectedly dispersed. Since the soil was mixed with water to the liquid limit and slowly consolidated to a high pressure, the clay particles would have tended to consolidated in a dispersed arrangement rather than flocculated. This means the hydraulic conductivity will be greater horizontally. As **Figure 3.9** shows, this is also the case for the electro-osmotic conductivity. Since the fabric is dispersed, most of the pores are aligned somewhat parallel to the applied electric field, providing the highest equivalent electric field, as equation 3.73 shows.

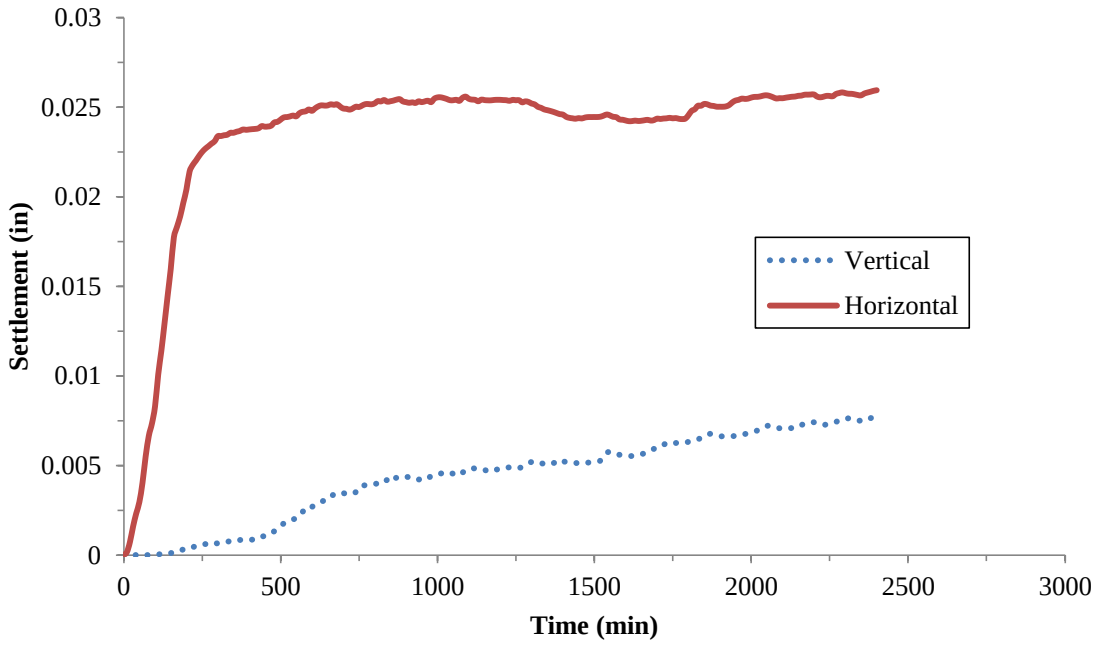

Figure 3.9 Settlement under a horizontal and vertical applied electric field.

3.9 Conclusions

The conventional model for the electro-osmotic conductivity of clayey soils is limited and does not consider important aspects of the clay-pore-water system. A new model was developed based on colloidal chemistry literature that better describes the flow of water between clay particles due to an electric gradient. The main contribution of this adapted model is that it considers the properties of the pore electrolyte. It also has more explanatory power; in essence, it can provide insight into why injection of saline solutions to the soil has been reported to improve electro-osmotic consolidation. The model also might be able to correct our understanding about the influence of pore sizes on electro-osmotic flow through soils. The model has also been expanded to account for the anisotropy of natural soils, making it possible to obtain more accurate predictions of

the utility of electro-osmotic consolidation for a particular soil as well as enriching our understanding of the mechanism at play during electro-osmotic consolidation.

The theoretical and experimental work described in this chapter leads to and demonstrates an important conclusion. The electro-osmotic conductivity is a vector. It is different horizontally and vertically for a given soil. This has important implications for the application of electro-osmotic consolidation in field applications. The clay soil fabric plays a significant role and should be investigated. It is possible that for some cases where electro-osmosis shows low efficiency simply changing the direction of the applied electric field could improve the results significantly. Based on this new insight, the performance of electro-osmosis can be assessed more accurately.

CHAPTER 4

ELECTRO-OSMOSIS AND SECONDARY CONSOLIDATION

4.1 Introduction

There is much that is still not understood about the mechanisms taking place during electro-osmotic consolidation. One such issue is what known type of work is electro-osmosis replacing, if any. If electro-osmosis is creating an effect currently achieved through other methods, then comparing and quantifying the efficiency of electro-osmotic consolidation is simple. However, if it is creating a whole new effect then measuring its usefulness, especially in field applications, becomes more difficult. It is proposed in this section that electro-osmosis has similar effects to secondary consolidation. Therefore, a comparison can be made and more accurate conclusions can be drawn about the efficiency of treating a soil with electro-osmosis. The contents of this chapter are being published in Martin and Meegoda 2019d.

4.2 Soil Compression

When foundation structures are built, they cause an increase in stress on the soil below them. This leads to compression of the soil mass. In general, this compression is observed in three ways

a. Ejection of water or air from the space between solid particles (voids);
b. Deformation of the solid particles; and
c. Relocation of soil particles.

According to Das and Sobhan 2018 settlement can be categorized as follows:

1. Elastic settlement (or immediate settlement), which is caused by the elastic deformation of dry soil and of moist and saturated soils without any change in the moisture content. This is mostly relevant in granular soils.

2. Primary consolidation settlement, which is the result of a volume change in saturated cohesive soils because of expulsion of the water that occupies the bulk of the void spaces.

3. Secondary consolidation settlement, which is observed in saturated cohesive soils and organic soil and is the result of the plastic adjustment of soil fabrics. It is an additional form of compression that occurs at constant effective stress over time. It is relatively slow but can be very significant depending on the type of soil.

When dealing with clays, primary and secondary consolidation typically govern any settlement considerations. Primary consolidation occurs relatively quickly under a new pressure due to the generation of excess pore water pressures and results in the removal of water molecules that are in the bulk part of the pore spaces. Once the excess pore water pressures are dissipated, primary consolidation ends and no more settlement of that kind is observed. Secondary consolidation on the other hand will continue to occur indefinitely and is generally understood to consist in the removal of water molecules that are chemically or otherwise attached to the solid particles. In the case of organics, which are composed of high amounts of water, significant secondary consolidation settlements are observed as they break down and release the water molecules that composed their organic structure. In the case of pure clays, water is chemically bonded to the particles in the double layer. This water is tightly held to clays and will not be released under stresses caused by an applied load, but will usually slowly do so over a long period of time. Depending on the type of clay, the double layer water content can be significant. For example, in the case of Na-montmorillonite the soil can easily reach water contents in the hundreds. The magnitude of the secondary consolidation is calculated as

$$S_s = \frac{H}{1 + e_p} C_\alpha \log\left(\frac{t_2}{t_1}\right) \tag{4.3}$$

4.3 Electro-Osmosis and Secondary Consolidation

Theoretically, applying an electric field to a clay soil should mobilize the water molecules in the particle double layer. Electro-osmosis does not mobilize water in the bulk of the pore because positive and negative ions are balanced, resulting in zero net flow. As shown in Chapter 1, this is evidenced by the fact that electro-osmosis can achieve drainage and settlement even after primary consolidation has finished, without any changes in pore water pressure. This suggests that electro-osmosis has a similar effect to secondary consolidation. If so, electro-osmotic consolidation could be used as a much quicker alternative to secondary consolidation efforts.

Primary and secondary consolidation tests were carried out on a sample of kaolin. The samples were consolidated to a pressure of 37.2 kPa and then allowed to undergo secondary consolidation for up to 2 months. This was carried out using a traditional one dimensional consolidation frame. Then, the load was doubled twice to induce new primary consolidation and study the trends of void ratio versus pressure.

At the same time, several electro-osmotic consolidation tests were carried out at different voltages. The same loading schedule was applied before and after electro-osmosis. This resulted in a variation of void ratio versus pressures for different voltages and for different secondary consolidation schedules.

4.4 Results and Discussion

Figure 4.1 shows the results for the consolidation tests in a void ratio versus pressure plot. The secondary consolidation tests exhibit a change in void ratio that is constant across different pressures. This corroborates that primary and secondary consolidation drained portions of the pore water. After adding additional load to a secondary consolidation test, the primary consolidation reveals an almost identical compression index as the test with only primary consolidation. The test that allowed for 2 months of secondary consolidation shows only minor improvements over 1 month, which is consistent with typical secondary consolidation tests. The process is very slow. After applying electro-osmosis, the effects are very similar to secondary consolidation but with a significantly higher change in void ratio. Additionally, the compression index remains almost the same before and after electro-osmosis. This is evidence that electro-osmotic consolidation has a similar effect as secondary consolidation. Only the test with 10 volts was reloaded for additional primary consolidation. Tests using other voltages were simply plotted to show the trend of change in void ratio with voltage. Compared to settlement due to primary consolidation, the test using 15 volts achieves a settlement equivalent to that caused by a surcharge load of 7.5 feet of soil in a 20 feet deep normally consolidated Kaolin clay.

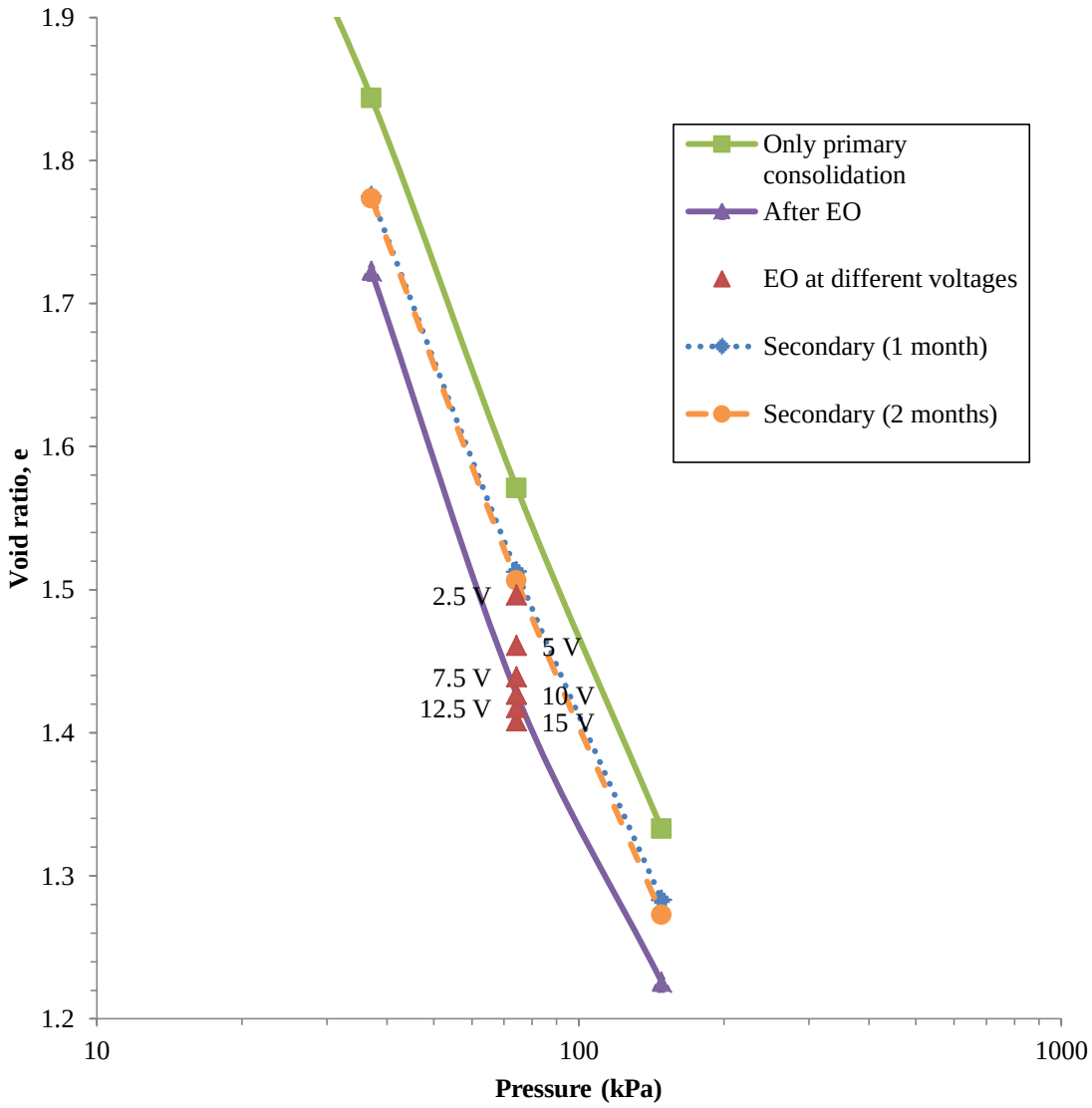

Figure 4.1 Settlements after primary, secondary, and electro-osmotic consolidation.

Figure 4.2 shows a time versus void ratio plot. This graph can be used to calculate the secondary compression index C_α, which had a value of 0.0243. This is within the typical range for normally consolidated clays (Das and Sobhan 2018). After about 24-36 hours, primary consolidation was completed and a voltage was applied for the electro-osmosis tests. This caused a steady decrease in void ratio (not shown) until a

final void ratio was reached (shown) usually within 48 hours. The graph demonstrates that for all the applied electric fields, electro-osmosis provided higher and quicker consolidation than the secondary consolidation period tested. However, the electro-osmosis tests reached a final void ratio, after which no further change was observed. This is caused by the different problems discussed in Chapter 2.

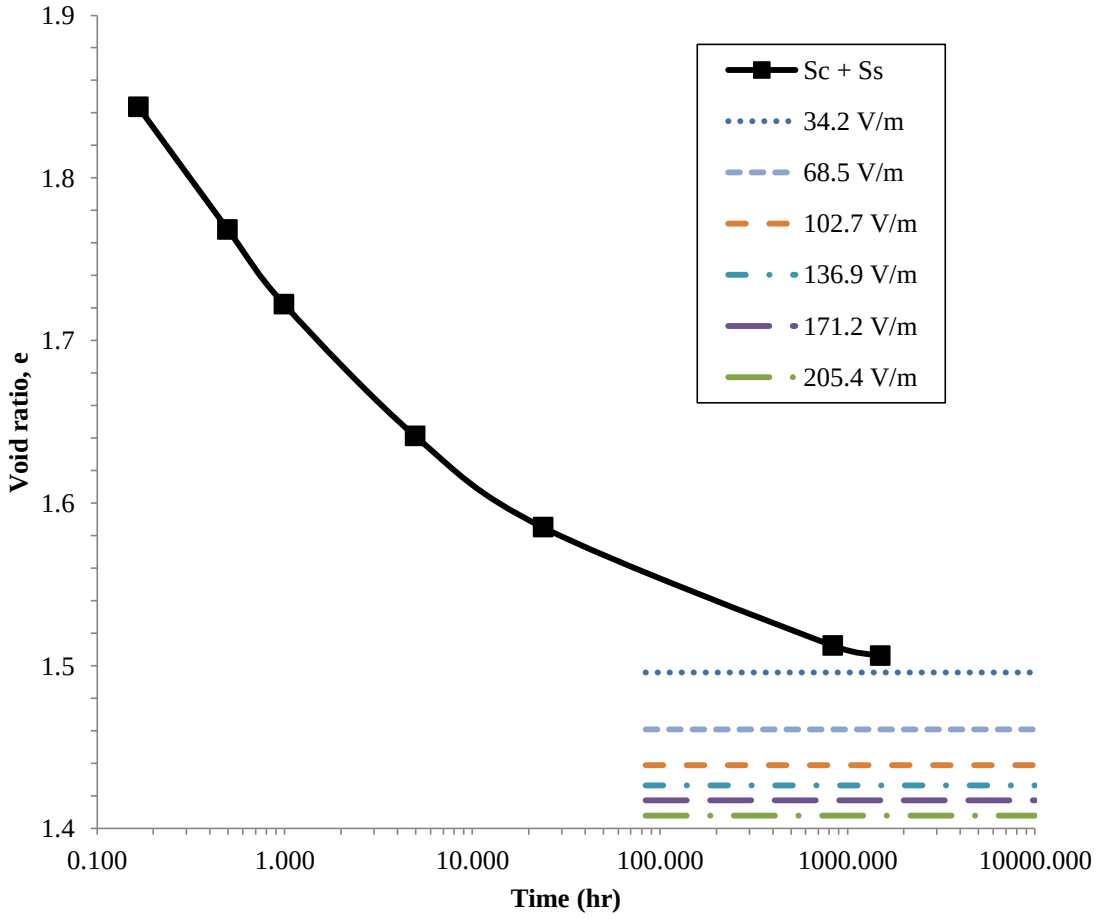

Figure 4.2 Secondary consolidation settlement and final settlement for electro-osmotic consolidation at different voltages.

Since secondary consolidation will continue to develop over time with no limit in a reasonable time scale, after some time it will reach the same void ratio changes as electro-osmosis. Using the secondary compression index, the time ratio for secondary

consolidation to achieve the same consolidation as electro-osmosis at different applied electric fields was calculated and shown in **Figure 4.3** in a log-log graph. The electric field values were nondimensinalized using the lowest electric field applied, $E_0 = 34.2\,V/m$. A trend line can be created to fit the data with an R^2 value of 0.998. This gives a relationship between the desired time that can be saved from secondary consolidation and the required voltage to achieve the needed change in void ratio. This relationship is governed by the equation

$$\frac{t_2}{t_1} = 1342\left(\frac{E}{E_0}\right)^{4.65} \tag{4.2}$$

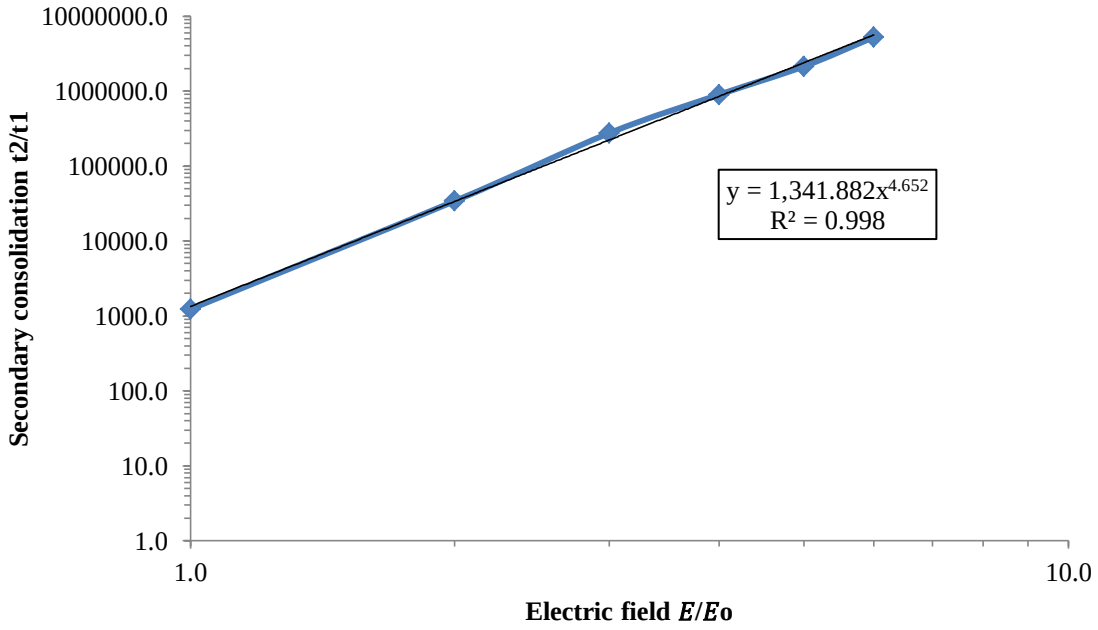

Figure 4.3 Relation between electro-osmotic consolidation at different applied electric fields and time required for an equivalent secondary consolidation.

Equation 4.2 is equivalent to

$$\log\left(\frac{t_2}{t_1}\right) = 4.65\log\left(\frac{E}{E_0}\right) + 3.13 \tag{4.3}$$

This can them be substituted into equation 4.1 to give

$$S_{EO} = \frac{H}{1+e_p} C_\alpha \left[4.65\log\left(\frac{E}{E_0}\right) + 3.13\right] \tag{4.4}$$

Here S_{EO} is the settlement caused by electro-osmosis. This is a significantly valuable relationship. It can be used to predict which voltage is necessary to achieve a desired degree of equivalent secondary consolidation using electro-osmosis requiring only simple laboratory tests for the secondary compression index and initial void ratio. Since electro-osmosis is completed in a minute fraction of the time secondary consolidation takes, and since their effects are similar in nature, this relationship can provide sufficient grounds for considering electro-osmosis as a viable option in the field. Electro-osmosis can effectively reduce soil preparation time for construction, by many years in some cases, in just a few days.

4.5 Conclusions

Secondary consolidation and electro-osmotic consolidation are shown to have similar effects in draining pore water from a kaolin clay both theoretically and experimentally. This suggests that a direct comparison is possible. Several tests were carried out to find the consolidation prowess of each technique. It was found that electro-osmosis provided

superior results and in a significantly shorter time. Additionally a relationship was found that allows the user to predict the voltage required to achieve the equivalent change in void ratio using electro-osmosis as a certain secondary consolidation. This new understanding has potential to reinvigorate the study of electro-osmosis. It also provides a clearer basis for comparing the efficiency of electro-osmotic consolidation. In this research, only one type of lab soil was used. Therefore, more extensive testing on different soils, especially field soils, is required to make wide ranging predictions. However, this lays the foundation for that work and demonstrates that electro-osmosis is relatable to known methods of consolidation.

CHAPTER 5

ION EXCHANGE MEMBRANES

5.1 Introduction

Electro-osmotic consolidation has long been of interest in the research community due to its potential to improve on current methods of clay soil consolidation. Unfortunately, as described in previous chapters, many problems hamper the process, especially the quick and drastic changes in pH in the soil around the electrodes. Many methods have been studied to remedy this problem with various levels of success but more work is needed to make electro-osmosis a viable option for consolidation of clays.

A potential solution is the use of ion exchange membranes to filter hydrogen ions. An ion exchange membrane (IEM) is a non-porous, membranous functional polymer having ionic groups. This technology has the potential to improve electro-osmotic consolidation by regulating the flow of ions resulting from hydrolysis at the electrodes. In the case of the anode, an anion exchange membrane (AEM) can be used to restrict the flow of hydrogen ions into the soil. This prevents the pH from decreasing and the zeta potential can be maintained at a higher level. Similarly, a cation exchange membrane (CEM) can be used at around the cathode to isolate hydroxyl ions so that they won't migrate into the soil and cause precipitation of metallic ions and clogging of the pores. The contents of this chapter are being published in Martin and Meegoda 2019a and Martin and Meegoda 2019e.

Ion exchange membranes differ from other polymer films in having charged groups, anionic and/or cationic, that are fixed on the polymer film. The particular

properties of the ion exchange membrane arise from the existence of the charge. The ion exchange membrane is ion conductive, namely, ions can permeate through the membrane together with water molecules. Because ion exchange membranes have ionic groups which are hydrated, these membranes are hydrophilic. Their characteristics are primarily decided according to the amount (ion exchange capacity) and species of the charged groups and their distribution in the membrane, and the amount of water molecules adsorbed on the membrane due to these groups (water content). The main characteristics of the membrane are:

1. Ion conductivity,
2. Hydrophilicity and
3. The existence of fixed carrier (ion exchange groups).

According to these characteristics, various applications have arisen. The most common of these is electro-dialysis, which is used in seawater desalination, industrial wastewater treatment of highly scaling waters, food and beverage production, and other industrial wastewaters treatments. IEM can improve electro-osmotic consolidation by preventing the flow of hydrogen ions into the soil so that no deterioration of clay particles' chemical and electrical properties occurs.

In ion exchange membranes, charged groups are attached to the polymer backbone of the membrane material. These fixed charge groups partially or completely exclude ions of the same charge from the membrane. This means that an anionic membrane (AEM) with fixed positive groups excludes positive ions but is freely permeable to negatively charged ions (see **Figure 5.1**).

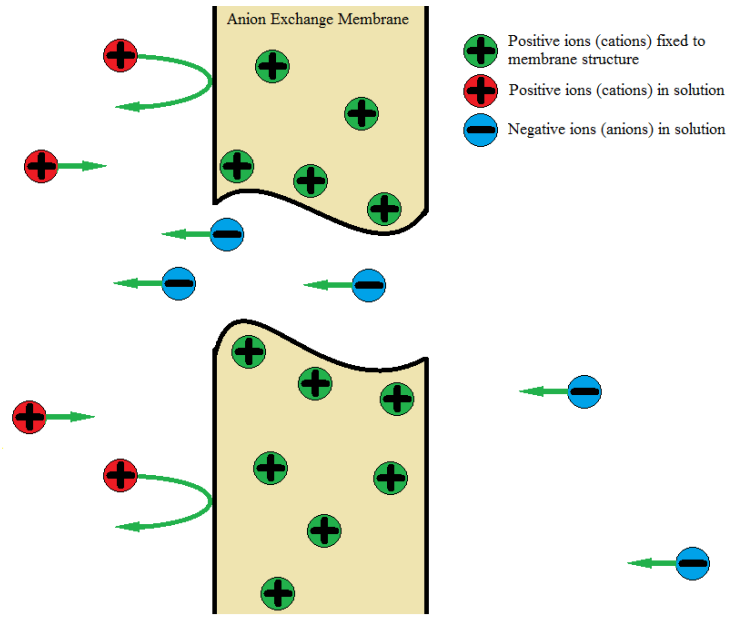

Figure 5.1 Anion exchange membrane excludes co-ions and allows movement of counter-ions.

Similarly, a cationic membrane (CEM) with fixed negative groups excludes negative ions but is freely permeable to positively charged ions. Ions that are rejected by the membrane are termed co-ions, since they share the charge type with the exchange groups of the membrane, while ions that are able to ion exchange into the membrane are called counter-ions. Ion exchange using membranes is based on the competitive adsorption between two ions at a charged surface. This process is reversible; the ion exchanger can be regenerated or loaded by washing with the appropriate ions (Giorno et al. 2015). The selectivity of the membranes is due to Donnan equilibrium and Donnan exclusion, and not due to physically blocking or electrostatically excluding specific charged species (Tanaka 2003).

5.2 Donnan Equilibrium

Donnan equilibrium, also known as the Gibbs–Donnan effect, refers to the behavior of ions near a semipermeable membrane. These ions fail to distribute evenly on both sides because some of the ions cannot cross the boundary. The presence of a different charged substance that is unable to pass through the membrane creates an uneven electrical charge. Equilibrium occurs when the electric gradient driving the movement of ions is balanced by a concentration gradient that generates diffusion. In the case of an ion exchange membrane there are fixed ionic groups that are attached to the polymer structure of the membrane and thus act as the impermeable ions. This effect is explained below.

An ion exchange membrane is placed next to a balanced solution of ions (see **Figure 5.2a**). In the membrane quaternary ammonium groups are bonded to the polymer structure, making it an anion exchange membrane. This restricts the flow of co-ions (cations) and stimulates the flow of counter-ions (anions). Chloride ions have migrated into the membrane during the membrane preparation process. On the solution side, there are chloride and potassium ions in concentrations that are equimolar with the ions in the membrane side.

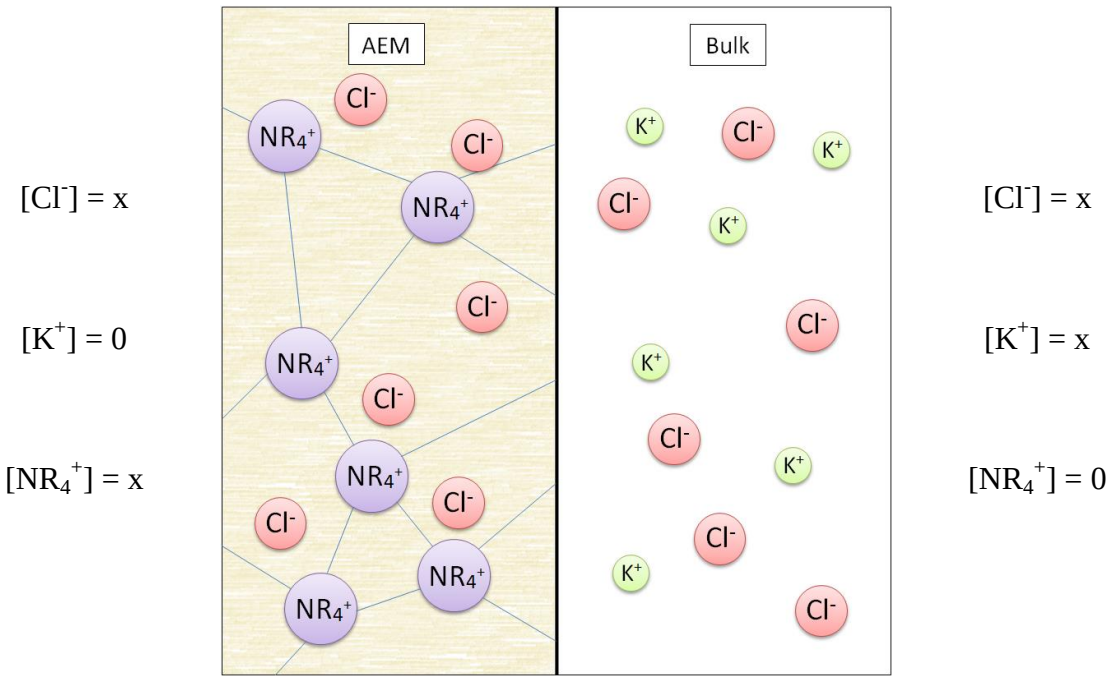

Figure 5.2.a Pretreated ion exchange membrane is introduced into a KCl solution.

Since the membrane side does not contain any potassium ions, these migrate into the membrane from the bulk side along a concentration gradient (see **Figure 5.2b**). The presence of positive potassium ions and quaternary ammonium ions makes the membrane side electro-positive with respect to the bulk side and creates an electrical potential difference.

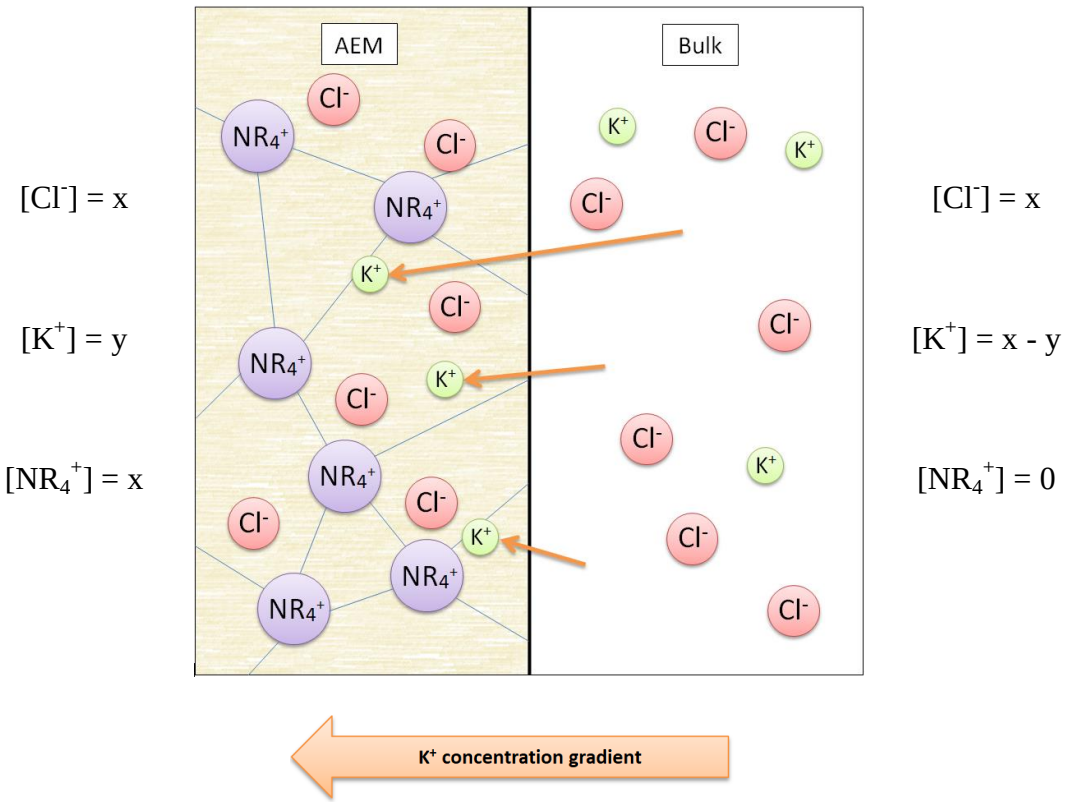

Figure 5.2.b K^+ ions move due to a concentration gradient.

The development of positive charge on the membrane side creates an electrical potential gradient that counter balances the concentration gradient for potassium ions, preventing the concentrations of potassium from becoming equal on both sides (see **Figure 5.2c**).

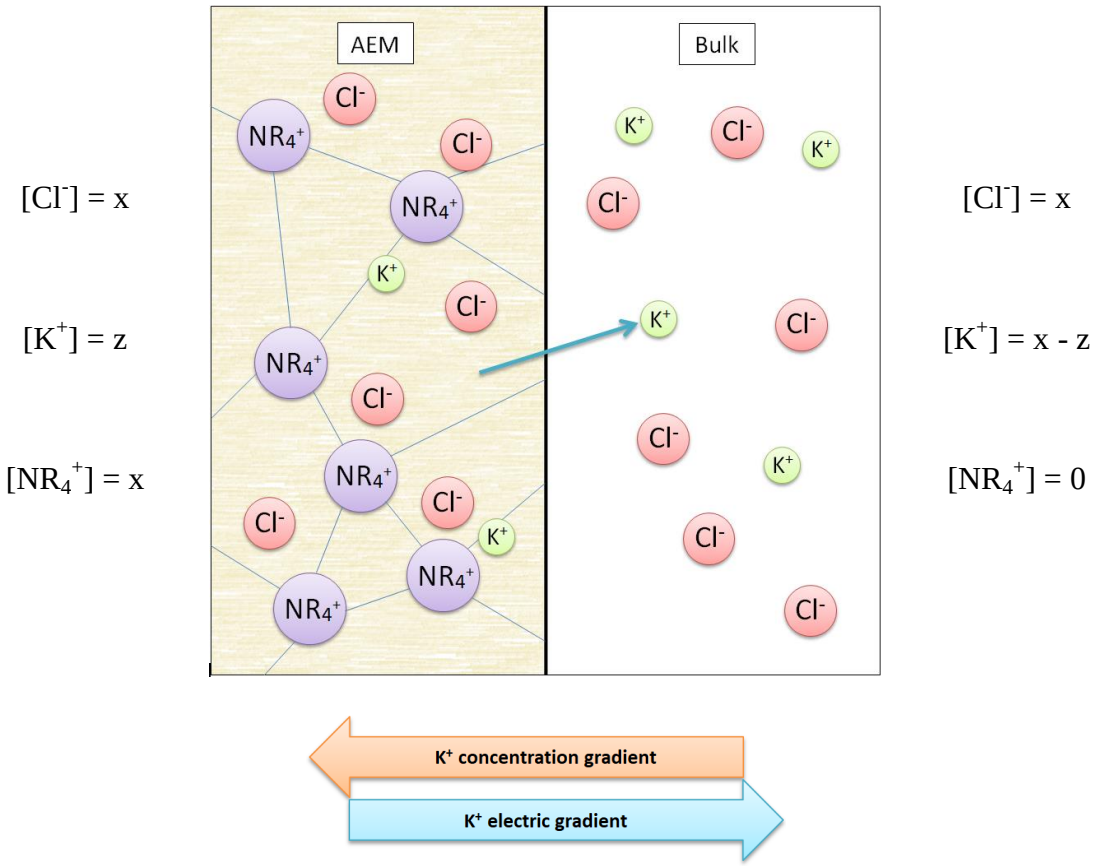

Figure 5.2.c K^+ ions move due to an electrical gradient.

Simultaneously, the net positive charge in the membrane side attracts the chloride ions from the bulk side to migrate into the membrane along an electrical gradient (see **Figure 5.2d**).

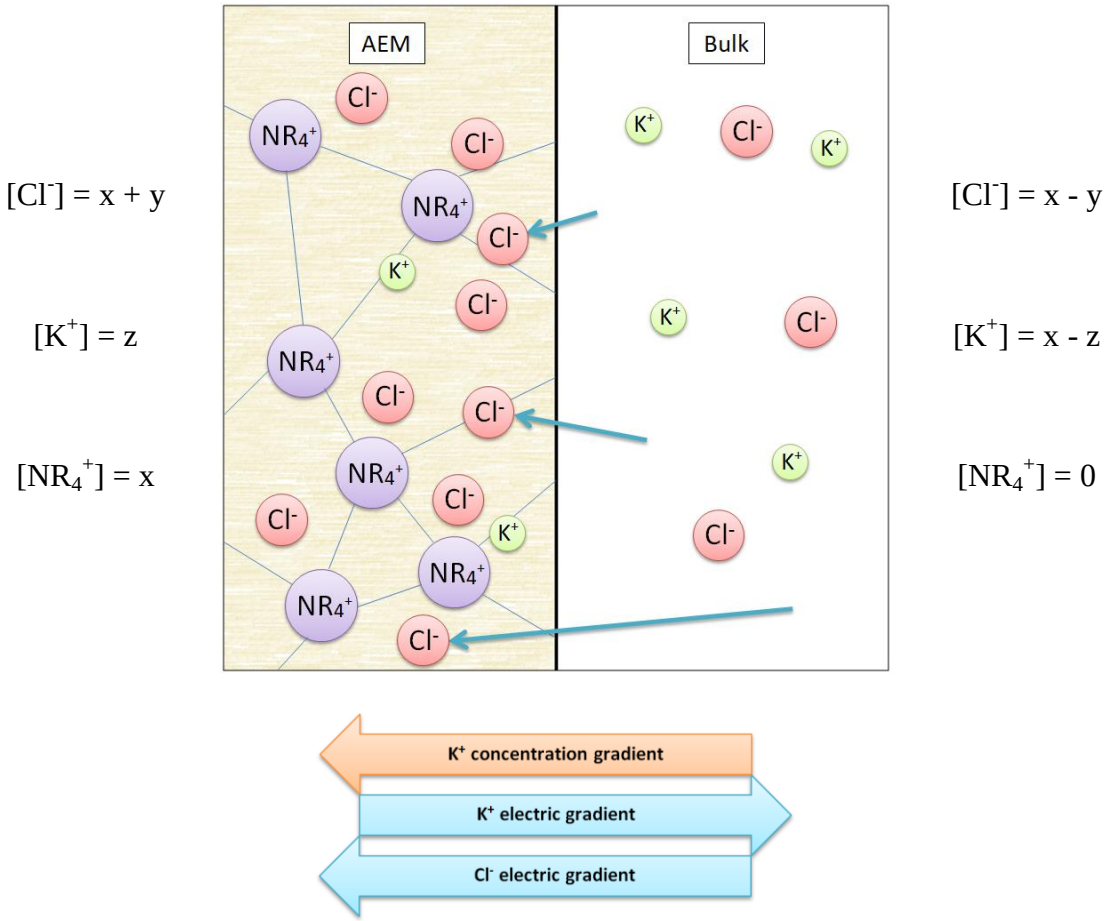

Figure 5.2.d Cl^- ions move due to an electrical gradient.

The concentration of chloride ions on the membrane side now exceeds that of the bulk side, and potassium ions will migrate from the membrane side to the bulk side along a concentration gradient (see **Figure 5.2e**).

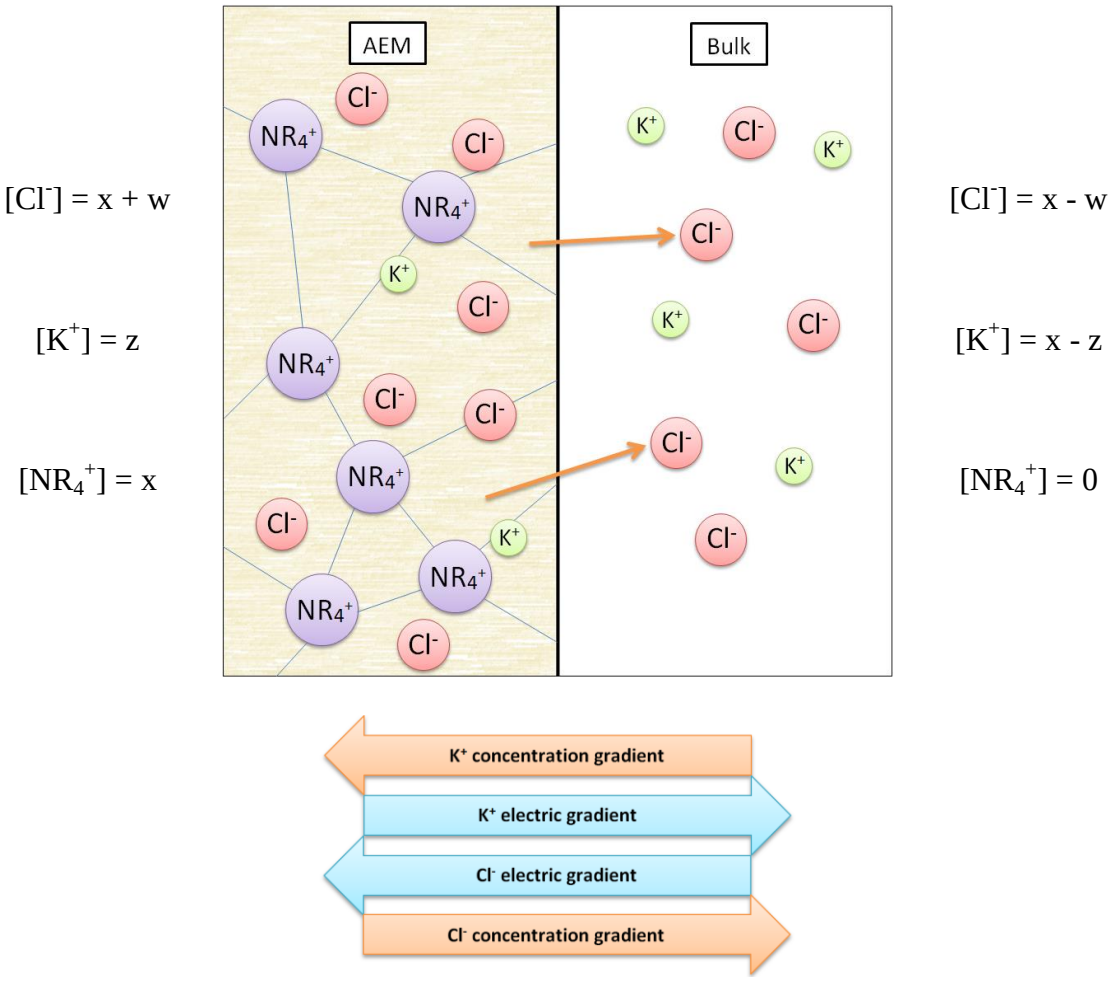

Figure 5.2.e Cl^- ions move due to a concentration gradient.

At equilibrium, the competing concentration and electric gradients for each ion are in balance (see **Figure 5.2f**). And there is no net flow of ions through the membrane. Chloride ions and potassium ions move back and forth between the membrane side and the bulk side in response to the electrochemical gradients such that each side remains electrochemically neutral within itself due to equimolar concentrations of cations and anions.

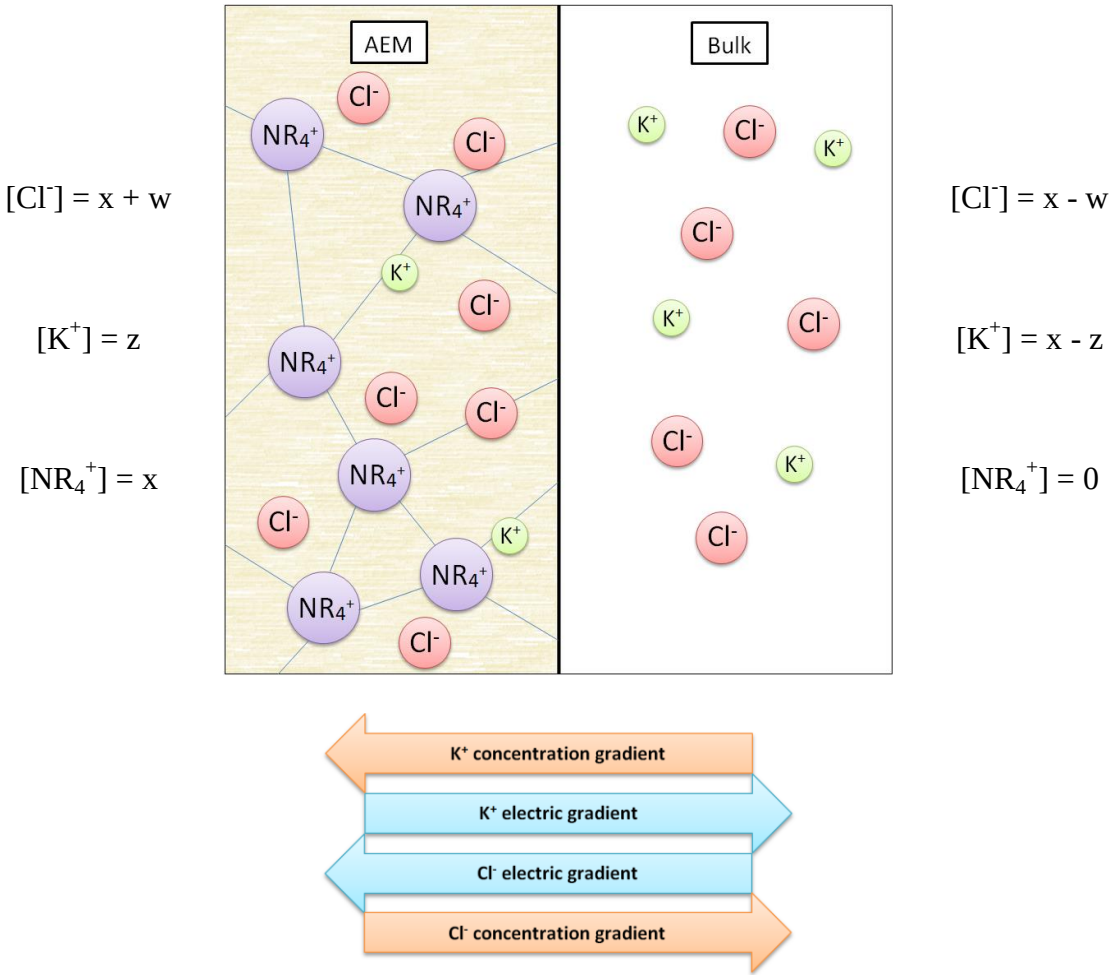

Figure 5.2.f Donnan equilibrium.

Between the two sides, there is an unequal distribution of permeable ions. This imbalance creates an electrical charge across the membrane boundary. In the above case, the bulk side is negative to the side with the impermeable cations. The voltage gradient at which an ion is in equilibrium with its diffusion gradient is called the Donnan potential. Applying an electric field will increase the electric potential gradients that drive ions movement.

5.3 Membrane Types and Properties

Ion exchange membranes can be classified based on their function, since this is dependent on the membranes' properties.

1. Cation exchange membranes, which have cation exchange groups (anionic charged groups), and cations selectively permeate through the membranes,
2. Anion exchange membranes, which have anion exchange groups (cationic charged groups), and anions selectively permeate through the membranes,
3. Amphoteric ion exchange membranes, in which there are both cation and anion exchange groups at random throughout the membranes,
4. Bipolar ion exchange membranes which have a cation exchange membrane layer and anion exchange membrane layer (bilayer membranes),
5. Mosaic ion exchange membranes, which have domains with cation exchange groups over cross-sections of the membranes and also domains of anion exchange groups. An insulator may exist around the respective domains.

Depending on the desired application, the properties of the membrane that are of interest will vary. Some of these are described in **Table 5.1**, based on typical specifications sheets for commercial membranes.

Table 5.1 Membrane Properties

Property	Description	Example / typical values	
		Units	Value
Membrane type	Membrane's function		anion exchange
Counter ion	Balancing fixed ions groups during shipment and storage before first use		Bromide (Br-)
Delivery form	Describes how the membrane will be shipped to customer. Can be either dry or wet and has implications for storage and preparation before use.		dry
Thickness (dry)	Thickness of the membrane sheet. Might change slightly when the membrane is hydrated	µm	110 – 140
Weight per unit area	Weight per unit area	mg/cm^2	10 – 13
Ion exchange capacity (in Cl^- form)	Related to the concentration of fixed charges in the membrane structure, it describes the ability of the membrane to attract counter ions and repel	meq/g	0.7 – 1.0
Area resistance	Resistance times cross-sectoinal area	$\Omega\ cm^2$	5.0 – 20.0
Specific conductivity	Measures a material's ability to conduct an electric current	mS/cm	1.0 – 2.5
Selectivity (e.g. in 0.1 / 0.5 mol/kg KCl at T = 25 °C)	Transport number of counter-ions in the membrane	%	93 – 98
Uptake in H_2O at T = 25 °C	Water content after preparation	wt %	5 – 15
Dimensional swelling in H_2O at T = 25 °C	Dimensional changes due to preparation	%	0 – 1
Proton transfer rate	Leakage rate of protons through AEMs due to interfacial transfer reactions	µmol/(min*cm^2)	60 - 400

5.4 Permselectivity

Permselectivity, which is a key property of IEMs, refers to the restriction of permeation of ions across a boundary or membrane wall on the basis of charge. The ion concentrations inside the membrane especially that of co-ions, is important for the membrane's permselectivity. A fully permselective membrane would completely exclude co-ions. This exclusion is termed the Donnan exclusion. The permselectivity of the membrane ($\psi^{membrane}$) can be calculated from the transport number of the counter-ions in the membrane ($T_{counter-ion}^{membrane}$) and the counter-ions ($T_{counter-ion}$) and co-ions ($T_{co-ion}$) of the outside solutions (Giorno et al. 2015):

$$\psi^{membrane} = \frac{T_{counter-ion}^{membrane} - T_{counter-ion}}{T_{co-ion}} \tag{5.1}$$

Under an applied electric field, the current carried by anions and cations is not necessarily equal. The transport number of a species is the fraction of the current carried by that species. Because of the Donnan effect, there is a very low concentration of co-ions in the membrane, thus they carry a very small portion of the current. Their transport numbers are usually between 0 and 0.05. Counter-ions on the other hand are abundant in the membrane and their transport numbers of these ions are around 0.95 to 1.0 (Baker 2004).

5.5 Limiting Current Density

Due to the great majority of counter-ions in the membrane the transport number of the counter-ions in the membrane is much higher than that of the counter-ions in the bulk

solution. As a consequence, a diffusion boundary layer is formed on both sides of the membrane. A conceptual concentration profile can be drawn as seen in **Figure 5.3** for an anion exchange membrane in steady state conditions.

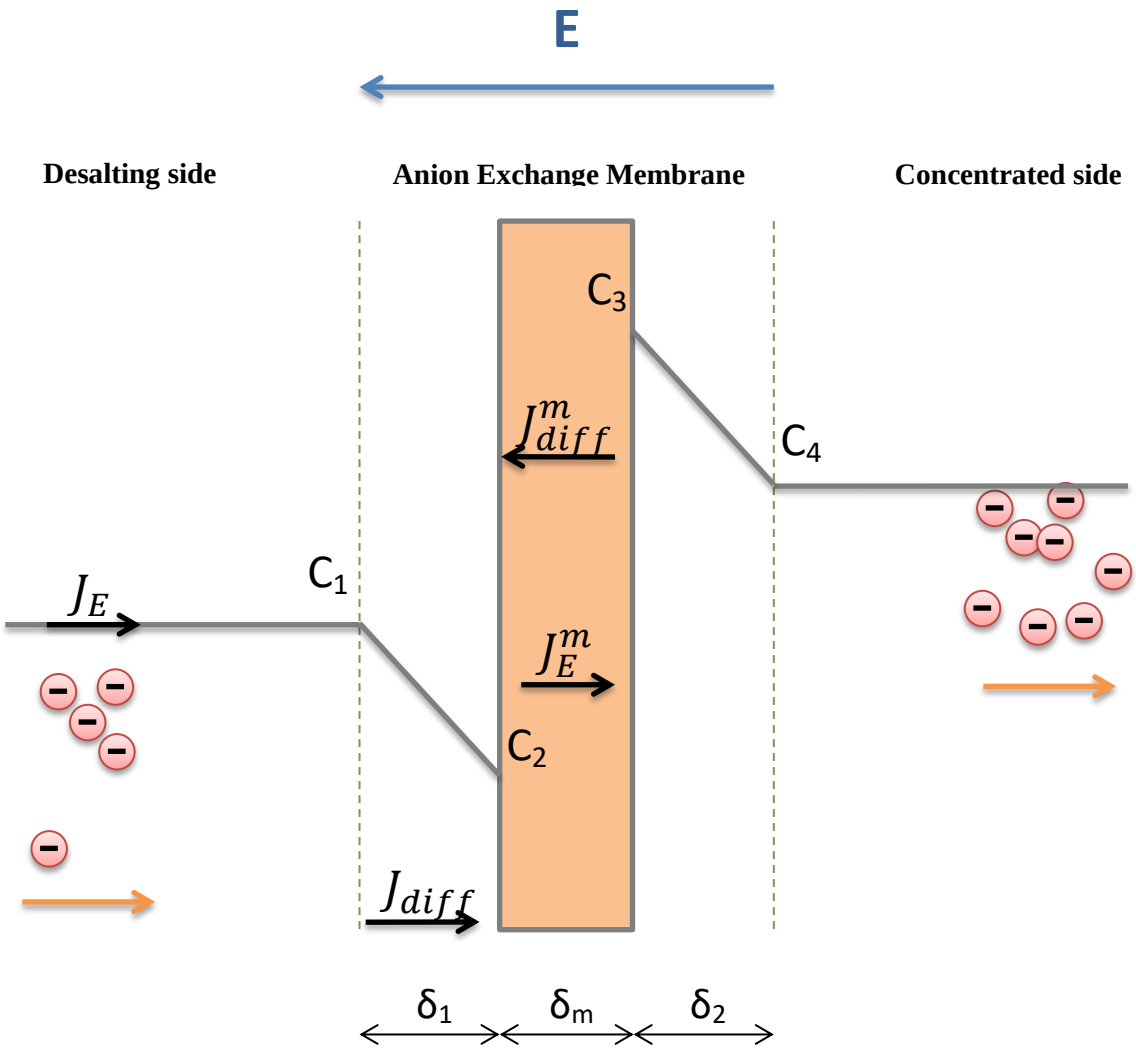

Figure 5.3 Conceptual concentration profile of counter-ions around an anion exchange membrane.

The mass balance equation for the anions moving from the desalting side into the membrane can be written as,

$$J_E + J_{diff} - J_{diff}^m = J_E^m \tag{5.2}$$

Hence, each of the flux values are

$$\frac{ia_-}{F} + \frac{D(C_1 - C_2)}{\delta_1} - \frac{D^m(C_3 - C_2)}{\delta_m} = \frac{ia_-^m}{F} \tag{5.3}$$

Where C_1, C_2, C_3, and C_4 are the anion concentrations in the desalting solution, in the membrane-desalting side interface, in the membrane-concentrated side interface, and in the concentrated solution, respectively. The mass balance can be rearranged as,

$$i = \frac{FD(C_1 - C_2)}{\delta_1(a_-^m - a_-)} - \frac{FD^m(C_3 - C_2)}{\delta_m(a_-^m - a_-)} \tag{5.4}$$

In general, the diffusion coefficient of the anions in the desalting solution is much greater than that in the membrane (Baker 2004). Thus the equation can be simplified to,

$$i = \frac{FD(C_1 - C_2)}{\delta_1(a_-^m - a_-)} \tag{5.5}$$

As the current density increases, C_2 will increasingly decay and eventually become virtually zero at higher currents. The current threshold at which C_2 is zero is called the limiting current,

$$i_{lim} = \frac{FDC_1}{\delta_1(a_{-}^{m} - a_{-})} \tag{5.6}$$

When electro-osmotic flow is carried out at a higher current than the limiting current density, water splitting will occur on the desalting side to provide ions to carry the charge. This will cause pH changes in the solution. In the above case, hydrogen ions (protons) will be generated and move towards the cathode. If the purpose of the membrane was to block the flow of protons, it is imperative to work at currents below the limiting current.

Two variables have a significant effect in maintaining a sufficiently high limiting current. First, the concentrations of counter-ions in the desalting (C_1) side needs to be sustained. If this depletes, the limiting current will also drop significantly. Second, the thickness of the diffusion boundary layer should be minimized. This depends on the structure of the system and the operating conditions. The limiting current can be determined by measuring the current-voltage relationship of the system.

5.6 Determination of Limiting Current Density

The limiting current density of ion exchange membranes has been studied for many decades, almost from the inception of ion exchange membranes. The basic method of determining its value has remained virtually the same (Sata et al. 1969). When a current is applied to the testing cell, the drop in voltage across the cell can be related as,

$$V = RI + V_e + V_c + V_p \tag{5.7}$$

Where RI is the ohmic drop, V_e is the electrode potential, V_c is the concentration potential, and V_p is the polarization potential. If we divide the equation by the applied current, I, we can get the following expression,

$$\frac{V}{I} = R + \frac{(V_e + V_c + V_p)}{I} \tag{5.8}$$

Here R is the resistance of the cell. For a given test with an applied current, the voltage can be measured, thus obtaining a plot of the voltage to current ratio and the current itself. A typical graph is shown in **Figure 5.4.a** below (Cowan and Brown 1959). As the current increases, the ratio of voltage to current will decrease somewhat uniformly. At some value of current, the voltage current ratio will develop a change in slope. This is due to a drop in efficiency in transporting electrolyte ions. When the limiting current is exceeded, some energy must be spent on splitting water molecules to create sufficient ions to carry the current. The negative slope of the initial part of the graph can be extended to intersect the positive slope of the second part of the graph. The point at which they intercept is defined as the limiting current.

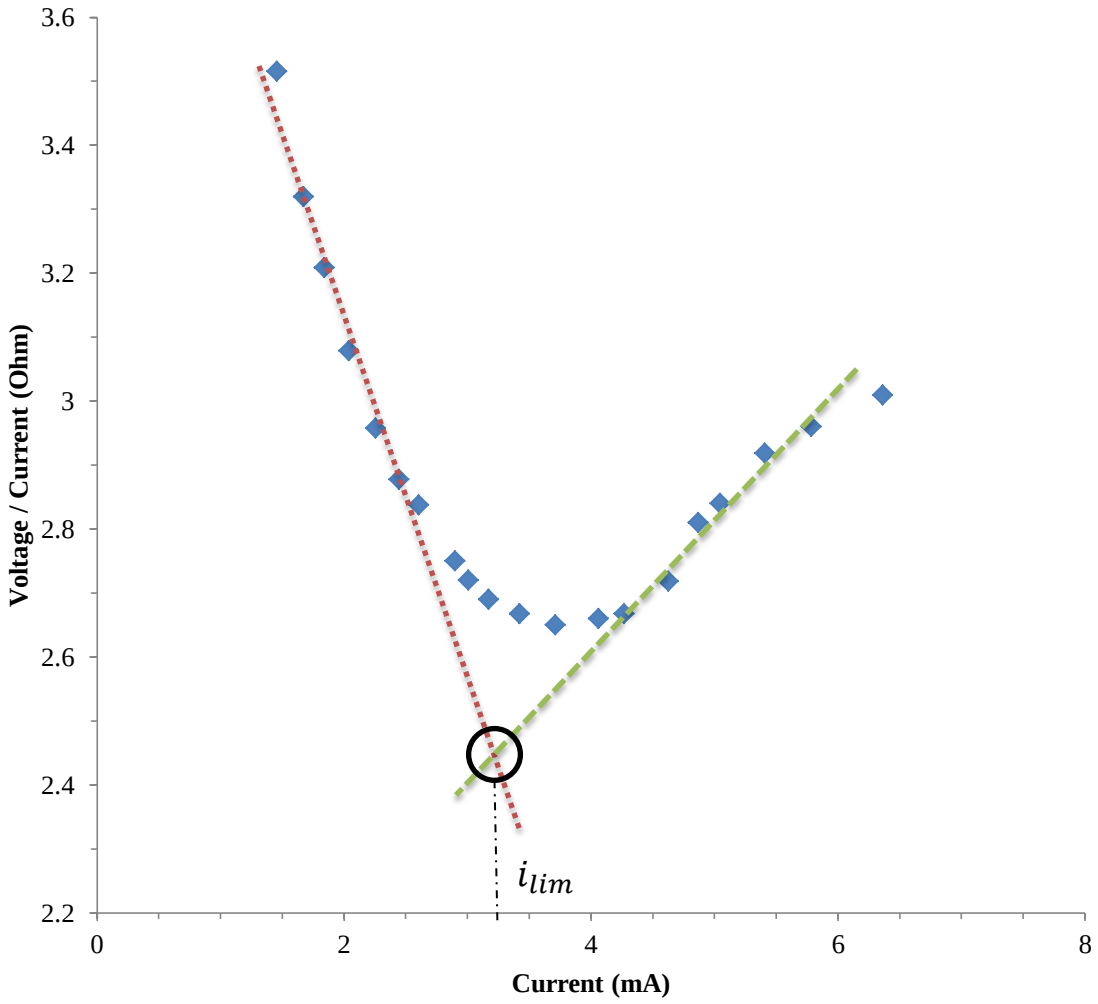

Figure 5.4.a Limiting current determination using a V/I graph.

Alternatively, the current can be plotted as a function of voltage. This will expose three areas of interest and also help estimate the limiting current. A conceptual graph can be seen in **Figure 5.4.b**.

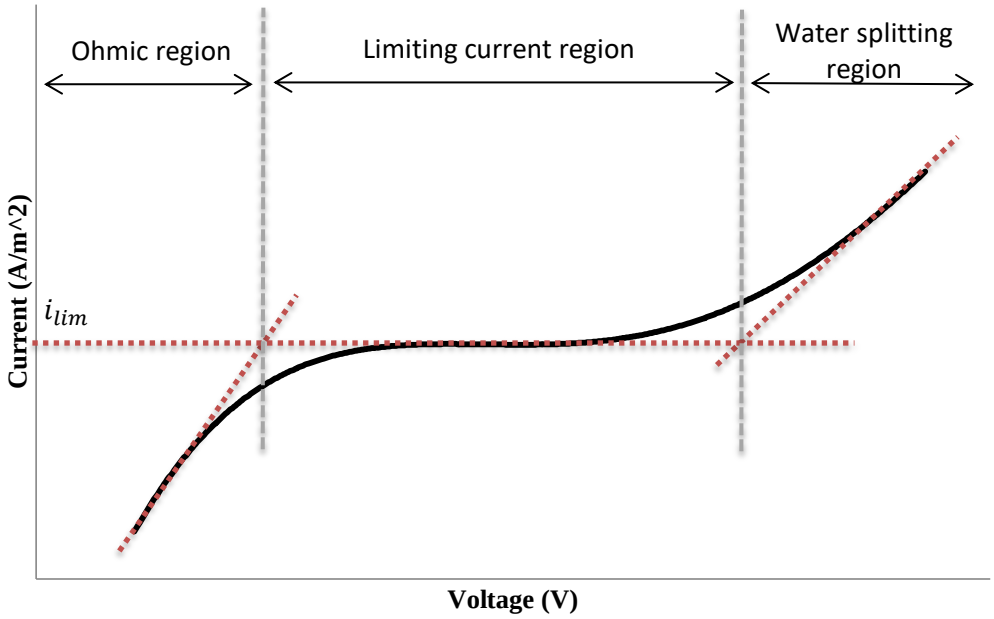

Figure 5.4.b Limiting current determination using a current vs. voltage graph.

The graph shows that as the applied voltage increases, the current reaches a maximum based on the properties of the electrolyte. Further increases in voltage do not initially increase current but eventually will by causing hydrolysis on the other side of the membrane. The limiting current corresponds to the current at which the curve flattens out. It is critical to determine the voltage and which the limiting current is reached and operate below it so as to not undermine the membrane.

5.7 Proof of Concept Test with Anion Exchange Membranes

5.7.1 Testing Process

A study was performed using two electro-osmosis tests. Test 1 was used as a control. After preparation, the sample was connected to a power supply and 15 volts of DC were

applied. During this time, an overburden pressure of 4 kPa was maintained to prevent crack formation. Water was drained from the cathode reservoir. Settlement and current were recorded. After 40 hours, the samples were disconnected and pH measured as per Hendershot et al. 2008. Test 2 introduced an AEM at the anode. For these tests, the anode reservoir was filled with deionized water to allow for hydrolysis to occur. A third test was later conducted to evaluate the effect of a cation exchange membrane. Contrary to expectations, the cation exchange membrane reduced the hydraulic conductivity of the system such that little water was drained throughout the test at the cathode, showing that drainage through the electrode will be insufficient. Thus, the data for that test is not included here. The configuration of the electro-osmotic process combined with both membranes is shown in **Figure 5.5**.

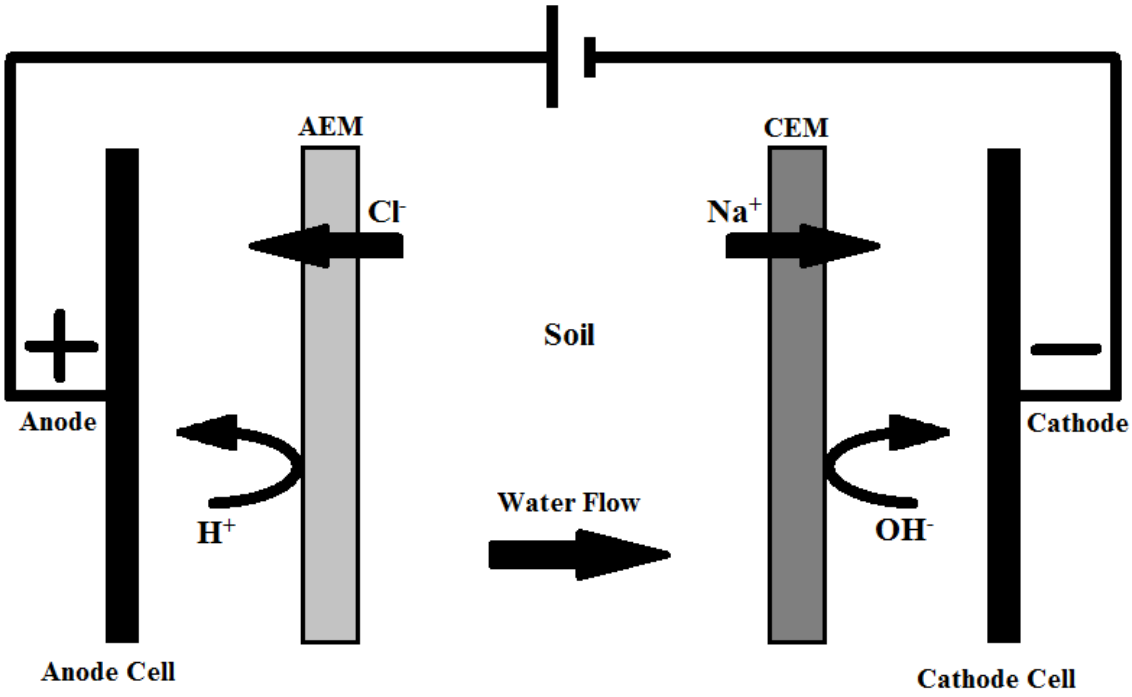

Figure 5.5 Schematic of electro-osmotic treatment of soil using ion exchange membranes.

5.7.2 Soil Sample

Sample soil preparation consists of first mixing 50% brown kaolin clay and 50% rock flour by weight. The mixture is mixed with water to a moisture content of 37.5%. The mixed sample is allowed to rest for 24 hours inside a vacuum oven to remove entrapped air. After this period, the sample is placed in the testing chamber and loaded to allow of normal consolidation to occur. Properties of the used samples are shown on **Table 5.2**.

Table 5.2 Soil Properties

Soil Composition (by weight)	Value
Brown Kaolin (%)	50
Rock flour (%)	50
Liquid Limit (%)	33.5
Plastic Limit (%)	16.9
Soil pH	6.13
Water content (%)	37.5

5.7.3 Membrane Preparation

For the AEM, it was prepared for use by soaking it in a 5% NaCl solution for 12 hours. This allowed the membrane to hydrate and expand. After this, the membrane was placed at the anode between the electrode and the soil. Membrane properties are listed in **Table 5.3**.

Table 5.3 Anion Exchange Membrane Properties

Property	Value
Membrane	*AMI-7001S*
Polymer Structure	*Gel polystyrene cross linked with divinylbenzene*
Functional Group	*Quaternary Ammonium*
Ionic Form	*Chloride*
Thickness (mm)	*0.45±0.025*
Electrical Resistance (Ohm*cm^2), 0.5 mol/L NaCl	*<40*
Maximum Current Density (Ampere/m2)	*<500*
Permselectivity (%), 0.1 mol KCl/kg / 0.5 mol KCl/kg	*90*
Total Exchange Capacity (meq/g)	*1.3±0.1*
Water Permeability (ml/hr/ft^2) @5psi	*<3*
Mullen Burst Test strength (psi)	*>80*
Thermal Stability (Celcius)	*90*
Chemical Stability Range (pH)	*1-10*

5.7.4 Testing Chamber

Figure 5.6 shows a schematic diagram and dimensions of the rectangular testing chamber. A small drainage tube in the cathode reservoir allowed for drainage of removed water. Graphite electrodes were used to prevent adding ions to the sample and deterioration of the electrode (Wu et al. 2015). This will also prevent corrosion due to

high pH in the anode reservoir, in addition, the acidic water can be easily drained by using hollow electrodes if necessary in the field. The membrane was placed between the electrode and the soil such that the electrode was not in direct contact with the soil.

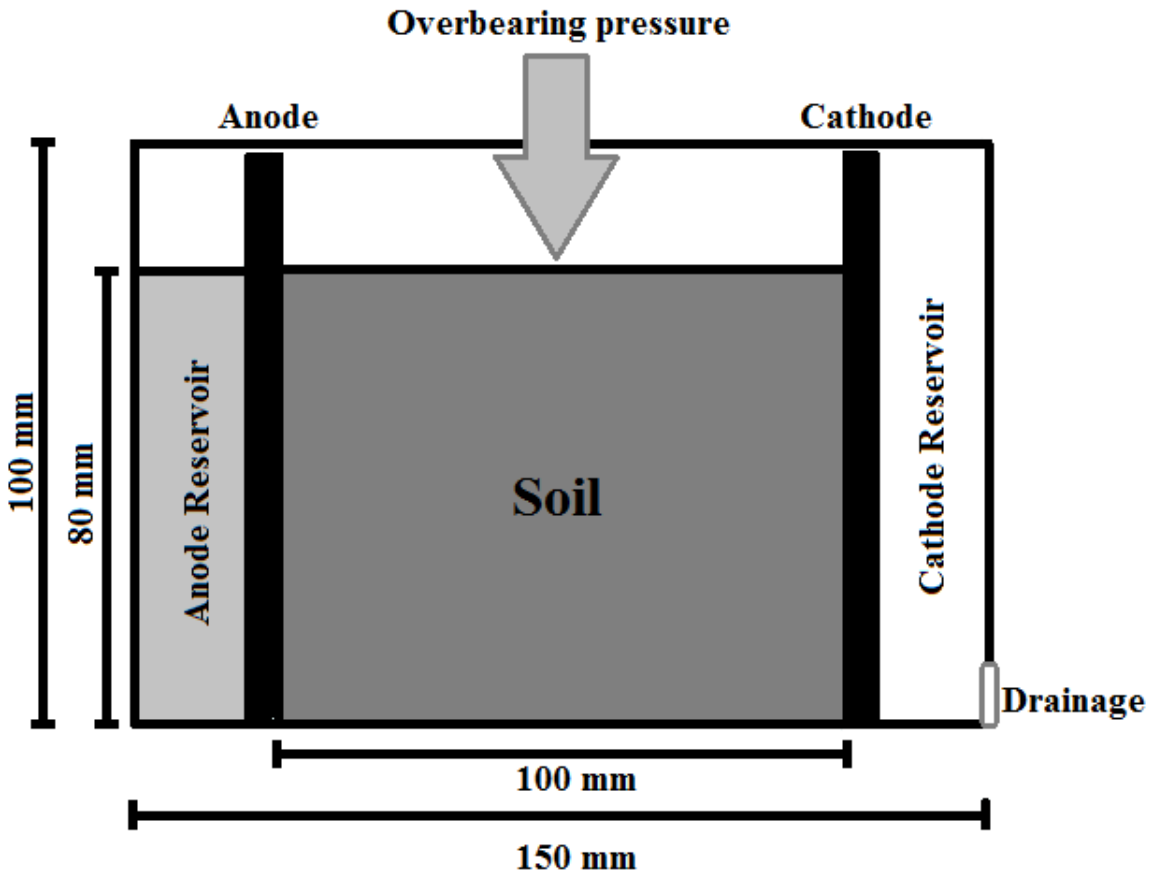

Figure 5.6 Schematic of testing cell.

5.8 Results and Discussion

5.8.1 pH

The variations of pH in the soil bed are shown in **Figure 5.7**. As the hydrolysis proceeds, hydroxide ions are produced at the cathode, whereas at the anode protons are produced, this results in a pH gradient across the soil (Yoshida 2000, Yuan and Weng 2003). The acid front near the anode and base front near the cathode migrate towards each other. The

acid front moves faster than the base front due to the higher mobility of H+ than OH-, and therefore low pH dominates the chemistry across the soil except for a small region close to the cathode (Alshawabkeh and Bricka, 2000). The control test reflects this phenomena. The pH around the anode drops to 3.9 and rises to 9.5 at the cathode, indicating that hydrolysis has occurred affecting the soil pH as expected. The pH at the center of the sample is acidic compared to the original, showing that the acidic front dominates.

Test 2 combines electro-osmosis with an AEM to prevent the flow of hydrogen ions into the soil near the anode and reduce the change in pH. The pH of Test 2 near the anode decreased to 5.0, even with in the presence of the membrane. This might be due to the exchange capacity of the membrane. As hydrolysis takes place, the membrane prevents the passage of H+ ions into the soil. However, eventually the membrane is depleted and ions can pass more freely. The time it takes for the membrane to be depleted is dependent many factors, such as soil type, electrode type, applied voltage, water content, type of ions in solution, type and size of membrane, and other; thus is usually not predicted (Sata 2004). The membrane used had a low hydraulic conductivity, thus passage of ions from the anode reservoir would still be partially thwarted even after depletion. The pH at the cathode is higher than that of the control. Since the membrane prevented the flow of hydrogen ions into the soil bed, the zeta potential of clay particles was better maintained. This is evidenced by the lower electrical resistance of Test 2 as shown in **Figure 5.8**. Consequently, the current throughout the test is higher (**Figure 5.9**) and hydrolysis occurs at a greater rate. This slightly greater generation of hydroxide ions increases the pH at the cathode to 10.1. At the center of the soil bed, the pH for Test 2 is

higher than the control. Since the hydrogen ions are trapped in the anode reservoir, the basic front generated at the cathode can migrate towards the anode and increases the pH of the soil. This further shows that the membrane prevented over acidification of the soil around the anode but the alkalinity around the cathode increase. Despite this, the results were still favorable as shown in **Figure 5.9** and **Figure 5.10**.

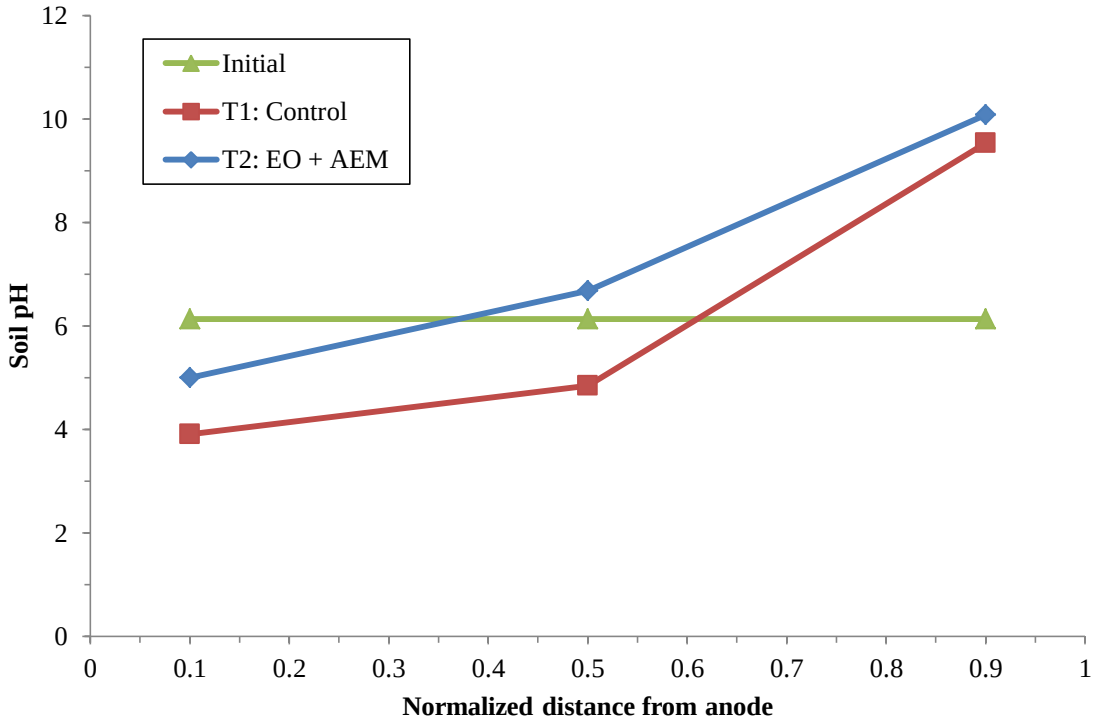

Figure 5.7 pH across soil bed after 40 hours of electro-osmotic treatment. Test 1: control; Test 2: electro-osmosis with anion exchange membrane.

The pH of the drained water and the water in the anode reservoir were also measured. These values are shown in **Table 5.4**. The drained water pH corresponded with the pH of the soil near the electrodes. Both had high pH, with Test 2 showing the higher value. Because the membrane prevented the generated hydrogen ions from flowing into the soil, the pH of the water in the anode reservoir decreased to below 1. This indicated

that the membrane succeeded in keeping the hydrogen ions from entering the soil bed. A yellowish coloration and faint smell also formed in the water.

Table 5.4 pH Measurements For Drained Water

	Test 1: Control	Test 2: EO + AEM
Drained water pH	10.17	10.79
Anode reservoir pH	-	0.5*

*The pH meter used had a minimum safe range of 1. Thus, the measurement obtained for the anode reservoir is below 1 but unreliable beyond that.

5.8.2 Electrical Resistance and Current

In accordance with the literature, the electrical resistance of the soil increased as electro-osmosis was carried out. The electrical resistance of the soil throughout testing was measured in one minute intervals for 40 hours. The results are shown in **Figure 5.8**. Both tests display an increasing electrical resistance. However, Test 1 experiences an electrical resistance 4.8 times greater than that of Test 2. The membrane does increase the electrical resistance in Test 2 by a fixed amount; however the trends still show its positive effects.

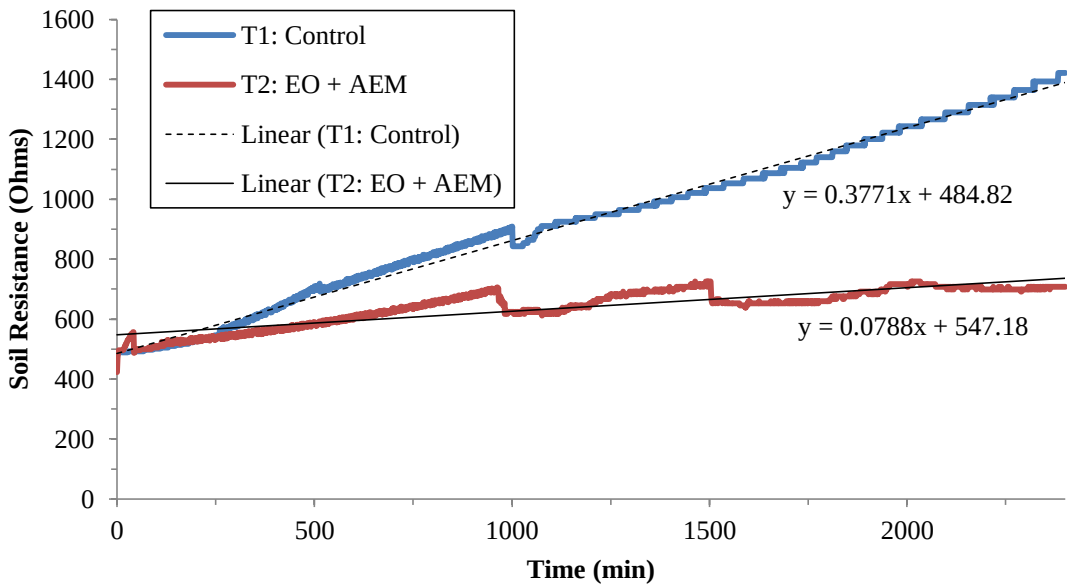

Figure 5.8 Soil resistance during 40 hours of electro-osmotic treatment. Test 1: control; Test 2: electro-osmosis with anion exchange membrane.

Figure 5.9 shows the variation in current through the soil over time. According to Ohm's law, the current is directly related to the electrical resistance, thus as electrical resistance increases the current decreases. While the current is still high compared to the initial value, and although the rate at which it decreases is low, the current can be expected to reach very low values, and even zero, if electro-osmosis is continued. If the test was continued until current reached zero, the membrane would have long been depleted and its effects likely nullified by the highly acidic water in the anode reservoir. Both **Figure 5.8** and **Figure 5.9** show some irregularities, especially at around 1000 minutes, which are common when making precise current measurements during electro-osmotic treatment (Micic et al. 2001, Sun and Ottosen, 2012, Hu et al. 2015).

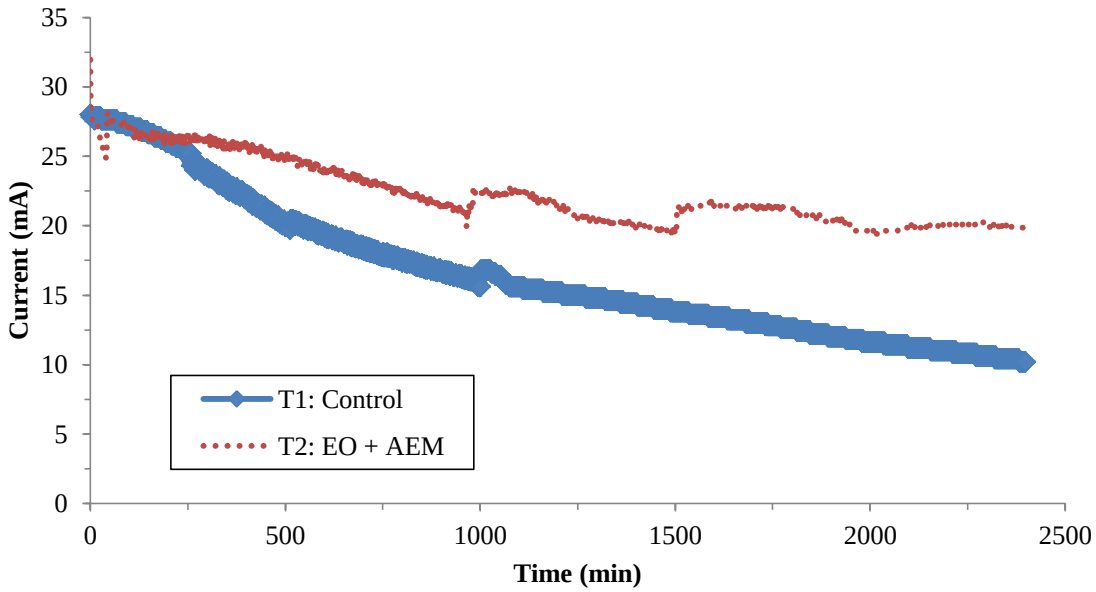

Figure 5.9 Current through the soil during 40 hours of electro-osmotic treatment. Test 1: control; Test 2: electro-osmosis with anion exchange membrane.

5.8.3 Settlement

A settlement gauge was placed on the center of the soil bed to measure the settlement of the sample as electro-osmosis was applied. **Figure 5.10** shows the settlement as a function of time. The application of a direct current induced settlement on both samples. Test 2 showed increased settlement due to the use of the AEM. Both tests show an initial high settling rate that plateaus after about 18 hours. Following this, settlement continues but at a much lower rate. Because the membrane prevented the flow of hydrogen ions into the soil bed, the absolute value of the zeta potential was not as affected and the electrical resistance in Test 2 did not increase as rapidly as Test 1. This allowed for a higher current and, thus, higher electro-osmotic flow, leading to increased consolidation.

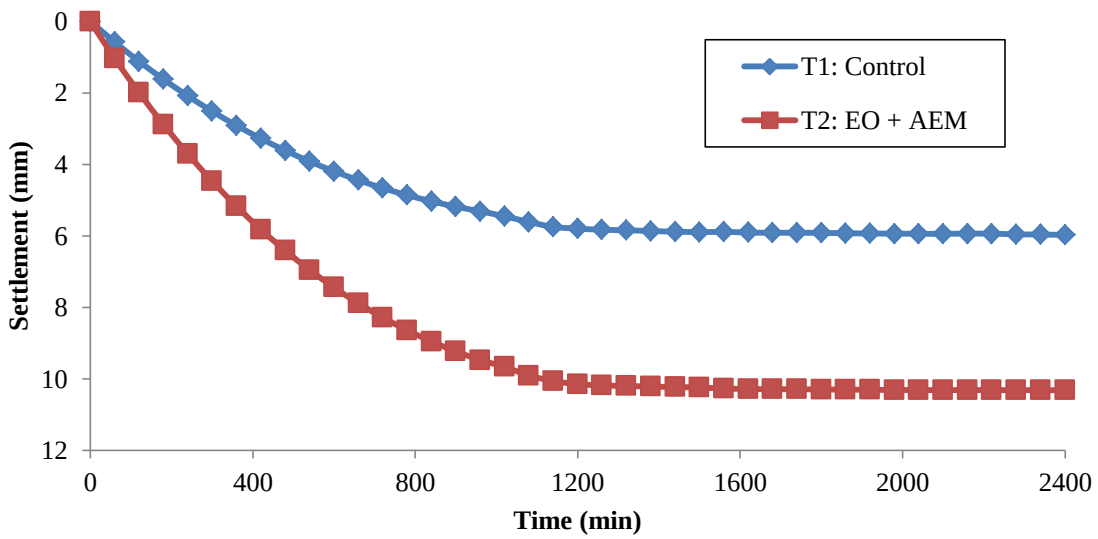

Figure 5.10 Settlement at the center of soil bed during 40 hours of electro-osmotic treatment. Test 1: control; Test 2: electro-osmosis with anion exchange membrane.

5.8.4 Summary of Proof of Concept Test

This small study assessed the possibility of use of AEMs at the anode to isolate hydrolysis of water around the anode and prevent the flow of hydrogen ions into the soil. The membrane showed positive results in all respects when compared to conventional electro-osmotic treatment. The pH of the soil around the anode did not decrease as much as with in the control test. It still decreased compared to the initial value. This is likely due to depletion of the exchange capacity of the membrane. The electrical resistance of the soil was shown to increase at a slower rate for the test with the membrane. This further affirms that the membrane produced a positive effect. The increased settlement of Test 2 was also very positive. The use of a membrane allowed for consolidation beyond that obtainable with simple electro-osmosis. Also of note is that despite using the membrane, the electrical resistance of the soil still increased. This demonstrates the

acidification of the soil around the anode is not the only force reducing electric efficiency.

5.9 Improving Electro-Osmosis with Anion Exchange Membranes

Several tests were carried out to quantify the efficiency of using anion exchange membranes in enhancing electro-osmotic consolidation. For this, consolidation tests were performed using different applied voltages to a soil sample with and without the membrane and the results were compared.

5.9.1 Soil

The soil used was commercially available brown kaolin with a liquid limit of 120. To prepare the soil for testing, it was thoroughly mixed with water to the liquid limit. After mixing and obtaining a homogeneous mixture, the soil was placed in a vacuum oven and a vacuum was applied to the soil capsule. The sample was stirred thoroughly and then left in the vacuum oven for 24 hours to remove any air voids.

5.9.2 Apparatus

To consolidate the soil, a Teflon cylinder was used. The cylinder had an inner diameter of 6.35 cm. The cylinder was closed on the bottom by a porous electrode plug that applies a voltage but also allows for water drainage. The plug consists of an electrode, porous stone, plastic disk, and base. The base contains a small orifice from which to control the liquid level at that electrode. On top of the electrode porous paper was placed to prevent the soil particles from clogging the electrode. This is not necessary when membranes are present. Both the electrode and plastic disk have multiple small holes to allow flow of liquid. The top of the cylinder has an extractable electrode with similar setup (see **Figure**

5.11). Load can then be applied on the top electrode to imitate stress conditions in the field. To track the settlement of the sample high precision GeoJac® settlement probes are placed on top of each cylinder.

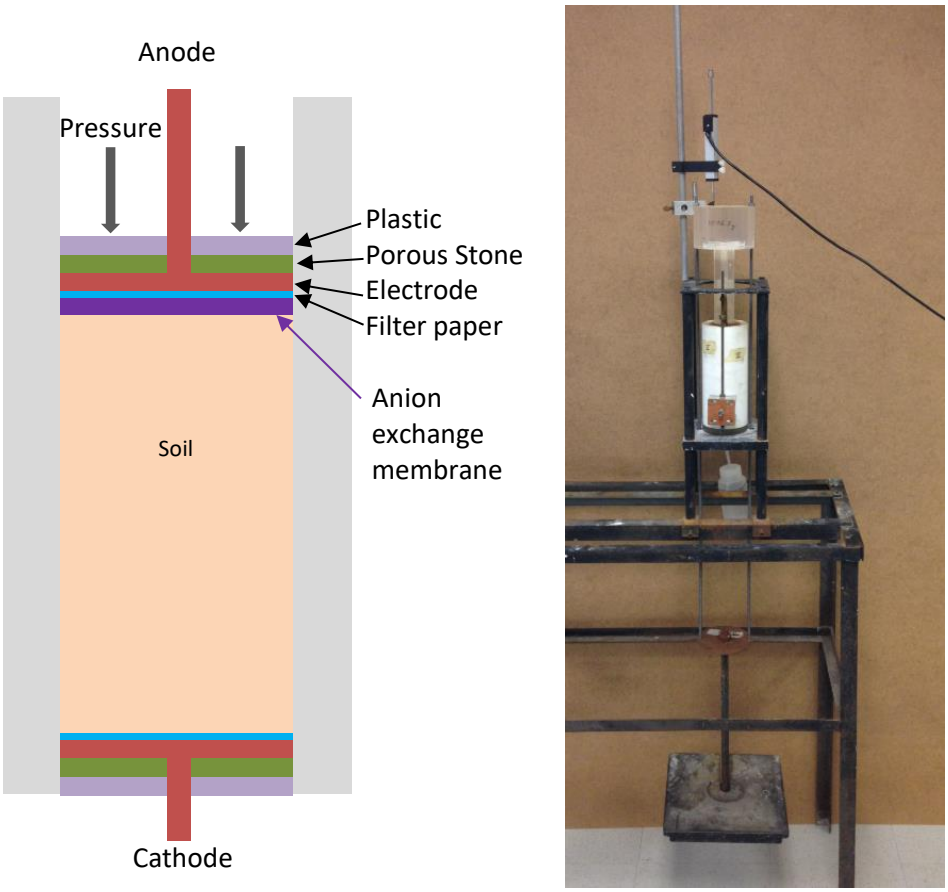

Figure 5.11 Testing cell and loading frame.

5.9.3 Preconsolidation

To achieve more relevant results, the soil is preloaded to the calculated stress found in the field. Assuming a depth of 10 feet, the vertical load to simulate field stress was calculated to be about 24 kg. After preparation with the vacuum oven, the soil was placed in the cylinder and allowed to settle by its own weight for 2-3 days. The soil was then loaded to 24 kg in 5 loading increments (1.5, 3, 6, 12, and 24 kg) to avoid undesired changes in soil

structure and its properties. In each load increment the settlement was monitored and timed. This is used to asses when the sample has reached full consolidation under the current load. The new load increment is then applied. After the calculated field vertical stress is applied and 100% primary consolidation is achieved, the samples are ready for electro-osmotic treatment.

5.9.4 Membrane Preparation

The AEM was prepared for use by soaking it in a 5% NaCl solution for 12 hours. This has to be done to allow the membrane to hydrate and expand. After this, the membrane was placed at the anode between the electrode and the soil. Membrane properties are listed in **Table 5.5**.

Table 5.5 Anion Exchange Membrane Properties

Counter Ion	Bromide (Br^-)
Thickness	110 - 140 µm
Electrical Resistance	5.0 - 9.0 $\Omega*cm^2$
Ion Exchange Capacity	0.7 - 1.0 meq/g
Selectivity	93 - 98 %
Proton Transfer Rate	60 - 400 µmol/(min*cm^2)

5.9.5 Testing

The samples were consolidated using electro-osmosis with and without a membrane and applying an voltage of 2.5, 5, 7.5, 10, and 15 volts. The settlement was tracked for each. The test was terminated once the settlement showed no further significant change. The maximum settlement achieved in each test was measured and the ratio of settlement using

the AEM to the settlement with regular electro-osmosis was calculated and plotted as a function of voltage. The limiting current was also measured.

5.9.6 Results and Discussion

The limiting current was tested four times to estimate the average voltage at which the membrane was undermined by producing hydrolysis. The result for one of these tests is shown on **Figure 5.12**.

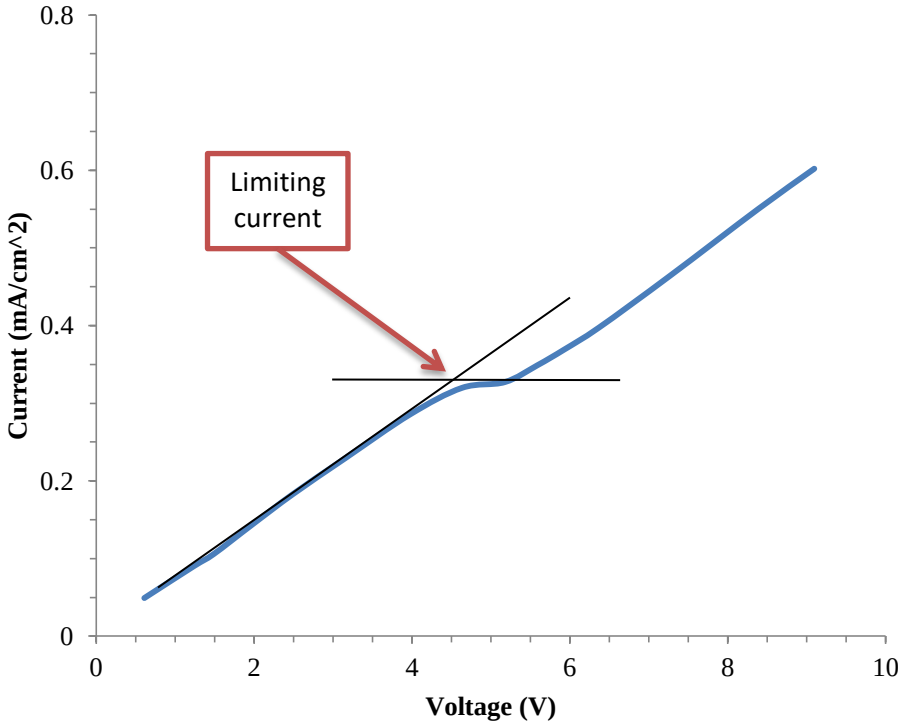

Figure 5.12 Limiting current test.

On average, at a voltage of 5.25 V, the limiting current was reached for the setup used. For the samples used, this corresponds to an electric field of 0.72 V/cm. Thus, if the applied electric field exceeds that value, the efficiency of the membrane should

significantly decrease. Based on this, the different voltages for the consolidation tests were selected.

Figure 5.13 shows the results of the consolidation tests using electro-osmosis with and without an AEM. The use of the AEM displays significant improvements over the conventional application of electro-osmosis. For all the voltages applied, the membrane outperformed regular electro-osmosis, especially for the lower voltages. This clearly demonstrates the potential of ion exchange membranes to enhance electro-osmotic consolidation and potentially make it commercially viable in construction.

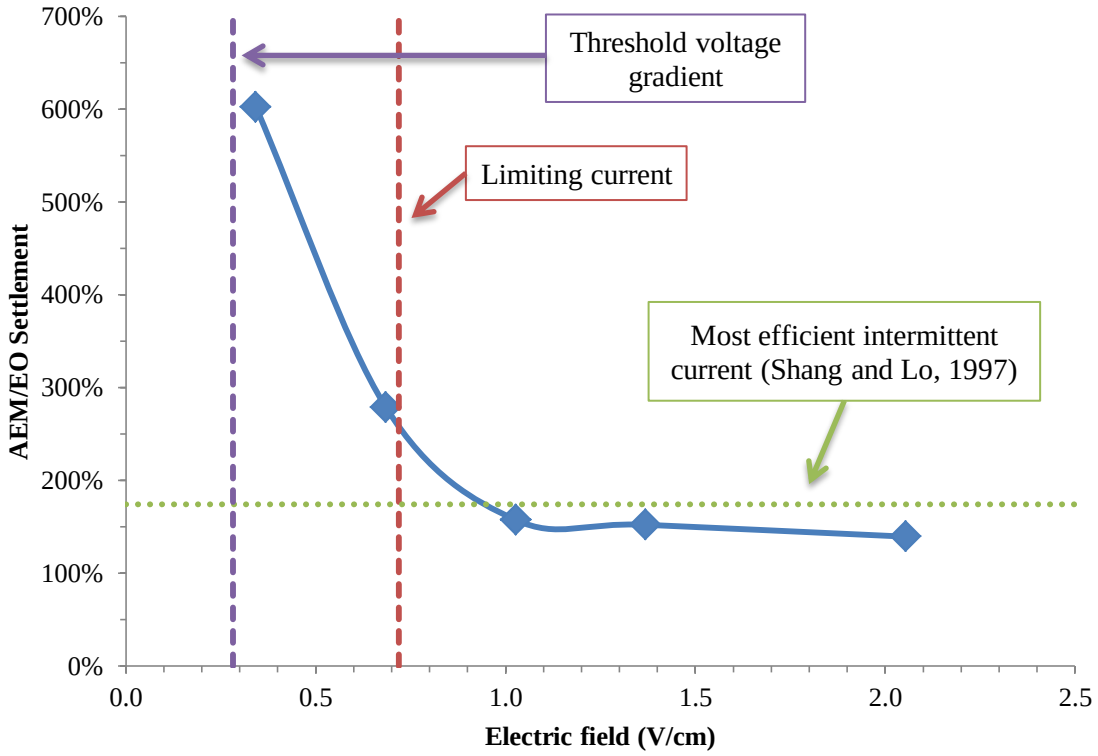

Figure 5.13 AEM efficiency at different voltages.

The graph matches the prediction based on the limiting current values reported in the literature. As the applied voltage increases, the efficiency of the AEM decreases,

though always staying positive. However, once the electric field corresponding to the limiting current is exceeded, the AEM has the lowest efficiency and is relatively constant. This happens because hydrolysis is occurring past the membrane and basically recreating the effects of regular electro-osmosis. It's as if a membrane wasn't being used. The small increase in efficiency at the higher electric fields is likely due to the initial delay of hydrogen ions, however small, from entering the soil. After this, the process continues normally. **Figure 5.13** also shows the best result from the other improvement techniques discussed in chapter 2. The best improvement was about 175% using intermittent current. This result is comparable to using the membrane at high voltages. However, using a membrane at low voltages still provides a substantially more significant enhancement. The threshold voltage gradient required for the hydrolysis reactions to take place is also shown. If the applied voltage gradient is below, in this case, 0.282 V/cm, electro-osmosis will not occur. The theoretical maximum improvement that could be achieved with a membrane in this setup is approximately 650%.

Figure 5.14 shows the settlement achieved for each test as a percentage of the total height right before application of the electric field. This graph reveals some interesting trends. First, regular electro-osmosis settlement increases with an increasing electric field but seems to peak around 1.3 V/cm. This corroborates Kaniraj et al., (2011) findings on the optimal voltage gradient. Applying a higher electric field causes the detrimental effects of the treatment to occur too quickly and the process is stifled before much consolidation can be achieved. The same effect occurs with the AEM tests. If and electric field higher than that corresponding to the limiting current is applied the tests behave like simple electro-osmosis tests and a peak is observed around 1.3 V/cm.

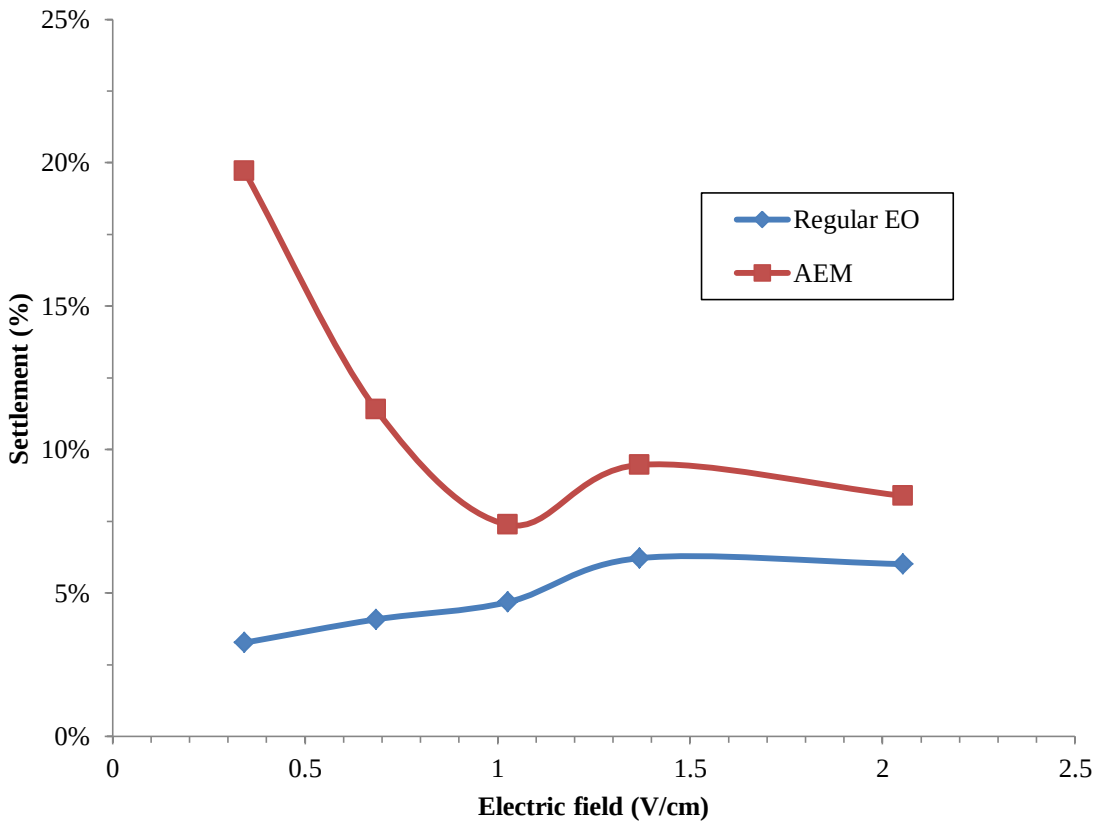

Figure 5.14 Settlement achieved for tests with and without an AEM.

Second, the efficiency of using AEM is always higher than regular electro-osmosis, even when comparing low AEM voltages versus high voltages without AEM. This means that the use of AEM produces significantly higher settlements with lower power consumption, showing that membranes have a high potential to make electro-osmosis a commercially viable option for consolidation.

5.10 Conclusions

The membrane successfully reduces an acid front of hydrogen ions that are generated due to electrolysis from moving into the soil, thereby preventing the deterioration of the

chemical structure of the clay particles. This results in higher settlements for less power consumed. The improvement might be significant enough to warrant the use of electro-osmotic treatment in soil treatment and preparation projects. However, there is a limiting current beyond which the electro-osmotic consolidation process is less effective. The limiting current for each particular application needs to first be calculated to maintain an optimal electric field. Then, using a composite electrode with a membrane, consolidation can potentially be achieved very effectively. Larger scale testing is still necessary to come to firm conclusions, but the work presented here proves the potential of ion exchange membranes and lays the foundation for future work in combining membranes with electro-osmotic consolidation.

CHAPTER 6

CONCLUSIONS AND RECOMMENDATIONS

6.1 Conclusions

The study described herein presents a new technology for consolidation of soft clayey soils. This technology involves the use of electro-osmosis enhanced by ion exchange membranes to electricity-driven create water flow though clay soil that achieve significantly greater settlements than conventional consolidation methods and more efficiently than other electro-osmosis techniques. A comprehensive review of other electro-osmotic consolidation methods was performed. Preliminary studies using ion exchange membranes showed that using membranes at the anode reduced the migration of hydrogen ions into the soil and significantly improved consolidation and electrical resistance. Several tests were performed to compare electro-osmotic consolidation with and without an anion exchange membrane at different voltages. A mathematical model was developed to describe the effects of electro-osmosis in clays. This model showed some improvements over previous models, especially with regards to the influence of the pore fluid and pore size. To describe natural soils, the model was expanded to account for anisotropy and a test was carried out to examine the electro-osmotic conductivity in different directions. The study also looked at the similarities between electro-osmotic consolidation and secondary consolidation. Multiple tests were carried out to estimate the relationship between secondary consolidation time and electro-osmotic consolidation at different voltages. The major findings from the research are summarized as follows:

1. Polarity reversal, intermittent current, injection of chemical solutions at the electrodes, and use of geo-synthetics increase the overall efficiency of electro-osmotic treatment. However, the improvements are not sufficient to justify widespread use of electro-osmotic dewatering.

2. The proposed equation for calculating electro-osmotic conductivities provides a comprehensive model by taking into account pore electrolyte properties, which the Helmholtz-Smoluchowski model overlooks. Hence the proposed model can provide accurate approximation of the effect of electro-osmotic consolidation.

3. The model also demonstrates that pore sizes do influence electro-osmotic flow through soils, contrary to what was previously thought.

4. The new mathematical model for estimating the electro-osmotic conductivity has more explanatory power in that it provides insight into why injection of saline solutions to the soil has been reported to improve electro-osmotic consolidation.

5. The model has been expanded to account for the anisotropy of natural soils, making it possible to obtain more accurate predictions of the electro-osmotic conductivity for a particular soil based on simple tests.

6. The electro-osmotic conductivity is a vector. It is different horizontally and vertically for a given soil. The clay soil fabric plays a significant role in electro-osmotic consolidation and should be investigated before application.

7. Secondary consolidation and electro-osmotic consolidation are shown to have similar effects in draining pore water from a kaolin clay both theoretically and experimentally. Electro-osmosis provided superior consolidation results and in a significantly shorter time. Additionally a relationship was found that allows the user to predict the voltage required to achieve the equivalent change in void ratio using electro-osmosis as a certain secondary consolidation.

8. Using an anion exchange membrane showed very positive results in all respects when compared to conventional electro-osmotic treatment. The pH of the soil around the anode did not decrease as much. The electrical resistance of the soil was shown to increase at a slower rate for the test with the membrane.

9. The membrane successfully reduces an acid front of hydrogen ions that are generated due to electrolysis from moving into the soil, thereby preventing the deterioration of the chemical structure of the clay particles. This results in significantly higher settlements for less power consumed.

10. There is a limiting current beyond which the electro-osmotic consolidation process is less effective. The limiting current for each particular application needs to first be calculated to maintain optimal voltage levels. Then, using a composite electrode with a membrane, consolidation can potentially be achieved very effectively.

6.2 Recommendations for Future Work

1. While other techniques were insufficient to make electro-osmosis viable, combining them might provide an increased efficiency in consolidation. Further studies should investigate the effectiveness of combining ion exchange membranes with other electro-osmosis techniques, especially intermittent current.

2. In this research, only one type of lab soil was used, a commercially available brown kaolin. Therefore, more extensive testing on different soils, especially field soils, is required to make wide ranging predictions.

3. Laboratory samples are uniform and not always representative of real soils. Therefore, testing with natural soils should be explored in future studies.

4. The new mathematical model can predict the electro-osmotic flow through a soil under an applied electric field. Further studies should compare predictions for different soils with test results.

5. The electro-osmotic conductivity was shown to be anisotropic. Further work should investigate other similarities to hydraulic conductivity. Knowledge of the properties of hydraulic conductivity could guide research of electro-osmotic conductivity of composite soils.

6. Different membrane structures should be tested to examine which works best with electro-osmosis on clays. A new membrane could potentially be synthetized for this purpose.

7. Large scale testing is still necessary to come to firm conclusions on the applicability and efficiency of these findings to field projects.

REFERENCES

Abdel-Meguid, M., El Naggar, M. H. and Shang, J. Q., 1999. Axial response of piles in electrically treated clay. *Canadian Geotechnical Journal,* Volume 36, pp. 418-29.

Abiera, H. O., Miura, N. and Bergado, D. T., 1999. Effects of using electroconductive PVD in the consolidation of reconstituted Ariake clay. *Geotechnical Engineering Journal,* 30(2), pp. 67-83.

Abou-Shady, A. and Peng, C., 2012. New process for ex situ electrokinetic pollutant removal. I: Process evaluation. *Journal of Industrial and Engineering Chemistry,* Volume 18, pp. 2162-2176.

Acar, Y. B. and Alshawabkeh, A. N., 1996. Electrokinetic remediation. I: Pilot-scale tests with lead-spiked kaolinite. *Journal of Geotechnical Engineering,* Volume 122, pp. 173-185.

Alshawabkeh, A. N. and Bricka, M., 2000. Basics and applications of electrokinetic remediation. In: D. L. Wise, et al. eds. *Remediation Engineering of Contaminated Soils.* New York, NY: Marcel Dekker, Inc., pp. 95-111.

Alshawabkeh, A. N. and Sheahan, T. C., 2003. Soft soil stabilization by ionic injection under electric fields. *Ground Improvement,* Volume 7, pp. 177-185.

Asadi, A., Huat, B. B. K., Nahazanan, H. and Keykhah, H. A., 2013. Theory of electroosmosis in soil. *International Journal of Electrochemical Science,* Volume 8, pp. 1016-1025.

Baker, R. W., 2004. *Membrane Technology and Applications.* 2 ed. Menlo Park, CA: John Wiley and Sons.

Bergado, D. T., Balasubramaniam, A. S., Parawaran, M. A. B. and Kwunpreuk, W., 2000. Electro-osmotic consolidation of soft Bangkok clay with prefabricated vertical drains. *Ground Improvement,* Volume 4, pp. 153-163.

Bhattacharya, A. K. and Basack, S., 2011. *A review of the use of the pre-loading technique and vertical drains for soil consolidation.* Kochi, Proceedings of Indian Geotechnical Conference.

Bjerrum, L., Moum, J. and Eide, O., 1967. Application of electroosmosis to a foundation problem in a Norwegian Quick Clay. *Geotechnique,* 17(3), pp. 214-235.

Burnotte, F., Lefebvre, G. and Grondin, G., 2004. A case record of electroosmotic consolidation of soft clay with improved soil–electrode contact. *Canadian Geotechnical Journal,* Volume 41, pp. 1038-1053.

Cameselle, C., 2014. Electrokinetic transport in soil remediation. In: G. Kreysa, K. Ota and R. Savinell, eds. *Encyclopedia of Applied Electrochemistry.* New York, NY: Springer, pp. 725-731.

Casagrande, L., 1949. Electro-osmosis in soils. *Geotechnique,* 1(3), pp. 159–177.

Chakraborty, S., 2015. Electrical double layers interaction. In: D. Li, ed. *Encyclopedia of Microfluidics and Nanofluidics.* Waterloo, NY: Springer Reference, pp. 735-742.

Chang, H. W. et al., 2010. Electro-osmotic chemical treatment - a study on distribution of calcium in kaolinite and its effect on strength and pH. *Clays and Clay Minerals,* Volume 58, pp. 154-163.

Chappell, B. A. and Burton, P. L., 1975. Electroosmosis applied to unstable embankment. *Journal of Geotechnical Engineering Division ASCE,* 101(8), pp. 733–740.

Chien, S., Ou, C. and Wang, M., 2009. Injection of saline solutions to improve the electroosmotic pressure and consolidation of foundation soil. *Applied Clay Science,* Volume 44, pp. 218-224.

Chien, S., Ou, C. and Wang, Y., 2011. Soil improvement using electroosmosis with the injection of chemical solutions: laboratory tests. *Journal of the Chinese Institute of Engineers,* 34(7), pp. 863-875.

Coelho, D., Shapiro, M., Thovert, J. F. and Adler, P. M., 1996. Electroosmotic phenomena in porous media. *Journal of Colloid and Interface Science,* Volume 181, pp. 169-190.

Conway, B. E., 1981. *Ionic Hydration in Chemistry and Biophysics.* New York, NY: Elsevier Scientific Pub. Co.

Cowan, D. A. and Brown, J. H., 1959. Effect of turbulence on limiting current density in electrodialysis cell. *Industrial and Engineering Chemistry,* Volume 51, pp. 1445-1448.

Das, B. M. and Sobhan, K., 2018. *Principles of Geotechnical Engineering.* 9th ed. Boston, MA: Cengage Learning.

Esrig, M. I., 1968. Pore pressure, consolidation and electrokinetics. *Journal of Soil Mechanics and Foundations Division, ASCE,* 94(4), pp. 899-921.

Fourie, A. B., Johns, D. G. and Jones, C., 2007. Dewatering of mine tailings using electrokinetic geosynthetics. *Canadian Geotechnical Journal,* Volume 44, pp. 160-172.

Giorno, L., Drioli, E. and Strathmann, H., 2015. Permselectivity of ion-exchange membranes. In: *Encyclopedia of Membranes.* Berlin, Germany: Springer.

Glendinning, S., Jones, C. and Pugh, R. C., 2005. Reinforced soil using cohesive fill and electrokinetic geosynthetics. *International Journal of Geomechanics,* 5(2), pp. 138-146.

Gray, D. H., 1970. Electrochemical hardening of clay soils. *Geotechnique,* 20(1), pp. 81-93.

Gray, D. H. and Somogyi, F., 1977. Electroosmotic dewatering with polarity reversals. *Journal of Geotechnical Engineering,* 103(1), pp. 51-54.

Hamir, R. B., Jones, C. and Clarke, B. G., 2001. Electrically conductive geosynthetics for consolidation and reinforced soil. *Geotextiles and Geomembranes,* Volume 19, pp. 455-482.

Hardin, J., Bertoni, G. P. and Kleinsmith, L. J., 2010. *Becker's World of the Cell.* 8th ed. San Francisco, CA: Benjamin Cummings.

Helmholtz, H. v. L., 1879. Studies of electric boundary layers. *Wied Ann,* Volume 7, pp. 337–382.

Hendershot, W. H., Lalande, H. and Duquette, M., 2008. Soil reaction and exchangeable Acidity. In: M. R. Carter and E. G. Gregorich, eds. *Soil Sampling and Methods of Analysis.* Boca Raton, FL: Canadian Society of Soil Science, pp. 173-175.

Hu, L., 2008. *Recent research and applications in the use of elecetro-kinetic geosynthetics.* Scotland, International Geosynthetics Society.

Hu, L., Wu, H., Meegoda, J. N. and Wen, Q., 2015. Experimental and numerical study of electro-osmosis on kaolinite under intermittent current. *Geotechnical Engineering Journal of the SEAGS and AGSSEA,* 46(4), pp. 47-51.

Hu, L., Wu, H. and Meegoda, N. J., 2016. Effect of electrode material on electro-osmotic consolidation of bentonite. *The 15th Asian Regional Conference on Soil Mechanics and Geotechnical Engineering*.

Hu, L., Wu, H., Ren, Y. and Wen, Q., 2016. *Experimental Study on Soft Soils Improvement by the Deep Electro-Osmotic Consolidation Technique.* Chicago, Geo-Chicago, pp. 235-244.

Hunter, R. J., 2001. *Foundations of Colloid Science.* 2nd ed. New York, NY: Oxford University Press.

Iwata, M., Tanaka, T. and Jami, M. S., 2013. Application of electroosmosis for sludge dewatering - A review. *Drying Technology*, Volume 31, pp. 170-184.

Jones, , C., Lamont-Black, J. and Glendinning, S., 2011. "Electrokinetic geosynthetics in hydraulic applications. *Geotextiles and Geomembranes,* Volume 29, pp. 381-390.

Jordan, A., 2014. *Lightening the clay (II).* [Online]
Available at: https://blogs.egu.eu/divisions/sss/2014/09/page/3/
[Accessed 2017].

Kaniraj, S. R., 2014. Soft soil improvement by electroosmotic consolidation. *International Journal of Integrated Engineering,* 6(2), pp. 42-51.

Kaniraj, S. R., Huong, H. L. and Yee, J., 2011. Electro-osmotic consolidation studies on peat and clayey silt using electric vertical drain. *Geotechnical and Geological Engineering,* Volume 29, pp. 277-295.

Lamont-Black, J. and Weltman, A., 2010. Electrokinetic strengthening and repair of slopes. *Ground Engineering,* pp. 28-31.

Lefebvre, G. and Burnotte, F., 2002. Improvements of electroosmotic consolidation of soft clays by minimizing power loss at electrodes. *Canadian Geotechnical Journal,* Volume 39, pp. 399-408.

Lockhart, N. C., 1983. Electroosmotic dewatering of clays. I. Influence of voltage. *Colloids and Surfaces,* Volume 6, pp. 229-238.

Lo, K. Y., Ho, K. S. and Inculet, I. I., 1991. Field test of electroosmotic strengthening of soft sensitive clay. *Canadian Geotechnical Journal,* Volume 28, pp. 74-83.

Lo, K. Y. et al., 2000. Electrokinetic strengthening of a soft marine sediment. *International Journal of Offshore and Polar Engineering,* Volume 10, pp. 137-144.

Mahmoud, A., Olivier, J., Vaxelaire, J. and Hoadley, A., 2010. Electrical field: A historical review of its application and contributions in wastewater sludge dewatering. *Water Research,* Volume 44, p. 2381–2407.

Martin, L., Alizadeh, V. and Meegoda, J. N., 2019. Electro-osmosis treatment techniques and their effect on dewatering of soils, sediments, and sludge: A review. *Soils and Foundations,* Volume 59, pp. 407-418.

Martin, L. and Meegoda, J. N., 2019a. Feasibility of ion exchange membranes to control ph during electro-osmotic consolidation. *Geotechnical Testing Journal,* Volume 42.

Martin, L. and Meegoda, J. N., 2019b. New method to predict electro-osmotic conductivity of clays. Submitted to *International Journal of Geomechanics.*

Martin, L. and Meegoda, J. N., 2019c. Calculating electro-osmotic conductivity of clays based on anisotropy and porosity. Submitted to *Geotechnique*, July 2019.

Martin, L. and Meegoda, J. N., 2019d. Prediction of applied voltage for electro-osmotic consolidation based on coefficient of secondary consolidation. To be submitted to *ASCE Journal of Geotechnical and Geo-environmental Engineering,* August 2019.

Martin, L. and Meegoda, J. N., 2019e. Anion exchange membranes to enhance electro-osmotic consolidation. Submitted to *Soils and Foundations,* August 2019.

Meegoda, J. N. and Ratnaweera, P., 2008. Prediction of effective porosity of contaminated soils using electrical properties. *Geotechnical Testing Journal,* 31(4), pp. 344-357.

Micic, S. et al., 2001. Electrokinetic strengthening of a marine sediment using intermittent current. *Canadian Geotechnical Journal,* Volume 38, pp. 287-302.

Mitchell, J. K. and Soga, K., 2005. *Fundamentals of Soil Behavior.* 3rd ed. Hoboken, NJ: John Wiley and Sons, Inc.

Mohamedelhassan, E. E., 1998. *Electro-Osmotic Permeability of a Marine Sediment.* 1 ed. London, Ontario: University of Western Ontario.

Mohamedelhassan, E. E. and Shang, J. Q., 2003. Electrokinetics-generated pore fluid and ionic transport in an offshore calcareous soil. *Canadian Geotechnical Journal,* Volume 40, pp. 1185-1199.

Mohamedelhassan, E. E. and Shang, J. Q., 2001. Effects of electrode materials and current intermittence in electro-osmosis. *Ground Improvement,* Volume 5, pp. 3-11.

Otsuki, N., Yodsudjai, W. and Nishida, T., 2007. Feasibility study on soil improvement using electrochemical technique. *Construction and Building Materials,* 21(5), pp. 1046-1051.

Ou, C., Chien, S. and Chang, H., 2009. Soil improvement using electroosmosis with the injection of chemical solutions: field tests. *Canadian Geotechnical Journal,* Volume 46, pp. 727-733.

Ozkan, S., Gale, R. and Seals, R., 1999. Electrokinetic stabilisation of kaolinite by injection of Al and PO43-ions. *Ground Improvement,* Volume 3, pp. 135-144.

Paczkowska, B., 2005. Electro-osmotic introduction of methacrylate polycations to dehydrate clayey soil. *Canadian Geotechnical Journal,* Volume 42, p. 780–786.

Pamukcu, S., Weeks, A. and Wittle, J. K., 1997. Electrochemical extraction and stabilization of selected inorganic species in porous media. *Journal of Hazardous Materials,* Volume 55, pp. 305-318.

Pazos, M., Sanroman, M. A. and Cameselle, C., 2006. Improvement in electrokinetic remediation of heavy metal spiked kaolin with the polarity exchange technique. *Chemosphere,* Volume 62, pp. 817-822.

Perrin, J., 1904. Mecanisme de l'électrisation de contact et solutions colloÏdales. *Journal of Chemical Physics,* Volume 2, pp. 601-651.

Rabie, H. R., Mujumdar, A. S. and Weber, M. E., 1994. Interrupted electroosmotic dewatering of clay suspensions. *Separation Technologies,* Volume 4, pp. 38-46.

Reuss, F. F., 1809. Memoires de la societe imperiale des naturalists. *Impr. de l'Université impériale,* Volume 2, pp. 327-337.

Rittirong, A. et al., 2008. Effects of electrode configuration on electrokinetic stabilization for caisson anchors in calcareous sand. *Journal of Geotechnical and Geoenvironmental Engineering,* 134(3), pp. 352-365.

Rutigliano, L. et al., 2008. Electrokinetic remediation of soils contaminated with heavy metals. *Journal of Applied Electrochemistry,* Volume 38, pp. 1035-1041.

Saichek, R. E. and Reddy, K. R., 2003. Effect of pH control at the anode for the electrokinetic removal of phenanthrene from kaolin soil. *Chemosphere,* Volume 51, pp. 273-287.

Sata, T., 2004. *Ion Exchange Membranes - Preparation, Characterization, Modification and Application.* Cambridge, United Kingdom: The Royal Society of Chemistry.

Sata, T., Yamane, R. and Mizutani, Y., 1969. Concentration polarization phenomena in ion exchange membrane electrodialysis. 1. Studies of the diffusion boundary layer by means of six different measurements. *Bulletin of the Chemical Society of Japan,* Volume 42, pp. 279-284.

Schmid, G., 1950. Zur elecktrochemie feinporiger kapillarsystems I. *Zhurnal fur Elektrochemie,* Volume 54.

Schmid, G., 1951. Zur elecktrochemie feinporiger kapillarsystems II. *Zhurnal fur Elektrochemie,* Volume 55.

Shang, J. Q., 1997. Zeta potential and electroosmotic permeability of clay soils. *Canadian Geotechnical Journal,* Volume 34, pp. 627-631.

Shang, J. Q., 1998. Electokinetic dewatering of clay slurries as engineered soil covers. *Canadian Geotechnical Journal,* 34(1), pp. 78-86.

Shang, J. Q. and Lo, K. Y., 1997. Electrokinetic dewatering of a phosphate clay. *Journal of Hazardous Materials,* Volume 55, pp. 117-133.

Shang, J. Q., Lo, K. Y. and Huang, K. M., 1996. On factors influencing electro-osmotic consolidation. *Journal of Geotechnical Engineering,* 27(4), pp. 23-26.

Smoluchowski, M., 1914. *Handbuch der Elektrizitat und Magnetismus.* 2 ed. Leipzig, Germany: J. A. Barth.

Smoluchowski, M., 1921. Elektrische endosmose und stromungsstrome. *Handbuch der Elektrizitat und des Magnetismus,* Volume 2, pp. 366-428.

Spiegler, K. S., 1958. Transport processes in ionic membranes. *Transactions of the Faraday Society,* Volume 54, pp. 1408-1428.

Sprute, R. H. and Kelsh, D. J., 1976. Dewatering and densification of coal waste by direct current: laboratory tests. *Energy Citations Database.*

Sun, T. R. and Ottosen, L. M., 2012. Effects of pulse current on energy consumption and removal of heavy metals during electrodialytic soil remediation. *Electrochimica Acta,* Volume 86, pp. 28-35.

Tanaka, Y., 2003. Concentration polarization in ion-exchange membrane electrodialysis—the events arising in a flowing solution in a desalting cell. *Journal of Membrane Science,* Volume 216, pp. 149-164.

Tuan, P. A., Jurate, V. and Mika, S., 2008. Electro-dewatering of sludge under pressure and non-pressure conditions. *Environmental Technology,* Volume 29, p. 1075–1084.

Vane, L. M. and Zang, G. M., 1997. Effect of aqueous phase properties on clay particle zeta potential and electro-osmotic permeability: Implications for electro-kinetic soil remediation processes. *Journal of Hazardous Materials,* Volume 55, pp. 1-22.

Veder, C., 1981. *Landslides and their stabilization.* Hilbert R ed. New York, NY: Springer.

Wu, H., Hu, L., Zhang, L. and Wen, Q., 2015. Transport and exchange behavior of ions in bentonite during electroosmotic consolidation. *Clays and Clay Minerals,* 63(5), pp. 395-403.

Yoshida, H., 2000. Electro-osmotic dewatering under intermittent power application by rectification of A.C. electric field. *Journal of Chemical Engineering of Japan,* 33(1), pp. 134-140.

Yoshida, H. K., Kitajyo, K. and Nakayama, M., 1999. Electroosmotic dewatering under A. C. electric field with periodic reversals of electrode polarity. *Drying Technology,* 17(3), pp. 539-554.

Yuan, C. and Weng, C. H., 2003. Sludge dewatering by electrokinetic technique: Effect of processing time and potential gradient. *Advances in Environmental Research,* 7(3), p. 727–732.

Zhou, D., Deng, C., Alshawabkeh, A. N. and Chang, L., 2005. Effects of catholyte conditioning on electrokinetic extraction of copper from mine tailings. *Environment International,* Volume 31, pp. 885-890.